STIMULI-RESPONSIVE MEMBRANES FOR TARGETED DELIVERY OF ACTIVES

Rita Del Pezzo

UNIVERSITAT ROVIRA i VIRGILI

Stimuli responsive membranes for targeted delivery of actives

RITA DEL PEZZO

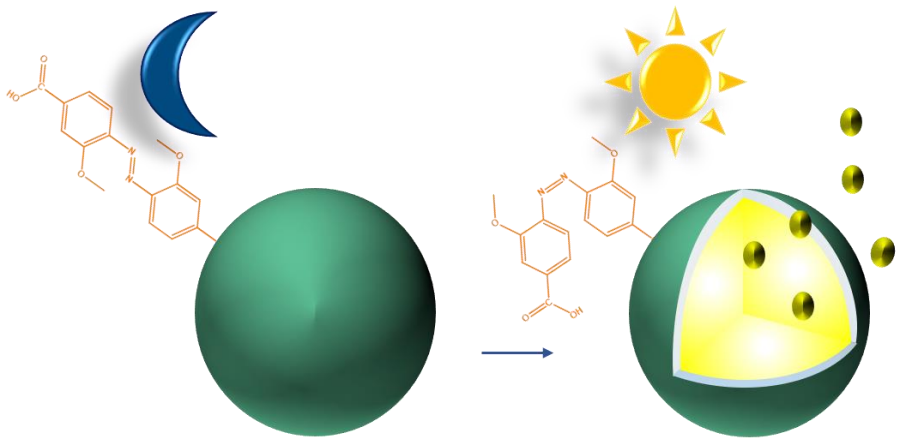

DOCTORAL THESIS

2020

Stimuli-responsive membranes for targeted delivery of actives

by

Rita del Pezzo

Doctoral Thesis

Supervisors:

Marta Giamberini

Johan Smets

Universitat Rovira i Virgili

Tarragona

2020

UNIVERSITAT ROVIRA I VIRGILI

Department d'Enginyeria Química
Campus Sescelades,
Avda. Països Catalans, 26
43007 Tarragona
Tel: 977 55 97 87
Fax: 977 55 96 21

Marta Giamberini, Associate Professor at the University Rovira i Virgili, Department of Chemical Engineering.
Johan Smets, Research Fellow, Procter & Gamble.

We state that the present study, entitled "Stimuli responsive membranes for targeted delivery of actives", presented by Rita del Pezzo for the award of the degree of Doctor, has been carried out under our supervision at the Chemical Engineering Department at the University Rovira i Virgili, and that it fulfils all the requirements to be eligible for the Doctor International Mention.

Tarragona, February 2020

Supervisors of the doctoral thesis

Dr. Marta Giamberini

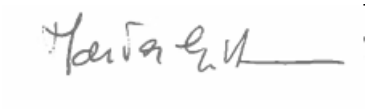

Dr. Johan

Smets

Acknowledgments

I have been extremely lucky, to have on my side, during this growth period, by two fantastic women; they have been always wise, strong but able to love and guide the others with a lot of caring. Two women of science that guided and helped me with the tough challenges I needed to face during these three years, teaching me the art of the research, of the science, of the communication with others, of the sharing, to not get difficulties get you down. My huge thanks goes, thus, to Marta and Susana, for their tireless patience and joy in teaching, the science as the life. I really want to thank you for believing in me to the very end, for pushing me, sometimes even hard, to grew when I didn't know how to do it. I know I still have a lot to learn from you two, and I am really looking forward to re-starting doing it.

Thanks to Johan, for his support to our program, for his contribution to my project and for his contagious passion for innovation. Thank you very much also to Bartek, for all the things he taught me; as office-mate, for more than a year, I thank you for your unique ability to really understand me, for your ability to listen, to advice, to reprimand, to laugh together. I would like to thank Raul, for the relationship we built in these years, for teaching me that, especially in our job, it is not possible to base our actions on assumptions, but also for being always available for a constructive talk, whenever I needed, or I wanted to. Thanks to Toni, Ricard and Angels, they welcomed not only me, but all of us, from the very beginning, as you would do in a family.

When I started this journey, as a big leap in the dark, I thought I was alone; the biggest joy for me, was to realize how many new friends were enriching me during time. Mario, Mimmo, Gianmarco and Jie were my family during these three years and I am sure they will keep doing so in the future. We took care of each other, always: when we didn't understand absolutely nothing due to the impact with the new languages, when we had no idea how to behave,

when we were scared, when we had beetles invasion, when there was few light, few time, few motivation, few food, few space, when everything was changing, when we did mistakes, when we were happy, a lot, together! I already miss the Sundays at home submersed by ice-creams, the dancing in the red-lighted laboratory, the gossiping, the nights in the Totem, the Chinese dinners, the basket matches in the basket bean, the football-table, everything!

Thanks to all the friends from the laboratory in Tarragona: Xavi, Ruben, Dailyn, Alberto, Lorena, Cristina, Isaac, Pere, the people from the CTQC, Benedetta, Montse, Anya, Ada, Monika, has been great to grow up with you, from the Erasmus to the PhD!

I really do not know how I would have managed my life without meeting my safety nets, my friends, Lorenza, Chiara and Silvia; each of you, at different times, in different places and in different ways, helped me to open my mind, made me laugh a lot, gave me advices as only a sister would have done, lean on me when you needed..there is nothing better that this in a friendship.

The big, ever-changing, always-growing family of Brussel, deserve also a big thank you! Non only for the kilos we gained together, but also for the great company; it has been a no-stop of lunches and dinners together, naps together, laugh together, lot of music..it was always a party! Thanks to Luca, Gianmarco P, Livio, Fabiana, Ines, Peppe, Giusy, Alessandro, Licia! Many thanks also to my old friends, Federica, Giulia and Anna, because also if we live far away from each other, and we have been far from long time, the love and the caring continues to be felt. I hope that, even if the Brasil account is not ready to meet our expectations, we will do better in the future to be present in each other's' life. Thank you for the support, for the ability to make me feel that everything is possible, for being always ready to fight on my side.

Thank you to Simone, unluckily for you I am following you around Europe because I discovered how good is to have you around! Lo, I taught you how to do the ostrich, but you addressed me to the love of my life; I do not think it is

exactly comparable, but I will try to repair during life! I love you! Tanks to Francesco in the last two years I freaked out less than usual, I improved my diet, I gave the proper importance to things, I made (more often) good decisions, I became more responsible; I do not want to imagine how I would be without you at this point, but I am so happy that you are here now, to make my life better and to fill my heart. Thanks for the love, for not giving up, for the patience of each days. I cannot help myself to not see this achievement as an additional step towards our life together.

Thanks to my family, it is amazing to have a family like mine. Thanks to Marco, for the many critics and the big love, thanks to my sister, because whenever I am there crying as a baby, you are always able to fix everything. Thanks to my dad, for supporting me in all my choices. But the person who had the strength to tell me “go”, to keep the smile on her face even when her hart was hurt, to be happy for me even when not agreeing, to encourage me even when it meant being apart, to say “let’s try” even when it meant lot of sacrifice, was my mom. I look at myself today and I know that everything I am, everything I achieved, it’s thanks to you and all what you thought me.

My beautiful niece born in these three years, so what can I say more.. couldn’t be better!

Ringraziamenti

Ho avuto la fortuna di essere accompagnata, durante questo percorso, da due donne fantastihce, sagge, forti ma capaci di amare e di guidare l'altro con tanto affetto. Due donne di scienza che mi hanno guidato ed aiutato nelle decisioni difficili che mi sono trovata a fronteggiare durante questi anni, insegnandomi l'arte della ricerca, della comunicazione con gli altri, della condivisione, a non abbattersi mai davanti alle difficolta. Il mio enorme grazie va quindi a Marta e Susana per la loro instancabile pasienza e gioia nell'insegnare, la scienza quanto la vita. Vi ringrazio per aver creduto in me fino alla fine e per avermi spinto, alle volte anche con forza, a crescere quando io non sapevo come farlo. So che ho ancora tanto da imparare da entrambe e non vedo l'ora di ricominciare a farlo.

Grazie a Johan, per il suo contributo al nostro progetto, per I suoi consigli e per la contagiosa passione che mette nel suo lavoro.

Un grazie speciale va a Bartek, per tutte le cose che mi ha insegnato; come mio compagno di ufficio, per ben un anno, ti ringrazio per la tua prontezza nel capirmi, per la tua capacita di ascoltare, di consigliare, di riproverare e di ridere insieme a me. Vorrei ringraziare Raul, per il rapport che abbiamo costruito durante questi anni, per avermi insegnato che nel nostro lavoro sempre tutto e' da essere provato e che non ci si puo adagiare a supposizioni, ma anche per essere stato sempre presente e disponibile quando ho avuto la necessita, o anche solo la voglia, di un confront costruttivo. Grazie a Toni, Ricard e Angels che hanno accolto, non solo me, ma tutti noi, come si fa in una famiglia.

Quando ho iniziato questo percorso e sono partita, come un salto nel vuoto, avevo paura e pensavo di essere da sola; la soddisfazione piu grande e' stata quella di capire, durante il tepo, di quante amicizie mi stavo arricchendo. Mario, Mimmo, Gianmarco e Jie hanno costituito la mia famiglia durante questi tre anni, e sono sicura che continueranno a farlo anche in futuro. Ci

siamo presi cura l'uno dell'altro, sempre: quando non capivamo assolutamente nulla per la difficolta delle lingue nuove, quando non sapevamo come comportarci, quando abbiamo avuto paura, quando c'e' stata l'invasione degli scarafaggi, quando c'era poca luce, poco tempo, poca voglia, poco cibo, poco spazio, quando tutto stava cambiando, quando abbiamo fatto degli errori, quando siamo stati felici, tanto felici, insieme. Le domeiche a casa sommersi da gelati, le sessioni di ballo nel labpratorio rosso, le sessioni gossip, le serate al totem, le cene cinesi, le canzoni che mi avete insegnato, le partite a basket nel cestino della spazzatura, il bilardino mi mancano tanto di gia!

Grazie a tutti i compagni di laboratorio all'universita, Xavi, Ruben, Dailyn, Alberto, Lorena, Isaac, tutto il team del CTQC, Benedetta, Montse, Anya, Ada, Monika, e' stato molto bello crescere con voi dall'Erasmus fino al dottorato!

Non so come avrei fatto senza aver incontrato le mie ancore di salvezza, Lorenza, Chiara e Silvia; ognuna di loro, in tempi, modalita e luoghi diversi mi ha Saputo aprire la mente, far ridere da morire, consigliare come avrebbe fatto una sorella, si e' affidata a me quando ne aveva bisogno..non c'e' cosa piu bella in una amicizia.

La grande, enorme, mutevole famiglia di Brussels merita un garnde grazie! Non solo per gli n-esimi kili in piu, ma per tutta la compagnia che ci siamo fatti a vicenda, come uno strano accord silenzioso per cui nessuno doveva mai restare solo; e allora era una no-stop di pranzi insieme, cene insieme, riposini insieme (a casa nostra), risate (tante), musica..era sempre festa! Grazie Luca (promotore del casino), Gianmarco P, Livio, Fabiana, Ines, Peppe, Giusy, Alessandro, Licia!

Un grazie alle mie amiche di sempre Anna, Federica e Giulia, perche anche se siamo lontane, e siamo state per molto lontane, il bene che ci vogliao continua a sentirsi. Il raggiungimento di questo traguardo mi ricorda che posso fare meglio, che non si smette di fare errori come non si smette di imparare. Mi auguro che, anche se il conto Brasile non e' pronto per le nostre aspettative,

riusciremo a dedicare piu tempo a noi. Grazie per aver il supoorto che mi avete sempre dato, per tutti I miei picci che siete bravissime ad accogliere, per aver dimostrato tanta voglia di condividere, per essere pronte a lottare anche per le mie battaglie! Grazie a Simone, purtroppo per te tis to seguendoin giro per l'Europa perche ho capito come e' bello averti vicino!

Lo, io ti ho insegnato a fare lo struzzo ma tu mi hai dato il coraggio di fare scelte importanti e mi hai spinto nelle braccia dell'amore della mia vita..non credo sia comparabile ma ptovero a rimediare nel corso della vita! Ti voglio bene, tanto! Grazie a Francesco durante gli ultimi due anni ho dato meno di matto, ho amngiato piu sano, ho dato il giusto peso alle cose, ho preso (piu) scelte giuste, sono divenatata piu responsabile; non voglio immaginare come sarei stata senza di te a questo punto, ma sono cosi felice che ci sei, a migiorare la mia vita e a riempirmi il cuore. Grazie per la stim ache hai di me, per averci creduto, per la pasienza di ogni giorno. Non posso fare a meno di vedere questo traguardo raggiunto, come un passo in piu verso la mia vita futura insieme a te.

Grazie alla mia famiglia, e' bello avere una famiglia come la mia! Grazie a Marco per le critiche costanti e le costanti dimostrazioi di affetto, grazie a mia sorella perche alla fine quando piango a dirotto sei sempre tu a risolvere tutto. Grazie a papa per appoggiarmi sempre incondizionatamente nelle mie scelte. Ma chi ha avuto la forza di dirmi vai, di mantenere il sorriso sul volto anche quando dentro voleva piangere, di essere felice per me anche quando non era d'accordo, di incoraggiarmi anche se questo voleva dire allontanarsi, di dire proviamo anche se questo significava sacrificio, e' stata mia mamma. Mi guardo oggi e, consapevole dei miei mille limiti, so che tutto quello che sono e che ho raggiunto, lo sono e l'ho raggiunto grazie a te e d a quello che mi hai insegnato tu.

I miei due bellissimi nipoti sono nati durante questi tre anni! Non potevano ezsere anni migliori!

Table of Contents

Summary

In this work the attention will be mainly drawn on the design, the preparation and the characterization of light sensitive microcapsules, which are able to release the payload under white light irradiation. Although the main reason for encapsulation is the necessity to store and protect an active ingredient into a physically and chemically stable shell, in commercial applications can be important also to control the release over time and to drive it in a specific place and in a specific moment. This is the main reason why we want to develop an easy, cheap and robust chemistry to produce capsules responsive to external stimuli. Among other external stimuli light was selected to control the release of fragrances and optimize it overtime, boosting the release during day-life and deactivating it during night. For this purpose, the core-shell capsules morphology was found to be the most suitable, and the azobenzene, among other chromophores, was selected as photo-isomerizable unit and building block of the capsule's polymeric shell. Azobenzene derivatives in fact, were designed and synthesised to be incorporated in the capsule's shell as its main constituent. The design included the functionalization of un-modified azobenzene with proper side groups which allow the isomerization of the whole molecule to undergo with white light, and subsequent incorporation of the new light-sensitive unit into different systems as polymeric linear chains or crosslinked nets.

First, the synthesis and characterisation of the photosensitive azobenzene units will be discussed and analysed; their behaviour, as a consequence of exposure to white light, will be investigated. The synthesis and characterization of linear polymeric chains and crosslinked polymers, both containing the synthesized photosensitive azobenzenes, will be examined and debated in depth.

The preparation of microcapsules based on such photosensitive systems will also be explored in the following sections of this work; the microcapsules are filled with perfumes which have business interest and importance. In some cases, the applicability of such microcapsules in consumer good products is also explored and consumer tests are designed and conducted.

The study of the controlled and triggered release of the active has been carried out in aqueous environment and evaluated mainly *via* dynamic head space measurements (DHS). *Via* DHS it is possible to identify and measure what is released from capsules, in a controlled volume, over time and after exposure to different conditions as light or UV irradiation, temperature, aggressive components, pH variations, etc. In this work the aqueous solution was selected as the least aggressive environment for capsules and for the active encapsulated, if compared with real life finish products which always contain a certain amount of surfactants; surfactants in fact, due to their amphiphilic nature, may force the encapsulated active to leak out from the capsules and thus, what is measured with the DHS, would not only be the active released due to light irradiation but also the one released due to forced leakage.

Citing a few lines from a recent review on microencapsulation from Bansode et al. it is important to underline that microencapsulation is both an art and a science. There's no one single way to do it, and each new application provides a fresh challenge. Solving these riddles requires experience, skill and the mastery of many different technologies.[1]

Sommario

Questo lavoro di tesi è principalmente incentrato sul design, la preparazione e la caratterizzazione di microcapsule fotosensibili, capaci di rilasciare l'attivo incaspulato, grazie all'irradiazione di luce visibile.

Il concetto di incaspulazione, così come la tecnica ed il processo, nasce principalemnte dalla necessità di immagazzinare e proteggere un determinato materiale, solido o liquido, dall'ambiente esterno. La protezione viene più spesso ottenuta tramite un involucro polimerico, stabile chimicamente e fisicamente. In alcune applicazioni commerciali, la possibilità di rilasciare l'attivo incapsulato nel tempo ed in maniera controllata, sta suscitando un interesse sempre maggiore; in questo modo il materiale attivo potrebbe agire in un luogo specifico ed in un determinato istante. Per questo motivo è sempre più attuale la ricerca di chimiche robuste ed economiche per la produzione di capsule sensibili a stimoli esterni che possano attivarne il rilascio.

Tra i diversi stimuli esterni a cui è possible pensare, l'irradiazione con luce ricadente nello spettro del visibile è stata scelta, nell'ambito di questo lavoro di ricerca, come controllo estrno ed interruttore per l'attivazione del rilascio del materiale incapsulato. Le capsule che verranno sviluppate in questo contesto sono utilizzate per l'incapsulazione di fragranze e per ottimizzare il loro rilascio durante il tempo, accrescendolo durante il giorno e disattivandolo durante la notte, quando la luce non è più coinvolta. Per raggiungere questo scopo la morfologia core:shell è stata scelta come la piu adeguata, e l'azobenzene, tra altre molecule fotosensibili, è stato selezionato come composto di base per la sintesi delle specie fotoattive che verranno utilizzate in questo lavoro. Composti derivati dell'azobenzene infatti, sono stati attentamente sintetizzati per essere poi incorporati nei gusci polimerici delle capsule, come suoi principali costituenti. Molecule di azobenzene non moficato, capaci di assorbire l'irradiazione di luce UV, sono state funzionalizzate con gruppi elettron-attrattori ed elettron-donatori, tali per cui, l'assorbimento della molecola finale, risulta essere spostato nel range della luce visibile. Le nuove specie chimiche ottenute sono poi state incorporate in catene polimeriche lineari o polimeri reticolati ad alto grado di crosslinking.

Nella prima parte di questa tesi, la sintesi e la caratterizzazione delle molecole fotosensibili basate sull'azobenzene, verrà analizzata e discussa; il loro comportamento, come conseguenza dell'esposizione alla luce visibile, sarà investigato.

La sintesi e la caratterizzazione di polimeri lineari e reticolati, contenenti le molecule fotosensibili basate su azobenzene modificato, verrà approfondita.

La preparazione di microcapsule basate sui sistemi fotosensibili descritti in precendenza, e contenenti fragranze ad interesse commerciale fornite dalla P&G, sarà affrontata nel capitolo 3, per quanto riguarda i polimeri lineari, e nei capitoli 4 e 5, per quanto riguarda i sitemi reticolati. In alcuni casi le microcapsule ottenute saranno testate all'interno di prodotti comemrciali per lo studio della loro stabilità, e test olfattivi con consumatori saranno condotti per lo studio delle performance.

Lo studio del rilascio innescato dalla luce visibile verrà condotto in ambiente acquoso e principalemnte quantificato *via* dynamic head space (DHS) attraverso il quale è possible misurare il rilascio delle fragranze in un volume controllato, nel tempo e sotto diverse condizioni di luce/buio.

Citando alcune frasi da una recente review sulle tecniche di microincapsualzione di Bansode et al., è importante sottolineare che la microincapsualzione è da considerarsi tanto una scienza come un' arte; non c'e un solo modo per farla e portarla a termine e, ogni nuova applicazione consiste in una nuova sfida. Risolvere questi enigmi richiede esperienza, skills e la conoscenza di differenti tecniche.[1]

Resumen

En aquest treball l'atenció es dibuixarà principalment en el disseny, la preparació i la caracterització de les microcàpsules sensibles a la llum, que són capaces d'alliberar la càrrega útil sota irradiació de llum blanca. Encara que la raó principal per a l'encapsulació és la necessitat d'emmagatzemar i protegir un ingredient actiu en una closca físicament i químicament estable, en aplicacions comercials pot ser important també per controlar l'alliberament al llarg del temps i per conduir-lo en un lloc específic i en una determinada moment. Aquesta és la raó principal per la qual volem desenvolupar una química fàcil, barata i robusta per produir càpsules sensibles altimuli extern. Entre altres estímuls externs s'ha seleccionat llum per controlar l'alliberament de fragàncies i optimitzar-lo en hores extraordinàries, potenciant l'alliberament durant la vida quotidiana i desactivant-lo durant la nit. Per a aquest propòsit, es va trobar que la morfologia de les càpsules Core-Shell era la més adequada, i l'azobenzene, entre altres cromòfors, va ser seleccionada com a unitat de foto-isomerizable i bloc de construcció de la closca polimèrica de la càpsula. Els derivats azobenzene, de fet, van ser dissenyats i sintetitzats per a ser incorporats en la closca de la càpsula com a principal component. El disseny incloïa la funcionalització de l'azobenzene no modificada amb els grups laterals adequats que permeten l'isomerització de tota la molècula per sotmetre's a la llum blanca, i la posterior incorporació de la nova unitat sensible a la llum en diferents sistemes com cadenes lineals polimèriques o polímers reticulats.

En primer lloc, es debatrà i s'analitzarà la síntesi i caracterització de la unitat d'azobenzene fotosensible. La seva conducta, com a conseqüència de l'exposició a la llum blanca, serà investigada. La síntesi i la caracterització de les cadenes de polimèriques lineals i els polímers reticulats, tots dos que contenen els azobenzene sintetitzats fotosensibless, seran examinats i debatuts en profunditat.

La preparació de microcàpsules basades en aquests sistemes fotosensibles també s'exploraran en els següents apartats d'aquesta obra; les microcàpsules s' omplen de perfums que tenen interès comercial i importància. En alguns

casos, també s'explora l'aplicabilitat d'aquestes microcàpsules en els productes bons de consum i les proves de consum estan dissenyades i dirigides.

L'estudi de l'alliberament controlat i desencadenat de l'actiu s'ha dut a terme en medi aquós i es valora principalment a *través* de mesuraments de dynamic head space (DHS). *Via* DHS és possible identificar i mesurar el que s'allibera de les càpsules, en un volum controlat, amb el temps i després de l'exposició a diferents condicions com a llum o irradiació UV, temperatura, components agressius, variacions de pH, etc. En aquest treball la solució aquosa va ser seleccionada com el medi ambient menys agressiu per a les càpsules i per al encapsulat actiu, si es compara amb productes d'acabat de la vida real que sempre contenen una certa quantitat de tensioactius; tensioactius de fet, a causa de la seva naturalesa amfílica, pot forçar l'encapsulat actiu per fuites de les càpsules i per tant, el que es mesura amb el DHS, no només seria el llançament actiu a causa de la irradiació lleugera, sinó també la alliberada a causa de fuites forçoses.

Citant unes quantes línies d'una ressenya recent en Microencapsulació des de Bansode *et al*. és important subratllar que la microencapsulació és un art i una ciència. No hi ha una única manera de fer-ho, i cada nova aplicació proporciona un desafiament nov. Resoldre aquests enigmes requereix experiència, habilitat i domini de moltes tecnologies diferents. [1]

1. Introduction

This thesis work will focus on the description, the preparation and the characterization of stimuli responsive microcapsules. In the first chapter an overview on the morphologies of capsules and the main encapsulation techniques will be proposed. We will discuss the principal mechanisms of capsules payload release and possibility of triggers; special attention will be payed to light triggered capsules and the main families of chromophores which can induce such behaviour. Microcapsules are small spherical particles with a diameter size ranged between 1 μm and 1000 μm[2], which are able to entrap an active ingredient. The totality of the ingredients entrapped is more often called core, while the material used for the encapsulation is the shell. The objectives of the thesis work will be outlined in the final section of this chapter as stepping stones for the organization of this work.

1.1 Microcapsules

Spherical particles with small geometries can be considered microcapsules when sized between 1 and 1000 μm[3]. Microcapsules are tiny particles which can incorporate reasonably high concentrations of an active agent or core material, surrounding it with an external coating or shell. Commercial microcapsules typically have diameter between 3 and 800 μm and contain from 10 to 90 wt% core material.[2]

The main elements of a microcapsules are thus, the core material and the coating material.[4,5]

The core materials of microcapsules can be drugs, cells, fragrant oils, dyes, etc...[6] They can be solids, liquids or even gases, dispersed, dissolved or separated from the coating. The possibility to diversify the entrapped material, according to the design of the capsule system, makes the encapsulation a flexible and versatile technique suitable for many different fields and applications. The coating material needs to be carefully selected depending on (i) the final desired properties of the capsule, (ii) the active that needs to be

encapsulated and (iii) the final application we want to use the capsule for;[7] the coating material is in fact, responsible for the mechanical and optical properties of the entire final system, as well as for its stability and permeability. It can be a natural polymer as proteins or carbohydrates (starch, agarose, chitosan, etc.) or a synthetic polymer, and should be capable of forming a film that is cohesive, inert and chemically compatible with the core material. According to the final application and to the reason for the encapsulation, there can be other elements to be considered as part of the encapsulation system; this components are additives for the system as organic and inorganic solvents, colorants, plasticizers and surfactants, these last two need to be especially considered in the case of spray drying, liquid bed coating, interfacial polymerization or emulsification.[8]

Microcapsules can be classified based on their morphology, as showed in Figure1.1. According to their structure and internal geometry, in fact, it is possible to distinguish between:

1. C*ore-shell microcapsules* where a single active nucleus (solid or liquid) is surrounded by one or more continuous polymeric shells or membranes; it can be a mono or multi wall. This system is considered mono-cored with a single hollow chamber within the capsule.
2. M*icrocapsules with an active dispersed in the matrix* where the polymeric matrix is homogeneous with the multiple cores or actives (solid or liquid) dispersed into it; this system is considered as poly-cored with a variable number of internal chambers for the actives, of different shapes and sizes.
3. *Microcapsules with active dissolved in the matrix* where the polymeric matrix is homogeneous with the active (solid or liquid) dissolved into it. The active ingredient is integrated within the matrix.[9]

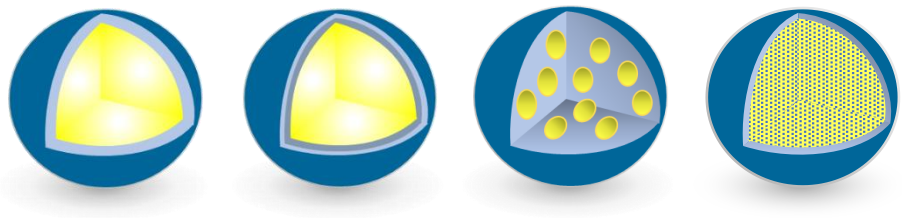

Figure 1.1 Microcapsule's morphology: core shell mono-wall, core shell multi-wall, poly-cored (active dispersed in the matrix), poly-cored (active dissolved in the matrix).

The process of encapsulation may provide many benefits and it can be utilized for different purposes and objectives. Considering that the uniqueness of microencapsulation is the smallness of the coated particles, it mainly represents an effective way to convert liquids into small solids and to provide the active material encapsulated with environmental protection (from oxygen, solvents, liquids, pH, temperature, surfactants, etc..); in some cases, it is important indeed, to avoid incompatibility between components or with the external environment, to mask the effect of volatility or to enhance the poor stability of some systems. Encapsulation should provide the desired coating properties such as strength, flexibility, impermeability, optical properties and stability and can be used to alter colloidal and surface properties of a system or to control the characteristics of release. In fact, with a proper selection and design of the wall material, it may be possible to tune the release of the active over time, allowing a sustained or prolonged release and even to drive the active delivery in a specific place and at a specific time.

Capsules should thus be stable in different mediums, protect the active and release it with a good control over a wide time scale. The specific function of the capsules and their future applications, depend strictly on the mechanical properties and the permeability of the shell, which are influenced by the capsule size, shell thickness and composition.[10] That is why, besides microcapsules morphology and structure of both membrane and interior, it is important to measure their porosity, tortuosity and crystallinity, as well as to characterize their permeability and leakage from release data.

1.2 Encapsulation techniques

Based on what discussed in the previous section, encapsulation can be defined as the process of incorporating an active material, into a small size particle unit. The word encapsulation relates thus, to technologies which enable to formulate one active compound inside individualized particles with specific geometries and properties.[3]

Encapsulation leads to the formation of a thin coating layer which enclose, acting as a wall, the core material. The encapsulation technology has been first developed in late 1930s, by Green and Schleicher from the National Cash Register Company, for the preparation of pressure-sensitive coatings for the manufacture of leuco-dyes based, carbonless copying paper, as an alternative to carbon paper and carbon ribbons used for cleaning.[5,11,12]

The methods for the obtainment of microcapsules are numerous and they can be classified according to different criteria. Regardless of the method, the core and/or the wall materials are, in most of the cases, dissolved in adequate solvents and then the process is divided in two steps:

1. droplet formation
2. droplet stabilization

The formation of the droplet is always obtained *via* dispersion of a liquid in air or in another liquid; the stabilization can be due to chemical reactions (polymerization, crosslinking, coacervation, etc..), solvent evaporation, solvent removal and polymer precipitation, etc. and mainly consists in the formation of the solid external layer of a capsule.

An exception can be the coating of a solid core; in this case only the wall material is dissolved into the solvent and then sprayed onto the solid active.

In this introduction the encapsulation techniques will be classified according to the nature of the material used for the obtainment of the capsule's shell/wall and thus, according to the process of stabilization. In some methods in fact, the starting material is a polymer and no chemical reaction is involved in the shell formation, but in other cases monomers or prepolymers are applied as starting material and chemical reactions occur during the capsules preparation.

It is easy to understand that the choice for a specific method is strictly related to the core-shell system, the composition and the final application of the capsule.

1.2.1 Interfacial and in-situ polymerization

Interfacial and in-situ polymerization are considered the most common chemical techniques of microencapsulation[13]. These are encapsulation techniques which require the development of a chemical reaction during the capsule formation and thus, they are called chemical methods; polymerization can be carried out in bulk, suspension or emulsion[14] and in each case a mixture of monomers and initiators is prepared, in order to start the polymerization. There are cases in which the polymerization needs to be initiated with an increase of the temperature and others where it is performed at room temperature.[4]

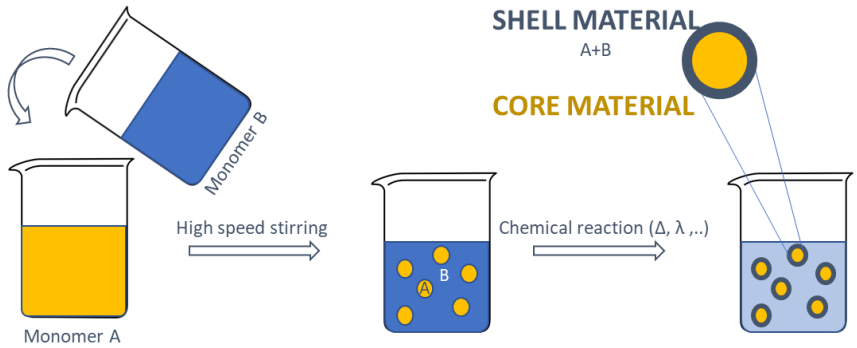

Figure 1.2 Schematic representation of encapsulation via Interfacial polymerization method.

As represented in Figure 1.2, in the interfacial polymerization, the reaction starts between complementary multifunctional monomers at the interface between two immiscible phases. A multifunctional monomer is dissolved in the core material, and this solution is dispersed in a second immiscible phase where a reactant to the first monomer is added and dissolved. Depending on the type of emulsion (oil-in-water or water-in-oil), it can be used for encapsulation of various core materials, including hydrophobic and hydrophilic drugs, as well as their solutions in water or in water-immiscible liquids. If the resulting polymer is soluble in the emulsion droplets, this process leads to the formation of microspheres. Otherwise, the polymer forms a shell around droplets which results in the microcapsule formation.[15] In this case the

polymerization quickly ensues at the surfaces of the core droplets forming, under the right conditions, thin flexible capsules walls. Interfacial polymerization can be used to prepare capsules with different diameter size ranges, but in most of the cases, commercial interfacial polymerization processes produce capsules in the 20-30 µm diameter range, or even smaller (3-6 µm). Interfacial polymerization has been largely applied in the last years for encapsulation of different actives; Lu et al. reported in 2018 a study for the formation of stable cross-linked shell microencapsulated phase change materials prepared by interfacial polymerization using butyl stearate and polyurethane as core and shell material respectively.[16] The same technique has been used by Zhang et al., coupled with microfluidics, to obtain a polyamine microcapsules for self-healing applications.[17]

Conversely, with the in-situ polymerization all the reactants are included in one single phase of the emulsion, organic or inorganic; the whole polymerization occurs in the phase which contains the monomers, rather than on both sides of the interface between the continuous phase and the core material, as it happens in the interfacial polymerization. The monomers first form a low molecular weight prepolymer and, as the prepolymer grows, it deposits on the interface/surface of dispersed phase, resulting in formation of microcapsules[18]. Examples of this method include urea-formaldehyde (UF) and melamine formaldehyde (MF) encapsulation systems.

The two techniques, *in situ* and interfacial polymerization microencapsulation, have many common aspects. In both cases, for example, the two-phase system is mixed under controlled conditions to form small droplets of one phase (dispersed phase) in the other one (continuous phase). The stability of the emulsion is strongly affected by the miscibility and by the interfacial tensions of the two phases; in case the emulsion is not stable, other methods can be considered, as the Pickering emulsion or the addition of higher amount of emulsifier agent. Then, under the right conditions, thin flexible walls form rapidly at the interface[1] due to polymerization. Condensations, reactions between amines, aldehydes as well as chlorides are examples of polymerization reactions. The addition of emulsifiers and stabilizers may be necessary to avoid coalescence during particles formation. Both processes moreover, are usually fast, and they lead to high molecular weight systems, but they can also lead to

the presence of unreacted monomer dispersed in the core or in the continuous phase. In some cases the polymerization results in highly crosslinked systems where the droplets are quickly hardened and converted into the corresponding microcapsule[19,20]. Finally, encapsulation *via* polymerization can lead to core-shell or matrix type capsules depending on the solubility of the polymer in the two phases.[21,22,23]

1.2.2 Phase inversion precipitation

Techniques which do not involve a chemical reaction, consider as starting materials polymers or oligomers which, indeed, needs to be solubilized or melted before the usage. These techniques include the phase inversion *via* solvent evaporation or solvent extraction, coacervation and phase separation, spray drying, etc.[4]

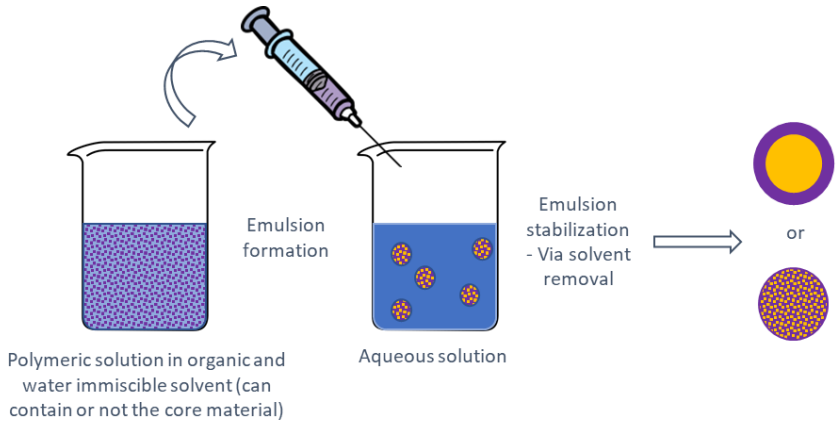

Figure 1.3 Schematic representation of encapsulation via phase inversion precipitation method.

In the solvent evaporation[24] or solvent extraction techniques, the polymer and the active are dissolved in a solvent which is immiscible or poorly miscible with the continuous phase. The polymeric solution is added to the continuous phase, which contains the immiscible non-solvent and a suitable stabilizer, to allow droplets and capsules formation *via* solvent removal and thus polymer precipitation. Many different strategies can be selected to bring the polymeric solution in contact with the coagulation bath of non-solvent; spray guns, high rpms stirring, micrometric nozzles or tubes are some examples. Once the polymeric solution gets in contact with the non-solvent, the polymer precipitates to form small capsules containing the active according to the interfacial tensions

between the phases involved; the removal of the solvent, and thus the precipitation of the polymer, can be obtained *via* evaporation, reduced pressure, extraction or dilution in the non-solvent bath[25,26]. Depending on the core-shell system and the rate at which the solvent abandons the polymeric system, it is possible to obtain both matrix and core shell capsules with different levels of shell porosity. This technique is applicable to a wide variety of core materials and of film forming polymers to be used as coatings[1]; moreover, it is a very flexible technology for the control of the particle size distribution (PSD) and the stabilization of the emulsion. The particles obtained *via* emulsion and solvent removal can either be dried, leading to a powder, or can be used as slurry. The influence of pressure, nature of the solvent and temperature on the morphology, surface and size of the capsules obtained, has been deeply studied in a recent review by Li et al.[27]. The porosity of these systems is difficult to control, and it is usually higher for capsules obtained *via* solvent extraction than in solvent evaporation due to the speed of solvent removal. The encapsulation efficiency is poor, and residue of solvent can be found after capsules formation.

1.2.3 Coacervation and phase separation

The technique of coacervation and phase separation is one of the first techniques used for the preparation of capsules in the industrial field, it does not involve chemical reactions and is nowadays widely used, especially for cellulose derivatives systems[28], in pharmaceutical, food, agriculture and textile industries. It is based on the properties of colloids to separate into colloid-rich and colloid-poor regions just before coagulation, resulting in a coating for the core material. A homogeneous polymeric solution can separate into two phases, one dense and rich in polymer, which is called coacervate, and the other liquid with low polymer content. Depending on the number of polymers involved, coacervation can be simple or complex.[3] Simple coacervation is based on the use of only one polymer and the phase separation can be triggered, when the core material is dispersed in the polymeric solution, by addition of inorganic salts, non-solvents or temperature change in the dispersed phase; the shell material (coacervate) starts to precipitate forming a continuous coating around the core droplets which is subsequently dried. This procedure is schematically represented in Figure 1.4.

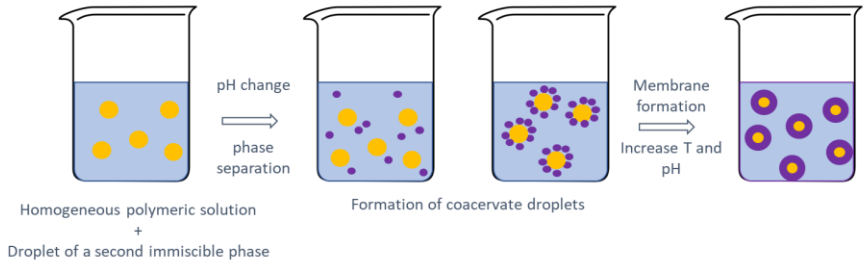

Figure 1.4 Schematic representation of microencapsulation via simple coacervation method.

On the other hand, complex coacervation involves oppositely charged polymers and their ability to interact in water and form polymer-rich phase. This second approach rely thus, on the attraction and subsequent neutralization of two oppositely charged polymers dissolved in two immiscible solvents (complex coacervation); when they got attracted, based on electrostatic interactions, they start to precipitate at the interface forming the shell. The particle size strongly depends on the dispersion parameters as stirring speed, stirrer shape, surface tension and viscosity.[29] Stabilizer are needed to avoid agglomeration which makes the scale-up hard for capsules obtained with this technique.

1.2.4 Spray drying and spray congealing

The spray drying and the spray congealing techniques are based on the drying of a polymeric atomized solution containing the active, in air. Both techniques serve as for microencapsulation when an active material is dissolved or suspended in a melt or polymer solution and becomes trapped in the dried particle. In the spray drying the fluid to be dried is atomized into fine droplets, which are thrown radially into a moving stream of hot gas; the solvents evaporate due to the high temperature reached into the spray drier chamber, leading to spherical particles. This technique has advantages as well as some disadvantages: the process is continuous and allows uniform size particles, moreover atomization and particles formation can happen in one single step allowing easy manipulation of labile materials; on the other hand, the equipment required is bulky and expensive and due to the high temperatures reached in the chamber it is not possible to work with high volatility solvents or high volatility core materials. The spray congealing instead, is considered as an alternative to spray drying for the encapsulation of a solid core; a molten coating

material is congealed or solidified due to contact with low temperature air. These processes lead to relatively rapid solidification of the coating and to the formation of 1-100 μm microcapsule; traces of solvent in both cases are removed by vacuum drying. Both techniques, resulting in continuous one-step and close-system processes, are widely used in food, chemical, pharmaceutical, and biochemical industries for various applications leading to the formation of either microspheres or polynuclear microparticles.[3,30]

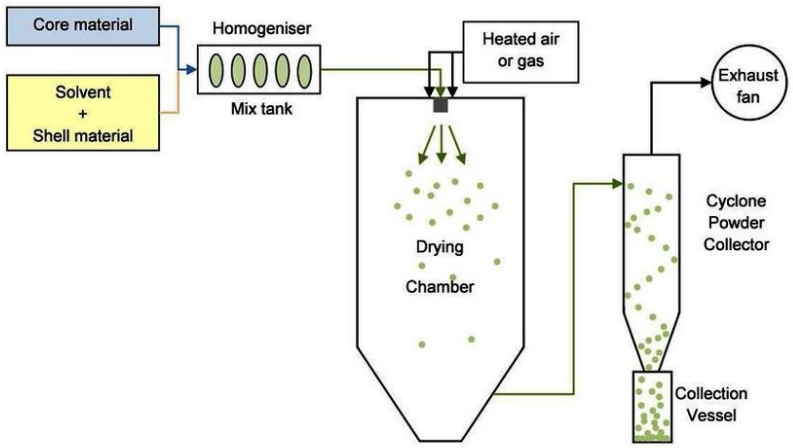

Figure 1.5 Schematic representation of encapsulation via spray drying (polymeric solution + hot air) or spray congealing (hot melt + cold air) methods.

1.2.5 Fluidized bed coating

The fluidized bed coating is another technique, mostly used for the protection of solid core materials. It is possible to refer to this technique also as an air-suspension coating of particles by solutions or melts. It involves suspension of the active material in high-velocity air stream, followed by the spraying with polymer solution; it gives good control and flexibility, especially in terms of variety of coating materials suitable. The particles are coated while suspended in an upward-moving air stream with coatings in the form of solvent solutions, aqueous solution, emulsions, dispersions or hot melts. The coating medium can be introduced in fluid bed chamber from the top, bottom, and tangentially. Solidification and subsequent microparticles formation, is simply achieved by solvent evaporation or cooling. This technique is highly scalable, easy and rapid

and most solid core materials can be effectively encapsulated, but agglomeration of the particles to some larger size may occur and can be difficult to avoid.[3] Also, the core must be around 50 µm big and the initial cost of the equipment is usually high.

1.2.6 Co-extrusion

The co-extrusion, which is widely applied in pharmaceutics and beauty care, is based on a dual fluid stream of liquid core and shell material that is pumped through a concentric tube and forced to form droplets under the influence of a certain vibration. This approach can be considered as a hybrid between the two categories of encapsulation techniques because the shell can be then hardened *via* solvent evaporation, crosslinking or cooling. Layer by layer deposition can be obtained immersing the capsules subsequently into substrates with opposite charges.

1.2.7 Expansion of supercritical fluids and Spinning disk

Another interesting and poorly investigated methodology is the obtainment of capsules *via* expansion of supercritical fluids as well as the spinning disc method. The first method is based on changes in solubility of the core material and the shell material into a supercritical fluid; at supercritical conditions of high pressure, the supercritical fluid is acting as a solvent for both the core and the shell material but as soon as the pressure decreases the system got saturated and the shell material precipitates at the interface, surrounding the core material. In the spinning disk method, rotational forces of a rotating disk are uses to create small droplets; the suspension of core material into shell material is dropped onto a rotating disk which throws the droplets out towards the circumference of the disk where the wall material solidifies through drying or chilling. The spinning rate can be carefully controlled and thus also the particle size distributions. Both processes, which are mainly used in the pharmaceutical industry, are based on simple operations and allow easy control with high production rates. In the table below the main encapsulation techniques, which have been also introduced in this paragraph, are listed together with the ranges of reachable loadings and size distributions (PSDs).

Table 1.1 Encapsulation techniques, PSD, payloads % and main fields of application. 2,31

	PSD [µm]	Loading [wt%]	Core material	Application
Interfacial polymerization	20-30	60-95	Liquid, solid	Crop protection, Catalysis, Drug delivery, Textile
In-situ polymerization	3-30	60-95	Liquid, solid	Crop protection, Catalysis, Drug delivery, Textile
Spray drying	1-100	50-60	Liquid, solid	Food technology
Coacervation	20-800	80-95	Liquid, solid	Drug delivery
Fluidized bed coating	50 - >1000	60-95	Solid	Biomedical, Pharmaceutical, Food technology
Solvent evaporation	1 - >1000	40-90	Liquid, solid	Drug delivery
Co-extrusion	3 - >1000	10-60	Liquid	Biomedical
Spinning disk	10-1000	50-60	Liquid, solid	Food technology, Pharmaceutical

1.3 Triggered devices

As already stated in the previous paragraphs, the final application of the capsules determines the desired morphology, the technique to be used for capsules fabrication and the nature of the core-shell system we will use.

It is possible to assert that the general aim of a microencapsulation application is the isolation of the core from its surroundings, for different reasons. The capsule is working as a carrier and its wall must thus be ruptured in the place and at the time of the final use. In many applications capsules' walls are ruptured by external pressure or mechanical stress, as in the case of copying paper, self-healing composites etc.; others can melt or dissolve under certain conditions, others can run into chemical or physical breakage *via* enzyme, pH or solvent actions. Other mechanisms that may take place in the release of the encapsulated material include biodegradation, erosion, osmotic pressure, diffusion, etc.[32]

Each mechanism depends on the composition of the capsule and also on its surroundings.[33,34] Microencapsulation can, though, also be used to control the

release over time, increasing or decreasing the release rate under different conditions, following a certain release pattern depending on the application.

It is possible to design a microcapsule with a desired release rate and obtain it by chemical or physical modification of the capsule itself. In the case of chemical alteration, the polymeric wall material can be completely modified, or an additive can be used. This allows the release of the active agent to occur in response to physical or chemical changes of the additive, stimulated by variations in the external environment. Physical modification more often involves the control of the shell porosity with strategies that increase or decrease the release rate if compared with unmodified systems. The purpose of developing an effective delivery system is thus, the controlled release over time; during the last decade, several triggers and their applicability have been investigated. Stimuli-responsive capsules can improve the delivery of fragrances, food preservation or drug effectiveness. The release can have a zero-order kinetic when the rate is constant and the microcapsules deliver a fixed amount of active per minute, or a first-order kinetic, in which the rate decreases exponentially with time until the active is completely exhausted[4]. Usually, for matrix capsules the mechanism of release is slow and associated to the degradation of the matrix itself, which gradually release the active; core-shell capsules release the encapsulated material mainly through membrane diffusion instead. In this last-mentioned scenario, it is possible to insert the concept of triggered release.

1.3.1 Physical release mechanisms

Osmosis, diffusion, external mechanical breakage, internal pressure, melting, etc. are examples of physical mechanisms. Diffusion, for example, occurs when a dissolution fluid (solvent) penetrates the shell, dissolves the core and makes it leak out through the interstitial channel pores of the wall; considering another approach, it can be also added directly to the organic phase before the microcapsule formation and it slowly leaks out changing the porosity of the microcapsule. With osmosis mechanism, the polymeric shell acts as semi-permeable membrane and allows the creation of an osmotic pressure difference between the inside and the outside of the microcapsule driving drug solution out of the microcapsule. As an example of melting-driven release,

polyurethane (PU) microcapsules chemically modified with side chain crystalline branches, were prepared by Yoon et al. to stimulate a faster release of the active due to temperature increase; this strategy of controlled release is mainly based on the different melting temperatures between PU and the added new polymer.[13]

1.3.2 Chemical release mechanism

Chemical release mechanism refers to a chemical reaction occurring between the shell and the external environment due to an external stimulus called thus trigger; the reactions lead to switching, disintegration, cleavage of crosslinking or depolymerization of the shell. It is worth to spend few words on the procedure of core release associated to each mentioned mechanism and the different stimuli which may trigger such reaction.

In the crosslink removal and in the depolymerization mechanism, it is possible to trigger the release *via* shell disintegration which is boosted by cleavage of bounds or removal of a polymeric chain group or monomer; both are irreversible. One example of chemically controlled release is reported by Shirley et al. with the incorporation of disulfide linkages into polymeric microcapsules prepared *via* in-situ polymerization; the release can be modified according to the amount of crosslinker and in alkaline conditions it increases rapidly due to bound cleavage.[35]

Of particular interest for this work are the mechanisms of switching and porosity change. The switching is mainly based on the possibility to reversibly control the porosity of a system and, in this case, of the shell wall. The porosity thus, can be controlled by bounds formation/cleavage or by conformational changes in the shell structure. This last is the case of many chemical species that can switch and move when light, electricity or sometimes temperature are applied, affecting the permeability of the system. Azobenzene derivatives, which will be treated and studied in this work, belong to this family; they can undergo a limited but still very high number of cycles of isomerization which results in cycles of opening and closing of the pores/gates for the passage of the active. The overall structure of the shell is always maintained, but little portions of it are able to move and change the porosity. They can thus work as controllable permeability devices.

In the case of triggered release capsules thus, it is not only matter of capsules preparation with the most suitable encapsulation technique for the specific system, but also great attention should be paid to triggering groups preparation, chemical design and external stimuli selection.

The release mechanisms can be activated *via* different external stimuli; light-activated mechanisms are relevant for targeted release in biological systems or for cosmetics and agricultural industries due to solar irradiation. Chemical and biological changes are widely used to trigger the release of perfumes in deodorants with changes in the pH of the system or in drug therapies to deliver the pharm in the right place when specific biological tissues or components get in contact with the capsule. Thermal trigger is useful in perfume release applications, cosmetics and in agriculture, to reach enhanced release of nutrients when the temperature is too high.[36]

In the next section, systems based on the light induced release will be discussed. Light can be used as the trigger for both physical and chemical release.

1.4 Light triggered microcapsules

Light triggered microcapsules which are based on photo-sensitive moieties, particles or fillers, open new horizons spanning both industry and academic research due to their numerous benefits over other external stimuli; light irradiation is durable and easy to control, the molecular response to light do not contaminate the reaction environment and can be tuned at different wavelengths through appropriate molecular design. Moreover, it is possible to reach a remote control triggered by external light without the need for direct contact or interaction. In some cases, as for environmental applications, drug release in medical delivery systems or in surface science applications, light can be considered as the only accessible stimulus to drive the systems and the development of photo-triggered capsules can be highly appreciated.[37] Nanoparticles and chromophores absorb light over a wide range of wavelengths and their absorption cross sections can be tuned both for one- and multi-photon absorption. For applications in cosmetics and agriculture, UV- and

visible light-sensitive capsules are used because of the abundance of near UV light, while near-IR-absorbing capsules are of greater interest in biological systems because of decreased light scattering in tissues at those wavelengths.[38]

1.4.1 Carbon nanotubes for light activation

Thanks to the promising property of carbon nanotubes to absorb infrared (IR) radiation, between 700 and 1100 nm, photosensitive microcapsules containing this material have been deeply studied. Pastine et al. developed, in 2009, microcapsules containing carbon nanotubes which can rapidly heat up the liquid content of the capsule when irradiated. For the obtainment of the sensitive capsules, the active material to be encapsulated was mixed with a small amount of carbon nanotubes and a commercial polymer. All reagents were continuously stirred, leading to the precipitation of the polymer and the formation of spheres that captured the nanotubes and the active material. When the laser was directed towards the capsule, the carbon nanotubes absorbed the light, promoting molecular oscillation and thus the heating of the surrounding environment. The heated internal liquid expanded leading to a huge influence on the capsule's diameter up to capsules explosion and release of the contents.[39] The same approach was also used to obtain photosensitive capsules with different wall materials comprising polyamides, urea-formaldehyde or organic materials for pharmaceutical applications; all these systems are activated *via* laser irradiation.[40,41]

1.4.2 Silver and gold nanoparticles for light activation

A similar result of triggered release can be obtained *via* incorporation into microcapsules, of silver and gold nanoparticles which can absorb light in the visible spectrum and then release their energy as heat in the surroundings. The release of heat can be harvested to release encapsulated substances from microcapsules either destructively or non-destructively. Caruso et al. developed polyelectrolyte capsules containing gold nanoparticles into the shell; they proposed that laser induced release involves a first heating of the capsule shell to high temperatures, thanks to nanoparticles light absorption, followed by the development of thermal stresses within the capsule shell because of the variations in thermal expansion coefficients of shell wall materials; this causes

changes in the permeability of the shell and, in some cases, capsule rupture.[42] Recently, Woong-Chan Jeong and co-workers[43] obtained ethyl cellulose photo- and thermo responsive microcapsules *via* water/oil/water double emulsion ; the ethyl cellulose capsule membrane was designed to contain interconnected pores that could be filled by a thermo-responsive hydrogel. To provide photo-responsiveness, gold nanorods were embedded in the hydrogel matrix to act as nano-heaters under near-IR irradiation. The microcapsules were shown to exhibit photo-triggered release of a model drug with high molecular weight, with the release event successfully occurring repeatedly over extended periods by a series of near-IR exposures. Capsules obtained with a biocompatible polymer as ethyl cellulose and containing gold nanoparticles, upon laser irradiation, could be useful in a wide range of medical therapies.

1.4.3 Titanium dioxide for light activation

In the field of photo-sensitive materials and composites also titanium dioxide particles are widely used due to their catalytic activity and oxidative potential, their low production costs and a strong absorbance in the UV region, which make them a smart choice of compound to sensitize thin films to UV light[44]. TiO_2 nanoparticles have been used in the last years in many applications as filler in transparent, flame-retardant thermally-insulating polymer composite films; to confer UV-blocking properties to such materials make them the best candidates to be used in fields as construction, transportation, electronics, aerospace and medicine[45]. Katagiri and co-workers recently showed that the UV irradiation of polyelectrolyte capsules coated with SiO_2/TiO_2 resulted in capsule obliteration due to the UV absorption of TiO_2..[46] Prior to UV irradiation, the particles have a spherical structure for both SiO_2-polymer and SiO_2/TiO_2-polymer capsules. After UV irradiation, the SiO_2-polymer capsules remain spherical and intact, whereas the SiO_2/TiO_2-polymer capsules completely decomposed. In addition to their triggering capabilities, these capsules have improved mechanical integrity resulting from the metal oxide coating when compared to other polyelectrolyte capsules. In the work from Wang et al. TiO_2 nanospheres were employed as typical photo-initiators, for the synthesis of various inorganic/polymer nanocomposites *via* photocatalytic surface-initiated polymerization. The excitation of TiO_2, deposited on the surface, by UV-light irradiation, produces electrons and holes which drive the free radical

polymerization at the surface, producing core/shell composite nanospheres. This approach opens new opportunities in the design and synthesis of inorganic and polymeric composite nanomaterials for a variety of applications.[47]

1.4.4 Photosensitive chromophores for light activation

The most interesting category of photosensitive capsules, especially in this thesis work context, is constituted by systems which contain a photosensitive chromophore into the shell. A chromophore is a molecule, or part of a molecule, that causes a conformational change of the molecule itself when hit by light; the photochromism indeed, is defined as the property to undergo a light-induced reversible change (of colour) based on a chemical reaction.[48]

It is worth to describe in detail the basic principles that characterize the phenomena of photochromism. The most common and simple model is the one that associate the photochromism to a two-way reaction between two molecular species A and B.[49] A and B are separated by a potential barrier, namely ΔE. If ΔE is low, B is metastable and can revert back spontaneously to A, for example due to the absence of light but, when the barrier is high, only the absorption of new photons can cause the back reaction and B is defined as a bi-stable system. Usually, photochromic systems are metastable; A absorbs in the UV or near-UV, with a characteristic absorption band at wavelength λ_A. The absorption coefficient of A at this wavelength is ε_A. When a photon at λ_A is absorbed, A is excited from the ground to the excited state B with a probability of $\phi_{A\rightarrow B}$ known as the quantum yield. B reverts back to A, with an analogous pattern when it is excited at λB, as shown in Figure 1.6.

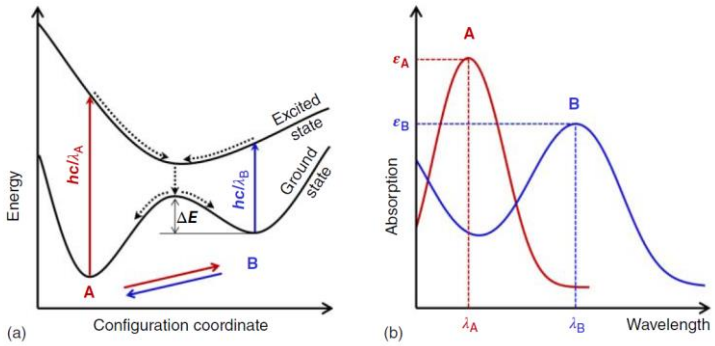

Figure 1.6 Photochromism: a two-way light-induced reaction between two molecules A and B. a) Potential energy diagram and b) the related schematic absorption spectra.

The historical reference of photochromism dates to ancient times (356–323 bC) when Macedonian head warriors were equipped with photochromic bracelets (the compound remains unknown up to now) exhibiting a colour change when exposed to sunlight. Such colour change was used by all warriors to indicate the right moment to begin the fight.

Over 2000 years later in 1867, Fritzsche reported for the first time the following peculiar behavior of tetracene solution: the initial orange colour of the solution fades when the sample is irradiated by sunlight but can be recovered completely when placed in a dark room. This is related to the conformational change observed for this molecule and reported in Figure 1.7.

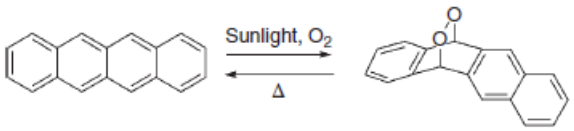

Figure 1.7 Photochromic reaction of tetracene.

Only in 1899 Markwald discovered the first solid-state photochromic organic compound and, after that, other families as fulgides, salicylideneanilines, stilbenes and nitrobenzylpyridines were discovered and studied. In the 1950s - 1960s a significant period for photochromic compounds started thanks to the advent of technologies and methods enabling their investigations, as for example, spectroscopy.[49] Many new molecules, both organic and inorganic, were then synthesized and further studies on the mechanism were conducted during this period. Reversible structural changes can thus, be induced through exposure to light in some photoactive groups. The response to external irradiation is different according to the type of chemical reaction involved during the photochromic process. The main mechanisms, as showed also in Figure 1.8, are I) an intramolecular proton transfer which allow the transformation of the molecule from one specie to another, called also excited state, II) homolytic cleavage of the C–X bond with formation of two radicals and III) cyclization reaction the reaction involves six π electrons delocalized over six different atoms, which produces a large change in electronic distribution. This is the case for spiropyran and diarylethenes. The last class of chemical reaction is IV) E–Z photoisomerization, the isomerization around a double bond which lead to

trans–cis (or *E–Z*) isomerism. Azobenzene derivatives represent the main family of photochromic molecules based on *trans–cis* reaction.

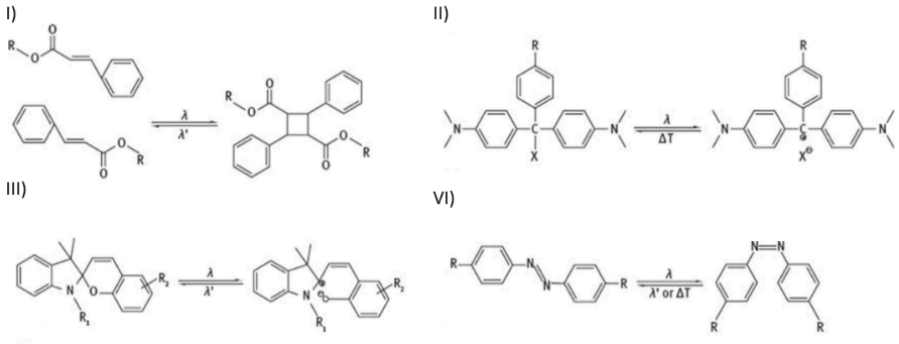

Figure 1.8 Traditional photo-switchable molecules I) proton transfer in the cinnamoyl group, II) homolytic cleavage of the C-X bond and dissociation of triphenylmethane leucoderivatives, III) Reversible photoisomerization of spirobenzopyran derivatives and IV) reversible trans - cis photoisomerization of azobenzene.

Azobenzene molecules, undergo a reversible E-Z photoisomerization and are accompanied by changes of dipole moment, size and shape; spyrobenzopyran, are characterized by ring opening and formation of zwitterionic species; triphenylmethane leucohydroxide, undergo dissociation into an ion pair and generation of charges, while cinnamoyls undergoes photodimerization. These transitions can further induce changes in the optical, mechanical and chemical properties of the system containing the chromophore.[50] Azobenzene derivatives, known centuries only as dyes, were intensively investigated for their photoswitching properties, while spiropyrans, diarylethene and spironaphthoxazines, were developed for their high fatigue resistance. Photochromism can be considered as being a fast-growing domain of research, especially with the implementation of azobenzene derivative compounds, as it can be substantiated by a simple survey on the evolution of the number of publications on this photosensitive compound (Figure 1.9).

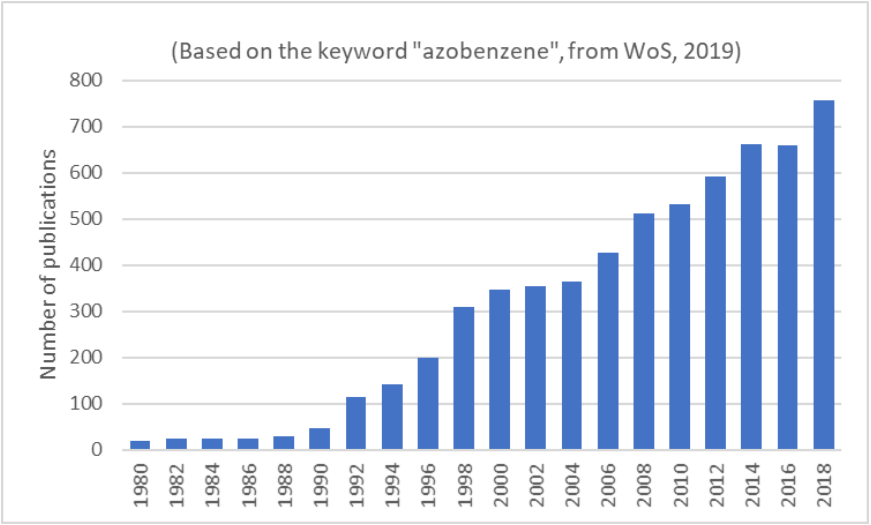

Figure 1.9 Number of publications on azobenzene per year. (Source: ISI Web of Science).

Currently, these chromophores are intensively investigated to implement light sensitivity in polymers as well as in the corresponding microcapsules.

Spirobenzopyran derivatives can be used to create polymers that are able to change their solubility when irradiated with UV or visible light. A water-soluble polymer dissolved in demineralized water and containing the spirobenzopyran, can associate into aggregates to create a large polymeric cluster when irradiated by UV light; this happens due to the reversible isomerization of the neutral spirobenzopyran into a zwitterionic merocyanine, which causes interaction between the polymeric chains. Upon exposure to visible light it is possible to revert the solubility and the clusters disintegrate as the spirobenzopyran returns to its neutral form.[51]

Microcapsules containing photoactive polymers bearing triphenylmethane leucohydroxide or nitrocinnamate have been studied. Kono's group prepared capsules with a partly crosslinked polymeric shell containing a leucohydroxide derivative.[52] Upon UV irradiation, the triphenylmethane derivative dissociated into an ion pair, thereby generating charges, and increasing the release rate of the encapsulated active material if compared with the release rate in the dark. They also showed that this light-triggered permeability control can be achieved over several cycles; the controlled release was caused by reversible degradation and cleavage of the photosensitive groups on the capsule shell. Microcapsules containing nitro-cinnamate derivative were also obtained *via*

reversible photo-crosslinking of the shell at λ > 275 nm, while destruction of the microcapsules, and release of the active, was achieved by photocleavage of the dimer linkages *via* illumination at λ = 254 nm.[53]

Koo and co-workers reported a new and different approach with microcapsules whose walls contain photoacid generators (PAGs).[54] By exposure to UV light with a wavelength of 254 nm, the PAGs used within the capsule walls were activated, which caused the release of protons from the capsules. This release of protons caused a decrease in the pH of the capsule solution, which then triggered microcapsules swelling. The authors reported that these microcapsules could be opened and closed *via* alternate repetition of exposure to UV light and washing with neutral water. Moreover, prolonged exposure led to breakage of the capsules.

N. Jiang et al. propose photo-switchable crosslinked microcapsules with a wall material based on coumarin and isocyanate group.[55] The capsules have been obtained *via* interfacial polymerization followed by photo-crosslinking reaction and a low initial leakage. Exploiting coumarin property to photo-dimerize while exposed to 365 nm light, and to photo-cleave upon 254nm irradiation, allows to obtain reversible crosslinking; this property leads to controlled release of an encapsulated dye upon specific UV light.

Azobenzene derivatives are the most studied photoactive groups thanks to their easy and reversible isomerization between the *E* and *Z* configurations by light and heat, the absence of side reactions associated to the isomerization itself, and the possibility to tune the wavelength to induce the transformation by incorporating substituents into the chromophores. Several studies demonstrate the possibility to obtain photosensitive microcapsules *via* implementation of azobenzene molecules either *via* incorporation of azo dyes into the shell walls, with alteration of the permeability of capsules exposed to visible light[56], or *via* incorporation of the azo-molecule directly into the polyelectrolyte backbone followed by alteration of the permeability of polyelectrolyte capsules upon light absorption by azobenzene moieties.[57]

Through the isomerization of azobenzenes it is possible to modulate the structure of the delivery systems and to obtain UV-sensitive microcapsules with a good light-induced release. The first study on the incorporation of azobenzene moieties in a photo-responsive system to affect release, was

published by Kano et al. in 1980.[58] The authors incorporated an amphiphilic azobenzene moiety along with a phospholipid, dipalmitoyl-phosphatidyl-choline (DPPC), at various molar ratios and were able to modulate the release profiles of encapsulated liposomes based on the azo moiety of choice, the composition of photo stationary state, and the degree of incorporation in the liposome. In this pioneering study the photosensitive release was not fully characterized; nevertheless, the authors also studied the resulting osmotic shrinkage of the vesicles upon incorporation of the azo compounds by measuring the optical density of the solutions, which gave an idea of the mechanism behind the controlled release.

Wang et al.[59] demonstrated for the first time the possibility of light-controlled self-assembly and disassembly of the block ionomer and surfactant microcapsules, tuning the amphiphilicity of the surfactants. The authors obtained the UV-responsive microcapsules through an electrostatic association between an azo-based surfactant and a double-hydrophilic block ionomer based on poly(ethylene glycol). They found that loading and release of fluorescent molecules included in the microcapsules could be achieved, respectively, by reversible self-assembly and disassembly under UV light irradiation. Azobenzene based microcapsules were also created *via* LbL assembly techniques, using the electrostatic interactions between oppositely charged polyelectrolytes. Several studies demonstrate that the presence of azobenzene derivatives into the capsule shell, has an impact on the size[60] and permeability of the microcapsules, and thus on the release of the encapsulated active.[61,62]

Since self-assembled microcapsules are generally not robust, reversible photo-responsive microcapsules have been also obtained *via* interfacial polymerization[63,64], which leads to more robust and crosslinked capsules. Tylkowski et al.[65] prepared lightly crosslinked liquid crystalline polyamide microcapsules that contained azobenzene moieties in the main chain, by using an interfacial polymerization method. They published results concerning the characterization of these microcapsules, which show that release could be easily triggered by irradiating with UV light at 364 nm for a few minutes.

1.5 Azobenzene and photoisomerization of azobenzene

In this thesis work, we will focus, among all the different triggers for the release of the encapsulated material, on the incorporation of chromophores into the polymeric shell; we will study in detail the effect of the isomerization of azobenzene molecules incorporated into the capsule shell. This is the main reason why we decided to dedicate a new paragraph to the study of the state of the art and the isomerization mechanism of this molecule.

Azobenzene (*(E)*-1,2-diphenyldiazene) is one of the most studied photochromic molecules of the last years. Azobenzenes (Figure 1.10) are organic molecules with two aromatic rings linked by an azo group, -N=N-. The azobenzenes are highly coloured, generally dark-yellow compounds, and belong to the group of so-called FD&C (food, drug and cosmetics) dyes. The simplest example within this family, the (*E*)-difenildiazene (azobenzene), features two unsubstituted phenyl groups.

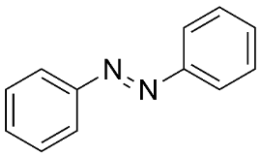

Figure 1.10 Simplest example of azobenzenes compounds, in its trans (E) isomer ((E)-1,2-diphenyldiazene).

Azobenzene was described for the first time in 1834, and in 1937, only one century later, G.S. Hartley published a study on the influence of light on the configuration of N=N double bonds.[66] The exposure of a solution of azobenzene in acetone to light allowed the discovery of the Z isomer. This was the starting point of the development of one of the best organic molecular switches described so far. Their properties have led to some applications of great importance, mainly for the chemical industry. Nowadays, azobenzene dyes represent approximately 60% of the world production of industrial dyes.[67]

The azobenzene has two geometric isomers, Z and E, around the N=N double bond; the E-isomer is ~12 kcal/mol more stable than the Z.[68] The energy barrier of the photoexcited state is ~23 kcal/mol, so that the E-isomer is predominant in the dark at room temperature;[69] this categorize the azobenzenes as metastable compounds. The E-azobenzene easily isomerizes to the Z form by irradiation with 365 nm UV light. The reaction is reversible, and the reverse Z-

to-E isomerization is induced by 450 nm light or heat. As we will see more in detail in the next chapter, the excitation caused by the wavelength and the wavelength of excitation itself, are dependent on the nature of the substituents of the aryl groups. For many azobenzenes, the two photochemical conversions occur on the scale of picoseconds, while the thermal relaxation Z-to-E is much slower (milliseconds to days). The absorption UV-Visible spectra of the E to Z and Z to E isomerization mechanism of azobenzene are reported in Figure 1.11.

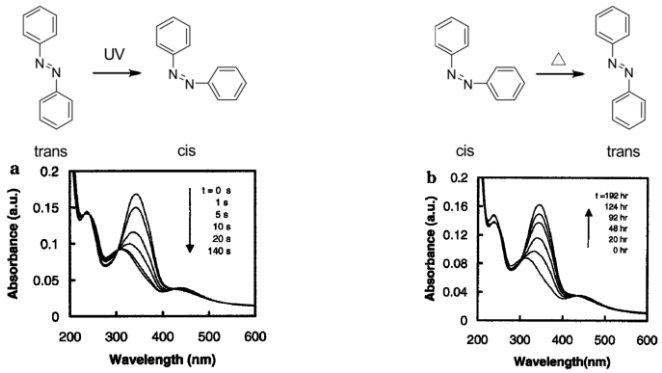

Figure 1.11 Time scale of photochemical conversion for azobenzene. E-to-Z (left) conversion in the scale of seconds and Z-to-E (right) conversion with temperature in the scale of days

The isomerization process involves also huge geometrical and conformational changes with a decrease in the distance between the two carbon atoms in position four of the aromatic rings of azobenzene, from 9.0 Å in the E form to 5.5 Å in the Z form.[70]

Moreover, the E-form is almost flat and has no dipole moment, whereas the Z-isomer presents an angular geometry and a dipole moment of 3.0 D (Figure 1.12). One of the rings rotates to avoid steric repulsions caused by the π clouds of the second aromatic ring. The isomerization is thus, accompanied also by a very significant change of the free volume of the molecule.

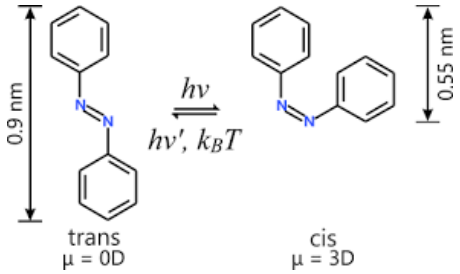

Figure 1.12 Azobenzene photoisomerization.

As it is possible to see from Figure 1.12, the *E*-isomer (left) can be converted to the *Z*-form (right) using an appropriate wavelength (UV at 300–350 nm) of light. A different wavelength (visible blue light >400 nm) can be used to convert the molecule back to the E form. Alternately, the molecule will thermally relax to the stable trans form. The isomerization is associated with a change in the length of the molecule from 0.9 nm to 0.5 nm and with a consistent change of the dipole moment from 0 D (E) to 3 D (Z).

Both isomers, E and Z, exhibit two characteristic absorption bands, π–π^* and n–π^*, the latter one lying in a lower energy region and being less intense, as it is symmetry forbidden. It is worth to mention that π–π^* and n–π^* are electronic transitions, due to absorption of energy, and for both of them an electron is excited from a full (low energy, ground state) orbital into an empty (higher energy, excited state) anti-bonding orbital. The possible transitions are: I) π-π^* or π- σ^* transition, when an electron is promoted from a π-bonding orbital to an antibonding π or σ orbital denoted with *, II) n-π^* or n-σ^* transition associated to free electron pairs denoted as n, to an antibonding π or σ orbital, and III) σ-σ^* or σ-π^* transition, when electrons occupying a highest occupied molecular orbital (HOMO) of a σ bond can get excited to the lowest un-occupied molecular orbital (LUMO) of that bond. They are reported in the below energy diagram (Figure 1.13):

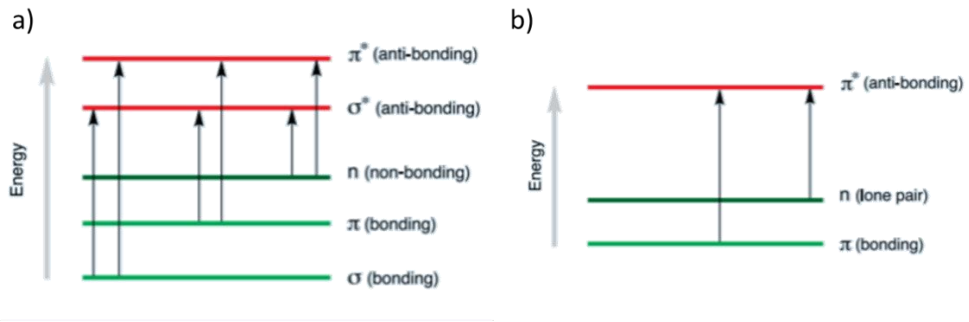

Figure 1.13 Electronic transition states.

Only π to π^* and n to π^* transitions occur in the UV-Visible region while, the σ to σ^* transition requires an absorption of a photon with a wavelength which does not fall in the UV-Visible range.

The two bands π–π^* and n–π^*, characteristic of the absorption spectrum of azobenzene, are clearly visible in the UV-vis absorption spectrum with two

separate peaks (Figure 1.14). The transition $\pi \rightarrow \pi^*$ is usually in the near UV region, while the electronic transition $n \rightarrow \pi^*$ is usually located in the visible region and is due to the presence of lone electron pairs of nitrogen atoms.[71] The absorption spectra of the two isomers differ mainly in the following aspects[72]:

– *E*-isomer: the absorption band π→π* is very intense, with a molar extinction coefficient (ε) ~ 2–3 × 10^4 $M^{-1} \cdot cm^{-1}$. The second band (n→π*) is much weaker (ε ~ 400 $M^{-1} \cdot cm^{-1}$) as this transition is not allowed in the *E*-isomer by symmetry rules.

– *Z*-isomer: the absorption band $\pi \rightarrow \pi^*$ is shifted to shorter wavelengths (hypsochromic effect) decreasing significantly in intensity (ε ~ 7-10 × 10^3 $M^{-1} \cdot cm^{-1}$). The electronic transition $n \rightarrow \pi^*$ (380–520 nm) is allowed in the *Z*-isomer, resulting in an increase in the intensity (ε ~ 1500 $M^{-1} \cdot cm^{-1}$) with respect to the *E*-isomer.

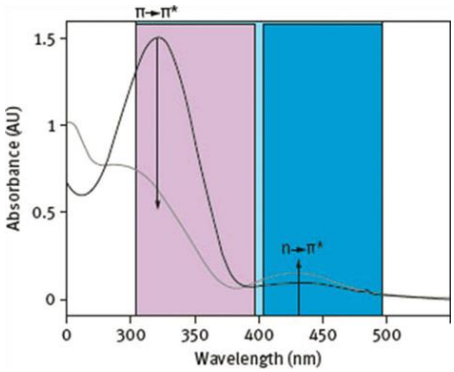

Figure 1.14 Absorption spectrum of the azobenzene.

1.6 Context of the work

When employed as storage and delivery systems, microcapsules gain considerable importance in a number of applications over a broad range of industries including adhesives and coating, dyes and inks, drugs, perfumes, consumer goods products, food additives, catalysts, etc. [37]

Capsules are widely used in medical and pharmaceutical applications as, for example, for the encapsulation of biosensors, DNA or drugs; in these applications, capsules are acting as sensors, protectors from a contaminated

environment and carriers. The technology enables controlled sustained delivery, as well as enhanced stability of microorganisms, taste masking and prolonged release dosage forms. Near-IR-sensitive capsules are highly considered as sustained release devices in this field due to the poor light scattering of biological systems at that wavelength. In the last years, the use of capsules has started to be considered as an effective and promising approach for new applications also in the field of architecture and construction as well as in the textile industry; in these cases, capsules are used to improve thermoregulatory properties of paints, textiles and building materials.[73–75] UV-sensitive microcapsules obtained *via* addition of TiO_2 nanoparticles has been recently investigated for applications in construction, transportation and electronics, where UV sensitive or photocatalytic degradative materials are required.[76]

Microcapsules can be also used for the quality and safety control in food, agricultural and environmental sector; encapsulated biosensors can be used to improve the control over pollution, food cold chain, etc. In the food industry, in agriculture and in cosmetics the application of capsules is more and more appreciated, considered and studied. While in the food industry capsules can provide *via*ble texture blending and appealing aroma release, in agriculture and cosmetics encapsulation means protection from light and oxidation as well as peculiar textures.[77] Also, in this case, photosensitive and UV-visible capsules are widely applied due to the abundance of near UV light.

It is worth to describe more in detail the reason for the need to introduce, in the industrial world which deal with fragrances, the idea of encapsulation and thus, the use on encapsulation in the consumers goods industries.

Fragrances, perfumes or aroma chemicals are an essential additive in consumer products such as household detergent and laundry products and they mainly provide control over the odor. Examples of typical fragranced consumer products are: air fresheners, bath additives, candles, cosmetics, deodorants, antiperspirants, perfumes, hair-care, household, oral hygiene, personal-care, shaving, skin-care and laundry products.

Detergent and laundry products, in general, have a fragrance level in the range 0.2–1 wt%, which is mainly added to: I) mask unpleasant odors, II) give the idea

of cleanness during storage and use and III) impart a nice smell to the fabric/ambient/skin etc.[78]

The general goal over industries is to improve the quality of the fragrances, not only making them more attractive but also making the aromas more durable and stable; for this reason, a good option is to look at controlled-triggered-release to extend fragrance longevity.

For fragranced consumer products, controlling costs is even more important than in pharmaceutical or food applications due to the high cost of fragrances combined with the ease in perfume loss during storage and application.

Encapsulation is an elegant way of controlling fragrance release, making it more durable and improving the performances, such as stability, substantivity, tenacity or endurance, of perfumes in washing products.

Their stability over time is indeed problematic due to surfactants contained in the washing products, which form micelles in water; as many fragrances are hydrophobic they tend to migrate to the micelles, rather than deposit on the substrate. Moreover, the performance of fragrances tends to fade by evaporation, interactions with other components, oxidation and chemical degradation. Encapsulation can thus reduce the reactivity of the fragrances protecting them from the outside environment, decreasing the evaporation rate and reducing the losses (of top notes) during repeated opening of the packages over storage.

The selection of a specific encapsulation route or delivery system depends on the nature of the product where the delivery system will be used, and on which property one wants to improve: this fact helps us to understand why the request for new encapsulation matrices and technologies is so high.

New technologies are being developed or adapted for household cleaning and detergents. For instance, encapsulation is already used in such products as Febreze from Procter & Gamble, a spray used for eliminating bad odors on fabrics; the same technology has been adapted also for use in fabric softener as Lenor; the same company also developed the Vicks® products using encapsulated mentholated vapors to help people to breathe freely. Alternatives are provided by Henkel's Neutralin technology or in personal care with the Kleenex® ColdCare facial tissues from Kimberly-Clark.

The past few years have witnessed particularly strong interest in the development of stimuli-responsive carriers, designed to release the active “on demand” in response to specific stimuli, in many fields.
Unsurprisingly, therefore, light-responsive nanocarriers have attracted major interest within the drug delivery field.[79] Both the wavelength and the power of the light used to trigger the release directly influences the effectiveness and safety profile of a light-responsive.[72] Among light-responsive carriers reported in the literature, photochromic molecules that undergo reversible isomerization upon irradiation are the most utilized, thereby functioning as gates or switches for the release of encapsulated compounds.

As a final remark, it is important to reemphasize that encapsulation is a technique which brings a lot of benefits, but has also some limitations; as already stated, no single encapsulation process is adaptable to all core material candidates or product applications. Therefore, they need to be carefully selected accordingly. Also, the coating of the active material can be incomplete and discontinuous, leading to non-uniform shells which may impact the release rate and also the stability and the mechanical properties of the system. Many factors and variables need to be considered during an encapsulation process: actually, this is what makes this technique fascinating, flexible and complex at the same time.

1.7 Objectives and problem statement

Conventional capsules used nowadays in consumer goods products are able to release perfume due to mechanical breakage resulting in a fast and constant release over time, as already stated in the previous sections. Microencapsulation techniques have been widely studied and employed in the design of controlled and sustained release systems as a response to the need of reaching a temporal delivery in specific applications. Temporal delivery refers to the control of perfume delivery rate in targeted circumstances and to the sustained duration of the capsules activity. In applications where no or low mechanical stress is involved, for example in beauty care applications or sprays for the home care, it is important to reach a controlled release of the perfume

over time. It is also important to explore the possibility to trigger and control such release by external factor as light, temperature, pH or others.

The objective of this work is to develop classes of compounds which are not only sensitive to external stimuli but are also able to encapsulate an active ingredient. In addition to that, we will focus on the preparation of light sensitive, core-shell capsules which are able to encapsulate a perfume with business interest for the Procter & Gamble Company (P&G), to reach long lasting perfume performances and high perfume release triggered by/associated with light irradiation.

The obtainment of photosensitive capsules is thus, strictly connected with the development of polymeric shells or the usage of polymeric and oligomeric additives, which are sensitive to external-source white-light irradiation.

The aim of this PhD work is to enrich commercial capsules with photosensitive activity by the formation of a polymeric shell based on an azobenzene moiety selected as photochromic material. To achieve this result, we will explore different strategies.

First, we will focus on the preparation of photosensitive capsules by microencapsulation processes such as emulsification and solvent evaporation; these capsules will be completely based on photosensitive azo-based linear polymers which contain the photosensitive unit in the main chain. The technique used in this case represent a valid alternative to *in-situ* polymerization or interfacial polymerization, two methods for the obtainment of microcapsules, broadly used in industrial applications. The same photosensitive azo-based linear polymer can be used in blend with commercially available polymers, to create stable capsules with a system where the amount of in-house synthesized photosensitive polymer used is decreased. Also, in this case it is possible to use physical methods of encapsulation which can be used in the management of non-crosslinked polymers.

Another approach is the addition of low percentages of light sensitive oligomers or monomers, properly functionalized, into commercial processes of microencapsulation. This approach leads to crosslinked shells and the photosensitive unit is incorporated in the network itself. With this technique it is possible to modulate and easily change the percentages of photosensitive

oligomer/monomer inserted into the shell and tune the properties of the final capsule. Also, with this approach and with the help of a good and effective molecular design, it is possible to obtain good capsules, changing the chemistry of the shell, without greatly modify the industrial process. Once selected the chemistry of the crosslinking reaction, it is possible to functionalize the stimuli-responsive molecule accordingly and incorporate it into the net. This strategy based on the combination of different chemical blocks in one single network, could help not only in the preparation of a wide range of stimuli-responsive systems and capsules, but could be also used to fulfil additional desired final shell characteristics, such as, for instance, biodegradability.

It is possible to schematize the objectives (1-4) and the main hypotheses (A-D) of this work, as follow:

1. Synthesis of chemical species which are sensitive to light irradiation (substituted azobenzene).
2. Synthesis of polymeric/oligomeric species containing the photosensitive azobenzene, as repeating unit, into the main chain.
3. Preparation and characterization of photosensitive capsules by microencapsulation processes such as emulsification and solvent evaporation.
4. Preparation and characterization of capsules containing low percentages of light sensitive monomers, into commercial processes of microencapsulation. This approach would lead to crosslinked shells with the photosensitive unit incorporated in the network itself.

The main hypotheses of this work are:

A) It is possible to obtain a red-shift in the absorption wavelength of the azobenzene molecule through functionalization of the parent azobenzene with both, electron-donor and electron-acceptor groups.

B) The preparation of polyesters with moderately high molecular weight and containing photosensitive repeating units, will allow the preparation of stable microcapsules.

C) The presence of ortho-substituted azobenzene moiety into the polymeric capsule shell, added in a proper concentration, will influence the mobility of the polymeric shell and help to achieve microcapsules which will release the core material under white light irradiation.

D) It is possible to prepare core-shell capsules starting from a pre-synthesized polymer, thrugh several encapsulation techniques, among which phase inversion precipitation; it is also possible to obtain core-shell capsules starting from single monomers, through interfacial polymerization encapsulation techniques.

Bibliography

1. Bansode, S. S., Banarjee, S. K., Gaikwad, D. D., Jadhav, S. L. & Thorat, R. M. Microencapsulation: a review. *Int. J. Pharm. Sci. Rev. Res.* **1**, 38–43 (2010).
2. Benita, S. *Microencapsulation: Methods and Industrial Applications,* Second Edition, CRC Press, 783 (2005).
3. Krajisnik, D., Čalija, B., Cekić, N., Polymeric Microparticles and Inorganic Micro/Nanoparticulate Drug Carriers: An Overview and Pharmaceutical Application. *In book Microsized and Nanosized Carriers for Nonsteroidal Anti-Inflammatory Drugs*, Academic Press, 31-67 (2017).
4. Azagheswari, B. K., Padma, S., Priya, S. P., A review on microcapsules. *Glob. J. Pharmacol.* **9**, 28–39 (2015).
5. Jabeen, M., Begum, S., Siddique, A., Fatima, S. S., Microencapsulation: A potential and promising approach in drug delivery system. *J. Invent. Biomed. Pharm. Sci. JIBPS*. **5**(2), 65–77 (2010).
6. Li, W., Zhang, X.-X., Wang, X.-C. & Niu, J.-J. Preparation and characterization of microencapsulated phase change material with low remnant formaldehyde content. *Mater. Chem. Phys.* **106**, 437–442 (2007).
7. Allen, V., Ansel, C., *Ansel's Pharmaceutical Dosage Forms and Drug Delivery Systems,* Lippincott Williams & Wilkins, (2013).
8. Chien, W. Y., Potential Development and New Approaches in Oral Controlled-Release Drug Delivery Systems. *Drug Dev. Ind. Pharm.* **9**, 1291–1330 (1983).
9. Thies, C., Microencapsulation. *In book Encyclopedia of Polymer Science and Technology*, American Cancer Society, (2004).
10. Chen, P. W., Erb, R. M., Studart, A. R., Designer Polymer-Based Microcapsules Made Using Microfluidics. *Langmuir* **28**, 144–152 (2012).

11. Venkatesan, P., Manavalan, R., *Microencapsulation: A Vital Technique in Novel Drug Delivery System*, Journal of Pharmaceutical Sciences and Research, 26-35 (2009).

12. Zhang, J., Coulston, R. J., Jones, S. T., Geng, J., Scherman, O. A., Abell, C., One-Step Fabrication of Supramolecular Microcapsules from Microfluidic Droplets. *Science* **335**, 690–694 (2012).

13. Ghosh, S. K. *Functional Coatings and Microencapsulation: A General Perspective*., John Wiley & Sons, Ltd, (2006).

14. Deladino, L., Alba, S. N., Miriam, N. M., Encapsulación de compuestos bioactivos con alginatos para la industria de alimentos. *Limentech Cienc. Tecnol. Aliment.* **10**, (2011).

15. Arshady, R. Microspheres and microcapsules: A survey of manufacturing techniques. Part 1: Suspension cross-linking. *Polym. Eng. Sci.* **29**, 1746–1758 (1989).

16. Lu, S., Shen, T., Xing, J., Song, Q., Shao, J., Zhang, J., & Xin, C., Preparation and characterization of cross-linked polyurethane shell microencapsulated phase change materials by interfacial polymerization. *Mater. Lett.* **211**, 36–39 (2018).

17. Zhang, H., Zhang, X., Bao, C., Li, X., Sun, D., Duan, F., ... & Yang, J., Direct microencapsulation of pure polyamine by integrating microfluidic emulsion and interfacial polymerization for practical self-healing materials. *J. Mater. Chem. A* **6**, 24092–24099 (2018).

18. Singh, M., Menra, J. S. D., Soni, M., Prasad, D. Microencapsulation and its various aspects: a review. *Int. J. Adv. Res.* **4**, 2094–2108 (2016).

19. Brandau, T. Preparation of monodisperse controlled release microcapsules. *Int. J. Pharm.* **242**, 179–184 (2002).

20. Arshady, R. Microspheres and microcapsules: A survey of manufacturing techniques. *Polym. Eng. Sci.* **29**, 1746–1758 (1989).

21. Berkland, C., Kim, K., Pack, D. W. Fabrication of PLG microspheres with precisely controlled and monodisperse size distributions. *J. Control. Release Off. J. Control. Release Soc.* **73**, 59–74 (2001).

22. Salaün, F., Devaux, E., Bourbigot, S., Rumeau, P. Preparation of multinuclear microparticles using a polymerization in emulsion process. *J. Appl. Polym. Sci.* **107**, 2444–2452 (2008).

23. Pascu, O., Garcia-Valls, R. & Giamberini, M. Interfacial polymerization of an epoxy resin and carboxylic acids for the synthesis of microcapsules. *Polym. Int.* **57**, 995–1006 (2008).

24. Arshady, R. Microspheres and microcapsules, a survey of manufacturing techniques: Part III: Solvent evaporation. *Polym. Eng. Sci.* **30**, 915–924 (1990).

25. Teeka, P., Chaiyasat, A. & Chaiyasat, P. Preparation of Poly (methyl methacrylate) Microcapsule with Encapsulated Jasmine Oil. *Energy Procedia* **56**, 181–186 (2014).

26. Peña, B., Panisello, C., Aresté, G., Garcia-Valls, R., Gumí, T. Preparation and characterization of polysulfone microcapsules for perfume release. *Chem. Eng. J.* **179**, 394–403 (2012).

27. Li, M., Rouaud, O., Poncelet, D. *Microencapsulation by solvent evaporation: State of the art for process engineering approaches*., Vol. 363 (2008).

28. Jyothi, N. V. N., Prasanna, P. M., Sakarkar, S. N., Prabha, K. S., Ramaiah, P. S., & Srawan, G. Y., Microencapsulation techniques, factors influencing encapsulation efficiency. *J. Microencapsul.* **27**, 187–197 (2010).

29. Arshady, R. Microspheres and microcapsules, a survey of manufacturing techniques Part II: Coacervation. *Polym. Eng. Sci.* **30**, 905–914 (1990).

30. Lam, P. L., Gambari, R. Advanced progress of microencapsulation technologies: in vivo and in vitro models for studying oral and transdermal

drug deliveries. *J. Control. Release Off. J. Control. Release Soc.* **178**, 25–45 (2014).

31. Oxley, J., Overview of microencapsulation process technologies. *In Microencapsulation in the food industry,* Academic Press, 35-46, (2014).
32. Paret, N., Trachsel, A., Berthier, D. L., Herrmann, A. Controlled Release of Encapsulated Bioactive Volatiles by Rupture of the Capsule Wall through the Light-Induced Generation of a Gas. *Angew. Chem. Int. Ed.* **54**, 2275–2279 (2015).
33. Korsmeyer, R. W., Gurny, R., Doelker, E., Buri, P., Peppas, N. A. Mechanisms of solute release from porous hydrophilic polymers. *Int. J. Pharm.* **15**, 25–35 (1983).
34. Higuchi, T. Mechanism of sustained-action medication. Theoretical analysis of rate of release of solid drugs dispersed in solid matrices. *J. Pharm. Sci.* **52**, 1145–1149 (1963).
35. Koppenhagen, V., Juanita E., Lee, K., Shirley, I., Wade, P., Follows, R., Acid-triggered microcapsules. U.S. Patent 6, 514, 439, issued February 4, (2003).
36. Esser-Kahn, A. P., Odom, S. A., Sottos, N. R., White, S. R. & Moore, J. S. Triggered release from polymer capsules. *Macromolecules* **44**, 5539–5553 (2011).
37. Del Pezzo, R., Bandeira, N. A., Trojanowska, A., Prieto, S. F., Underiner, T., Giamberini, M., & Tylkowski, B., Ortho-substituted azobenzene: Shedding light on new benefits. *Pure and Applied Chemistry*, 91(9), 1533-1546, (2019).
38. Vogel, A., Venugopalan, V. Mechanisms of Pulsed Laser Ablation of Biological Tissues. *Chem. Rev.* **103**, 577–644 (2003).
39. Pastine, S. J., Okawa, D., Zettl, A., Fréchet, J. M. J. Chemicals On Demand with Phototriggerable Microcapsules. *J. Am. Chem. Soc.* **131**, 13586–13587 (2009).

40. Yashchenok, A., Masic, A., Gorin, D., Inozemtseva, O., Shim, B. S., Kotov, N., Möhwald, H., Optical Heating and Temperature Determination of Core–Shell Gold Nanoparticles and Single-Walled Carbon Nanotube Microparticles. *Small*, *11*(11), 1320-1327 (2015).

41. Saito, H., Kato, N. Polyelectrolyte/carbon nanotube composite microcapsules and drug release triggered by laser irradiation. *Jpn. J. Appl. Phys.* **55**, 03DF06 (2016).

42. Radt, B., Smith, T. A., Caruso, F. Optically Addressable Nanostructured Capsules. *Adv. Mater.* **16**, 2184–2189 (2004).

43. Jeong, W.-C., Kim, S.-H. & Yang, S.-M. Photothermal Control of Membrane Permeability of Microcapsules for On-Demand Release. *ACS Appl. Mater. Interfaces* **6**, 826–832 (2014).

44. Dahl, M., Liu, Y., Yin, Y. Composite Titanium Dioxide Nanomaterials. *Chem. Rev.* **114**, 9853–9889 (2014).

45. Jiang, Y., Peng, Z., Zhang, S., Li, F., Liu, Z., Zhang, J., Wang, K. Facile in-situ Solvothermal Method to synthesize double shell ZnIn2S4 nanosheets/TiO2 hollow nanosphere with enhanced photocatalytic activities. *Ceram. Int.* **44**, 6115–6126 (2018).

46. Katagiri, K., Koumoto, K., Iseya, S., Sakai, M., Matsuda, A., Caruso, F., Tunable UV-Responsive Organic−Inorganic Hybrid Capsules. *Chem. Mater.* **21**, 195–197 (2009).

47. Wang, X., Lu, Q., Wang, X., Joo, J., Dahl, M., Liu, B., Yin, Y., Photocatalytic Surface-Initiated Polymerization on TiO2 toward Well-Defined Composite Nanostructures. *ACS Appl. Mater. Interfaces* **8**, 538–546 (2016).

48. Bouas-Laurent, H., Dürr, H. Organic photochromism, *Pure Appl. Chem.* **73**, 639–665 (2001).

49. Nakatani, K., Piard, J., Yu, P., Métivier, R. Introduction: Organic Photochromic Molecules. in *Photochromic Materials* 1–45, John Wiley & Sons, Ltd, (2016).

50. Li, M.-H., Keller, P. Stimuli-responsive polymer vesicles. *Soft Matter* **5**, 927–937 (2009).

51. Koňák, Č., Rathi, R. C., Kopečková, P., Kopeček, J. Photoregulated Association of Water-Soluble Copolymers with Spirobenzopyran-Containing Side Chains. *Macromolecules* **30**, 5553–5556 (1997).

52. Kono, K., Nishihara, Y., Takagishi, T. Photoresponsive permeability of polyelectrolyte complex capsule membrane containing triphenylmethane leucohydroxide residues. *J. Appl. Polym. Sci.* **56**, 707–713 (1995).

53. Yuan, X., Fischer, K. & Schärtl, W. Photocleavable Microcapsules Built from Photoreactive Nanospheres. *Langmuir* **21**, 9374–9380 (2005).

54. Koo, H. Y., Lee, H.-J., Kim, J. K., Choi, W. S. UV-triggered encapsulation and release from polyelectrolyte microcapsules decorated with photoacid generators. *J. Mater. Chem.* **20**, 3932–3937 (2010).

55. Jiang, N., Cheng, Y., Wei, J. Coumarin-modified fluorescent microcapsules and their photo-switchable release property. *Colloids Surf. Physicochem. Eng. Asp.* **522**, 28–37 (2017).

56. Tao, X., Li, J., Möhwald, H. Self-Assembly, Optical Behavior, and Permeability of a Novel Capsule Based on an Azo Dye and Polyelectrolytes. *Chem. – Eur. J.* **10**, 3397–3403 (2004).

57. Bédard, M. F., De Geest, B. G., Skirtach, A. G., Möhwald, H. & Sukhorukov, G. B., Polymeric microcapsules with light responsive properties for encapsulation and release. *Adv. Colloid Interface Sci.* **158**, 2–14 (2010).

58. Kano, K., Tanaka, Y., Ogawa, T., Shimomura, M., Okahata, Y., & Kunitake, T., Photoresponsive membranes. regulation of membrane properties by photoreversible cis–trans isomerization of azobenzenes. *Chem. Lett.* **9**, 421–424 (1980).

59. Wang, Y., Han, P., Xu, H., Wang, Z., Zhang, X., & Kabanov, A. V., Photocontrolled Self-Assembly and Disassembly of Block Ionomer Complex

Vesicles: A Facile Approach toward Supramolecular Polymer Nanocontainers. *Langmuir* **26**, 709–715 (2010).

60. Marturano, V., Ambrogi, V., Cerruti, P., Giamberini, M. & Tylkowski, B. Photo-triggered release in polyamide nanosized capsules. *AIP Conf. Proc.* **1599**, 234–237 (2014).
61. Xiao, W., Chen, W. H., Zhang, J., Li, C., Zhuo, R. X., & Zhang, X. Z., Design of a Photoswitchable Hollow Microcapsular Drug Delivery System by Using a Supramolecular Drug-Loading Approach. *J. Phys. Chem. B* **115**, 13796–13802 (2011).
62. Tao, X., Li, J., Möhwald, H. Self-Assembly, Optical Behavior, and Permeability of a Novel Capsule Based on an Azo Dye and Polyelectrolytes. *Chem. – Eur. J.* **10**, 3397–3403 (2004).
63. Tsuda, N., Ohtsubo, T., Fuji, M. Preparation of self-bursting microcapsules by interfacial polymerization. *Adv. Powder Technol.* **23**, 724–730 (2012).
64. Salaün, F., Bedek, G., Devaux, E., Dupont, D. & Gengembre, L. Microencapsulation of a cooling agent by interfacial polymerization: Influence of the parameters of encapsulation on poly(urethane–urea) microparticles characteristics. *J. Membr. Sci.* **370**, 23–33 (2011).
65. Tylkowski, B., Pregowska, M., Jamowska, E., Garcia-Valls, R. & Giamberini, M. Preparation of a new lightly cross-linked liquid crystalline polyamide by interfacial polymerization. Application to the obtainment of microcapsules with photo-triggered release. *Eur. Polym. J.* **45**, 1420–1432 (2009).
66. S. Hartley, G. The Cis-form of Azobenzene. *Nature* **140**, (1937).
67. Zollinger, H. *Color Chemistry: Syntheses, Properties, and Applications of Organic Dyes and Pigments*. John Wiley & Sons, (2003).
68. Rabek, J. F., Scott, G. W. Photochemistry and photophysics. Vol. 1. CRC Press, (1989).

69. Brown, E. V., Granneman, G. R., Cis-trans isomerism in the pyridyl analogs of azobenzene. Kinetic and molecular orbital analysis. Journal of the American Chemical Society 97, 621-627 (1975).

70. Koshima, H., Ojima, N. & Uchimoto, H. Mechanical motion of azobenzene crystals upon photoirradiation. *J. Am. Chem. Soc.* **131**, 6890–6891 (2009).

71. Bédard, M., Skirtach, A. G. & Sukhorukov, G. B. Optically Driven Encapsulation Using Novel Polymeric Hollow Shells Containing an Azobenzene Polymer. *Macromol. Rapid Commun.* **28**, 1517–1521 (2007).

72. Giamberini, M., Prieto, S. F., Tylkowski, B. *Microencapsulation: Innovative Applications*. Walter de Gruyter GmbH & Co KG, (2015).

73. Salaün, F., Devaux, E., Bourbigot, S., Rumeau, P. Thermoregulating response of cotton fabric containing microencapsulated phase change materials. *Thermochim. Acta* **506**, 82–93 (2010).

74. Sánchez-Silva, L., Rodríguez, J. F., Romero, A., Sánchez, P. Preparation of coated thermo-regulating textiles using Rubitherm-RT31 microcapsules. *J. Appl. Polym. Sci.* **124**, 4809–4818 (2012).

75. Sánchez, P., Sánchez-Fernandez, M. V., Romero, A., Rodríguez, J. F., Sánchez-Silva, L. Development of thermo-regulating textiles using paraffin wax microcapsules. *Thermochim. Acta* **498**, 16–21 (2010).

76. Giamberini, M., Prieto, S. F., Tylkowski, B. *Microencapsulation: Innovative Applications*. Walter de Gruyter GmbH & Co KG, (2015).

77. Arshady, R. Microcapsules for food. *J. Microencapsul.* **10**, 413–435 (1993).

78. Berger, R. G. *Flavours and Fragrances: Chemistry, Bioprocessing and Sustainability*. Springer Science & Business Media, (2007).

79. Jia, S., Fong, W.-K., Graham, B., Boyd, B. J. Photoswitchable Molecules in Long-Wavelength Light-Responsive Drug Delivery: From Molecular Design to Applications. *Chem. Mater.* **30**, 2873–2887 (2018).

2. Chemical modification of azobenzene molecules - Absorption of light in the visible range

In this chapter the attention will be focused mostly on the preparation and characterization of light-sensitive molecules, based on azobenzene. The photosensitive behavior of the synthesized molecule, and the kinetic of its *Z-E* isomerization process, will be studied in detail via Nuclear Magnetic Resonance and UV-Visible spectroscopy. Theoretical calculations demonstrate that visible light can act as a trigger for the isomerization of the synthesized molecule inducing, therefore, isomerization via two different mechanisms. It is important to give, first, a brief overview on the different ranges of light irradiation we are interested in, and on the basic principles of photon-induced electronic transitions.

Electromagnetic waves, which represent one of the many ways in which energy travels through space, can be classified according to the different wavelengths or frequencies; this classification is known as the electromagnetic spectrum (Figure 2.1) and the visible range only represents a small fraction of it. To the right of the visible spectrum, we find the energies that are lower in frequency (and longer in wavelength) than visible light. These types of energy include infrared (IR) rays, heat waves given off by thermal bodies, microwaves, and radio waves. To the left of the visible spectrum, we have ultraviolet (UV) rays, X-rays, and gamma rays.

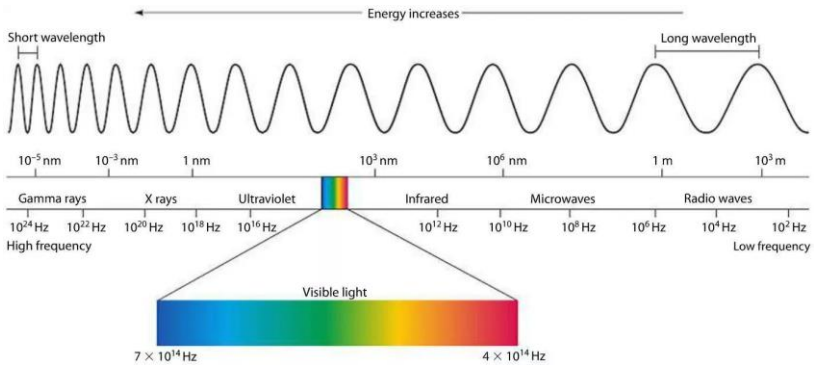

Figure 2.1 Electromagnetic spectrum.

We will focus our interest, in the context of this work, in how these waves, and in particular UV and visible radiation, interacts with the matter; this interaction translates in photon absorption which causes electronic transitions from the ground state to a high energy state. The ultraviolet region falls in the range between 200-400 nm, the visible region falls between 400-700 nm. As we will underline also later, lower frequency waves are lower in energy, and thus are not dangerous to our health, while higher frequency waves are harmful due to their high transported energy.

The starting point for the study of the photosensitive molecules used in this work is the un-modified azobenzene, the *(E)*-1,2-diphenyldiazene, described already in the first chapter. It can absorb in the UV light range, to isomerize from the *E* isomer to the *Z* isomer, via excitation of π-π^*. The reverse *Z*-to-*E* isomerization is induced by 450 nm light absorption (or by heating), but the presence of overlapping n-π^* bands for both isomers, prevents complete recovery of the *E* form.[1]

The UV light photoisomerization of most azobenzenes can be considered as a limit for a wide range of applications; for example, in applications in vivo or comprising the biological systems, the UV light is considered unhealthy and can trigger unwanted responses, including cellular apoptosis.[2] This is the main reason why, it is important, in order to broaden the range of applications of this molecule, to try to shift their absorption wavelength to low frequencies and thus, to the red region of the electromagnetic spectrum.[1] A red-shifted, fast photoisomerization that can occur entirely in the visible region would therefore be desirable and considered as a benefit in many fields.[3]

Several studies have already demonstrated that the introduction of ring substituents significantly influences the absorption wavelength of both isomers of azobenzene.[4] This shift has been attributed to three factors: I) electron-donating group on the rings lead to a red-shift of the absorbance of the *E* isomer, possibly due to raising the relative energy of the HOMO in the *E*-form[5], II) steric interactions reduces the sp^2 character of the N atoms, also raising the HOMO energy, leading to the red-shift absorbance,[6] and III) electron-withdrawing groups such as F atoms can lower the n-orbital energy of the Z isomer by reducing the electron density in the nearby N=N bond.[5] In Table 2.1

several example of the modification of azobenzene molecules and thus, azobenzene absorption spectrum, are schematically reported.

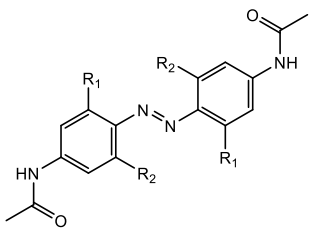

Table 2.1 Visible Light-responsive symmetric azobenzene derivatives. Adapted from[4].

R_1	R_2	λ_{max} ***E*** **isomer [nm]**	λ_{max} ***Z*** **isomer [nm]**
H	H	364	348 (π→π*), 473 (n→π*)
Methoxyl groups	Methoxyl groups	338 (π→π*), 480 (n→π*)	330 (π→π*),444 (n→π*)
Piperidine groups	H	445	-
F	F	364 (π→π*),370 (n→π*)	314 (π→π*),450 (n→π*)

The azo-compounds can, indeed, be classified according to the nature of the aromatic rings and their chemical substitution. Mainly it is possible to group the azobenzene derivatives in three different classes which have distinct absorption spectra and thus, distinct energetic electronic transitions $\pi \rightarrow \pi^*$ and $n \rightarrow \pi^*$. The classification is also reported in Figure 2.2. In the I) azobenzene type molecules, the $\pi \rightarrow \pi^*$ band is very intense in the UV region and there is one $n \rightarrow \pi^*$ weaker band in the visible region. They exhibit yellow colour; the colour of azobenzene is indeed, generally yellow but its substitution yields a bathochromic shift, providing an orange to red colour. The electronic nature of the aromatic rings is very similar to simple azobenzene (Ph–N=N–Ph) which indeed, belongs to this class. The category of the II) aminoazobenzene type molecules shows very close $\pi \rightarrow \pi^*$ and $n \rightarrow \pi^*$ bands and usually they collapse in the UV-visible region. What makes them different from the un-modified azobenzenes is the presence of electron-donating substituents (X) in the ortho or para positions. They exhibit dark orange colour. (o- or p-(X)–C6H4–N=N-Ar).

The third class of azobenzene derivative molecules is the one of III) pseudo-stilbenes; for this class of compounds the absorption band corresponding to the $\pi \rightarrow \pi^*$ transition is red-shifted, and inverted respect to the band $n \rightarrow \pi^*$ in terms of ppm. They can be described as an azobenzene modified with electron-donating (X) and electron-acceptor (Y) groups and, for this reason, they are also called push/pull system because of the double nature of the substitution which not only leads to a red-shift of the absorbance of the *E* isomer, but also greatly decreases the thermal stability of the *Z* isomer. This class of compounds exhibits red colour. [(X)–C6H4–N=N–C6H4–(Y)].[2]

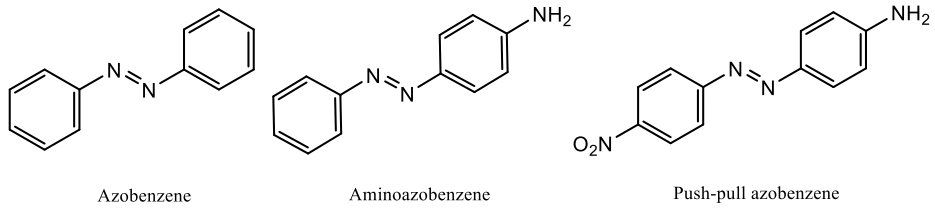

Figure 2.2 Classification of azobenzene compounds: un-modified azobenzene (azobenzene), azobenzene functionalized with one electron-donating group (aminoazobenzene), azobenzene functionalized with both electron-donating and electron-acceptor groups (push-pull azobenzene).[7]

Those compounds all exhibit the central azobenzene structure while they differ for the ring substitution patterns; this helps to hold the common properties of azobenzene such as the strong electronic absorption, whilst the ring substitution leads to a modification of the absorption spectrum with a shift in the absorption wavelength;[8] moreover, depending on the nature of the substituents on the aromatic group, not only the absorption wavelengths but also the equilibria between the *E* and *Z* isomers will change. To conclude, increasing electron density is a good strategy to red-shift the absorption and lower the energy barrier for the *Z*-to-*E* isomerization. Both effects are achieved in the "amino" and "push–pull" azobenzenes showed in Figure 2.2.[9]

2.1 Experimental

2.1.1 Materials

3-methoxy-4-nitrobenzoic acid (Sigma-Aldrich, 99), D-(+)-glucose (Sigma, 99.5 %), sodium hydroxide (Sigma-Aldrich), glacial acetic acid (Sigma-Algrich, 99.5 %), triethylamine (Sigma-Aldrich, 99 %), and thionyl chloride (Sigma-Aldrich, 97 %) were used as received without any further purification. All the solvents were supplied by Scharlau, Aldrich and Fluka and used without previous purification as received. Aqueous solutions were prepared using Milli-Q water.

2.1.2 Nucler Magnetic Resonance (NMR)

Nuclear Magnetic Resonance (NMR) spectroscopy is an analytical chemistry technique used in quality control and research for the determination of the purity of a sample, its molecular structure as well as the content of a specific species in a mixture. NMR spectroscopy is thus, one of the main techniques utilized for the study of molecular structures of organic compounds; it is a non-destructive technique and it requires 5-30 mg of samples depending on the accuracy desired on the final spectrum.

The principle behind NMR is that every nucleus has a characteristic spin and all nuclei are electrically charged. The spin can be integral, fractional or equal to zero. The most relevant and interesting isotopes, which will be analyzed in this thesis work, are the ^{1}H and the ^{13}C which both have a fractional spin equal to ½. When an external magnetic field is applied, two opposite spin energy state are possible for each isotope, ±1/2, one of lower energy +1/2 aligned with the external field and the other with higher energy -1/2 opposed to the external field. Between these two spins states an energy transfer is possible. Figure 2.3 illustrates that the two spin states have the same energy when the external field is zero but diverge as the field increases. At a field equal to B_x the energy difference is given by Equation 2.1:

$$\Delta B = \frac{\mu B_x}{I} \qquad (2.1)$$

where I=1/2 and μ is the magnetic moment of the nucleus in the field.

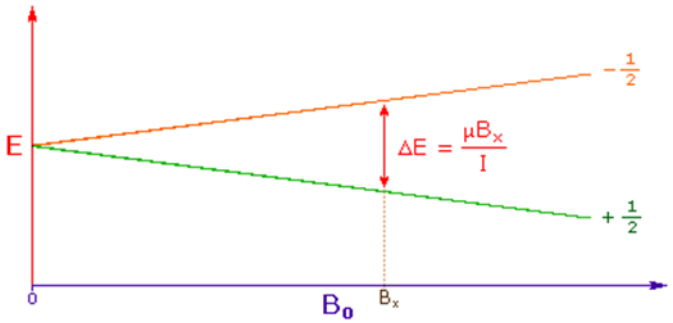

Figure 2.3 Energy diagram which explains the principle behind NMR spectroscopy: spin energy states as a function of the external applied magnetic field.

For NMR purposes, this small energy difference (*ΔE*) is usually given as a frequency in units of MHz ranging from 20 to 900 MHz, depending on the magnetic field strength and the specific nucleus being studied.

Irradiation of a sample with radio frequency (rf) energy corresponding exactly to the spin state separation will cause excitation of the nuclei from the +1/2 state to the higher -1/2 spin state. The energy transfer takes place at a wavelength that corresponds to rf and, when the spin returns to its base level, energy is emitted at the same frequency. The signal that matches this transfer is measured and processed to yield an NMR spectrum for the nucleus concerned. The precise resonant frequency of the energy transition is dependent on the effective magnetic field and on the electron shielding which is in turn dependent on the chemical environment. Information about the nucleus chemical environment can thus be derived from its resonant frequency. In general, the more electronegative the nucleus is, the higher the resonant frequency. Unlike infrared and UV-Visible spectroscopy indeed, where absorption peaks are uniquely located by a frequency or wavelength, the location of different NMR resonance signals is dependent on both the external magnetic field strength and the rf frequency. Since there are not two magnets with the same exact field, resonance frequencies will vary accordingly and an alternative method for characterizing and specifying the location of NMR signals is needed. To solve this problem, it is customary to adopt tetramethylsilane (TMS) as the proton reference frequency. As standard compound TMS is added to every sample analyzed and its signal is used as reference. To eliminate the dependence on the magnetic field thus, it is

convenient to express each NMR signal not in frequency but in terms of the chemical shift δ defined as follow (Equation 2.2):

$$\delta = \frac{v - v_{ref}}{v_{ref}} \qquad (2.2)$$

where v_{ref} is the resonant frequency of the reference signal and v is the frequency of the sample signal. This operation gives a locator number called the chemical shift, having units of parts-per-million (ppm), and designated by the symbol δ.

The molecules synthesized in this work, were characterized with ^{1}H-NMR and ^{13}C-NMR spectroscopy, using deuterated dimethyl sulfoxide (d-DMSO) or deuterated chloroford (CDCl3) as a solvent with a Varian Gemini 400 MHz spectrometer (^{1}H-400 MHz, TMS; ^{13}C-100 MHz, TMS). Measurements were carried out at room temperature using 10-15 mg or 30-40 mg of sample respectively for ^{1}H and ^{13}C analysis; the samples were dissolved in the adequate solvent, according to the polarity of the sample. ^{1}H-NMR measurements have been obtained with 400 MHz frequency, pulse delay time between consecutive pulses (d1) between 1 and 16 seconds, while ^{13}C-NMR spectra are recorded with 100.6 MHz frequency and lower d1 between 0.5 and 0.2 seconds. As previously described, for all the analysis TMS has been used as reference. ^{1}H-NMR analysis was also used to study the photosensitive behavior of the synthesized ortho-substituted azobenzene-4,4′-dicarboxylic acid. A Varian Gemini 400 MHz spectrometer equipped with a heating chamber was used for this purpose. Starting from a mixture of *E* and *Z* isomers, obtained through irradiation of the sample for 30 min by sunlight, the azo compound was heated into the NMR spectrometer and kept at fixed temperature for 30 min. The spectra were recorded every 5 min during a period of 30 minutes, to monitor how the concentration of the two isomers in the mixture changed and to study the kinetics of Z-E isomerization for the synthesized ortho-substituted azobenzene moiety. The described procedure was repeated at four different temperatures, namely 30, 50, 60, and 70 °C (± 2 °C), to study the thermal back isomerization and to calculate the activation energy E_a of this process.

2.1.3 UV-Visible spectroscopy (UV-VIS)

UV-Visible spectrophotometer can be used to measure the absorbance of ultra violet or visible light for samples which contain either C=C or N=N bonds, and therefore can absorb light in the region from 200 - 800 nm. The measurement can be either at a single wavelength or a scan over a certain wavelength range in the spectrum. The technique can be used both quantitatively and qualitatively. A schematic diagram of a UV-visible spectrometer is shown in Figure 2.4. The light source (a combination of tungsten/halogen and deuterium lamps) provides the visible and near ultraviolet radiation covering the 200-800 nm range. The output from the light source is focused onto the diffraction grating which splits the incoming light into its component colours of different wavelengths.

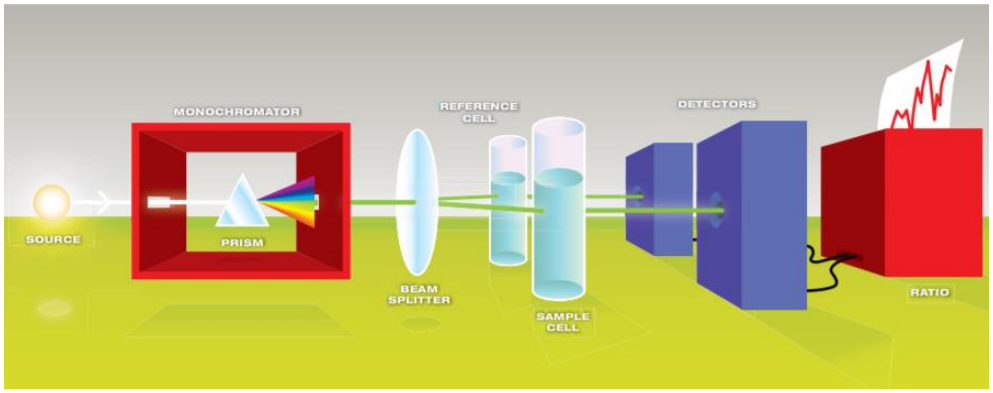

Figure 2.4 Schematic diagram of a UV-Visible spectrometer.

For liquids, the sample is held in an optically flat, transparent container, in our case in quartz, called a cell or cuvette. The reference cell or cuvette contains the solvent in which the sample is dissolved, and this is commonly referred to as the blank. For each wavelength the intensity of light passing through both a reference cell (I_0) and the sample cell (I) is measured. If $I \leq I_o$, then the sample has absorbed some of the light. The absorbance (A) of the sample is related to I and I_o according to the Equation 2.3:

$$A = \log_{10} \frac{I_0}{I} \qquad (2.3)$$

The detector converts the incoming light into a current, the higher the current the greater the intensity. The chart recorder usually plots the absorbance against wavelength in the UV and visible section of the electromagnetic spectrum.

Photoisomerization thus, was investigated by irradiating samples with a UV light source at 340 nm using a UV-1800 Shimadzu Spectrophotometer for the desired irradiation time and with scanning speed of 3'000 to 2 nm/min. The samples for UV-Visible spectroscopy were prepared via dilution of the sample into adequate solvent (DMSO) to give a final concentration in the range 0.9–2 g/L. UV-Visible spectra were recorded at room temperature (20 °C) in the wavelength range 190–600 nm using dissolved samples.
The photosensitive *E*-to-*Z* isomerization of dicarboxylic acid, the azobenzene-2,2′-dimethoxy-4,4′-dicarboxylic acid, at room temperature was studied via UV-Visible spectroscopy. Spectra were recorded with a UV-Visible spectrophotometer Shimadzu UV-1800 every 5 minutes over 30 minutes of total test. First, a 0.1% wt solution of the azobenzene-2,2′-dimethoxy-4,4′-dicarboxylic acid (0.05 g) in DMSO (25 mL) was prepared. The solution, kept in the dark, was first analysed at time t=0 then, to induce the isomerization, it was irradiated for 5 minutes with white light from an IDual bulb Adaptative LED (11W) and analysed again over the UV-Visible spectrometer. The process of analysis was repeated until the pss was reached.
The isomerization was studied assuming a first order kinetic (Equation 2.4):

$$v = -k\,[A] \qquad (2.4)$$

In the previous equation *v* is the *E-Z* isomerization rate, *k* is the rate constant and *A* is the concentration of the *E* (or *Z*) specie. The experimental data are, thus, analysed according to Equation 2.5.

$$In\frac{A_0 - A_\infty}{A_t - A_\infty} = k_i t \qquad (2.5)$$

where *t* is the irradiation time, A_0, A_t, and A_∞ are the *E* form absorbance corresponding to the time 0, t, and pps respectively.

The thermal back isomerization was studied via UV-Visible spectroscopy at 70°C and via NMR spectroscopy at different temperatures in order to study its kinetic. When the *Z*-to-*E* isomerization was studied with UV-Vis spectroscopy, the same DMSO solution prepared for the study of *E*-to-*Z* isomerization was used; an irradiated sample, which shows the absorption peaks characteristic for both *Z* and *E* isomers was considered as starting point. The sample was then placed in an oil bath heated at 70 °C and was analysed every 5 minutes until complete recovery of the *E* isomer was accomplished.

2.1.4 Fourier-Transform Infrared-Spectroscopy (FT-IR)

Infrared (IR) spectroscopy is one of the most common and widely used spectroscopic techniques employed mainly by inorganic and organic chemists to determine specific structures of compounds. Chemical compounds have different chemical properties due to the presence of different functional groups. In this technique infrared light (1-100 µm) interacts with a sample which can be solid or liquid. While a certain aliquot of the incident light goes through the sample, a certain amount gets absorbed by the molecules inside the sample. The absorption of IR light can be analysed in three ways by measuring absorption, emission and reflection. Each chemical bound can be visualized as a harmonic oscillator, whose resonant frequencies are related to the strength of the bond and the mass of the atoms at either side. Therefore, the frequency of vibration can be associated to a particular bond type and correlated to the presence of specific groups. Generally, stronger bonds and light atoms will vibrate at a high stretching frequency or wavenumber (1/h).

A common FTIR spectrometer consists of a source, interferometer, sample compartment, detector, amplifier, A/D convertor, and a computer as schematized in Figure 2.5. The source generates radiation which passes the sample through the interferometer which is used to split one beam of light into two so that the paths of the two beams are different and then they recombine into the detector.

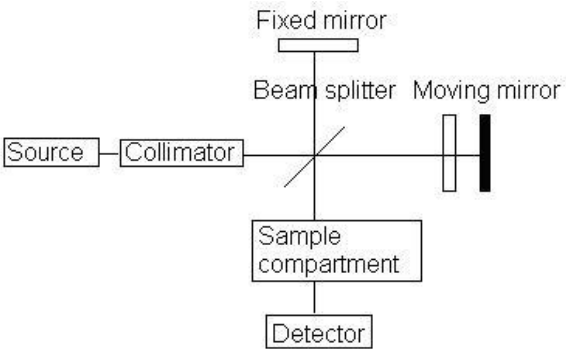

Figure 2.5 Schematized FT-IR spectrometer.

Then, the signal is amplified and converted to digital signal by the amplifier and analog-to-digital converter, respectively. The signal is transferred to a computer in which Fourier transform (FT) is carried out. The term FT-IR originates from the fact that a Fourier transform is required to convert the raw data into the actual spectrum. The interferogram obtained is a plot of the intensity of signal versus the optical path difference (OPD). Since a Fourier transform can be viewed as the inversion of independent variables of a function, the Fourier transform of the interferogram can be viewed as the inversion of the OPD. The unit of OPD is centimeter, so the inversion of OPD has a unit of inverse centimiters also known as wavenumbers.

In this work the infrared spectroscopy has been used qualitatively to determine mainly the progress of the reaction of chlorination and the degree of hydrolysis. All the FT-IR spectra were recorded at room temperature with a FT-IR spectrophotometer Bruker Vertex 70; the equipment has a resolution of 4 cm^{-1} in absorbance and transmittance modes and scanning speed of 2 mm/s. The spectrophotometer is equipped with an attenuated total reflection (ATR) tool with a diamond crystal.

2.1.5 Synthesis of 4,4′-bis(chlorocarbonyl)-2,2′-dimethoxy azobenzene (Azo-chloride)

The photo-sensitive monomer 4,4′-bis(chlorocarbonyl)-2,2′-dimethoxy azobenzene was synthesized in a two-steps procedure, which first involved the synthesis of azobenzene-2,2′-dimethoxy-4,4′-dicarboxylic acid (Azo-acid) and then, its conversion into the 4,4′-bis(chlorocarbonyl)-2,2′-dimethoxy azobenzene (Azo-chloride), through a slight modification of the procedure

reported in a paper from Tylkowski et al, in a paper from 2016.[10] In a typical experiment, 3.55 g (18.0 mmol) of 3-methoxy-4-nitrobenzoic acid were solubilized in a 14% wt solution of NaOH prepared via dissolution of 10 g (25 mmol) of NaOH in 60 mL of water. The mixture was heated until the solid completely dissolved. Then, a hot aqueous glucose solution (20 g of glucose in 30 mL water) was slowly added dropwise at 80 °C. A stream of air was passed into the mixture for 48 h. Then the solution was diluted with 200 mL millQ water and acidified with 25 mL glacial acetic acid, thus yielding ortho-substituted azobenzene-4,4′-dicarboxylic acid. The obtained orange solid was filtered, washed with 900 mL of distilled water and dried under vacuum at 40°C. ^{1}H-NMR (d-DMSO, TMS, δ ppm): 3.93 (s, 3H, -OCH_3); 7.50 (d 12 Hz, 1H); 7.62 (dd 12, 2 Hz, 1H); 7.74 (d, 2 Hz, 1H). ^{13}C-NMR (d-DMSO, TMS, δ ppm), 169.30 (s), 156.36 (s), 144.76 (s), 142.65 (s), 121.72 (s), 115.73 (s), 113.97 (s), 56.16 (s). Yield 49%. To get 4,4′-bis(chlorocarbonyl)-2,2′-dimethoxy azobenzene, 4,0 g (10.9 mmol) of ortho-substituted dicarboxylic acid was mixed with 15 mL of thionyl chloride and 0.2 mL of triethylamine. The mixture was heated on an oil bath up to 60 °C for three hours. Then, the solution was stirred overnight at room temperature. Unreacted thionyl chloride was removed by distillation under reduced pressure and the residue was washed with dry n-hexane (100 mL) and dried under vacuum at 40 °C. ^{1}H-NMR (d-CDCl3, TMS, δ ppm): 4.02 (s, 3H); 7.50 (d 12 Hz, 2H); 7.60 (dd 12, 2 Hz, 2H); 7.68 (d 2 Hz, 1H). Yield 92%.

2.1.6 Simulation study on ortho-substituted azobenzene photoisomerization

Simulation study and computational investigation of the two main electronic transitions of the modified azobenzene, to study its structural distortion and interconversion processes, were conducted in collaboration with Dr. Nuno A. Bandeira from the University of Lisbon. Herein, a computational characterization of the monomeric unit previously synthesized, the ortho-substituted azobenzene, was conducted to elucidate and predict its structural features in the microcapsules shell.

The dynamics of the photochemical and thermal processes were analysed by a potential energy surface analysis and by the calculation of the transition states (TSs), following both the inversion and rotation reaction coordinates and using spin flip time-dependent density functional theory (TDDFT) methodology.

The computational analysis was performed taking as a model 4,4'-(diazene-1,2-diyl)bis(3-methoxy-Nmethylbenzamide) but the obtained results can be considered valid also in the case of the 4,4'-(diazene-1,2-diyl)bis(3-methoxybenzoic acid) (Figure 2.6).

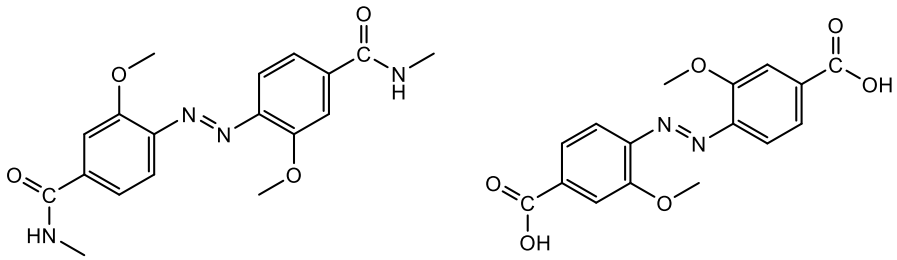

(*E*)-4,4'-(diazene-1,2-diyl)bis(3-methoxy-*N*-methylbenzamide) (*E*)-4,4'-(diazene-1,2-diyl)bis(3-methoxybenzoic acid)

Figure 2.6 Chemical structures of the two photo-responsive monomers of importance for the understanding of this chapter.

2.2 Results and discussions

2.2.1 Synthesis of 4,4′-bis(chlorocarbonyl)-2,2′-dimethoxy azobenzene

In a review from Hamon et al. a comprehensive overview on the different paths for the synthesis of azobenzene derivatives is provided (from 1998 to 2008).[7] In this study we selected one of those approaches, for the synthesis of ortho-substituted azobenzene which is thus conducted through reduction reactions of aromatic compounds having nitro groups. This strategy was already explored by Tylkowski et al.[10] to obtain a symmetrical modified azobenzene and a modified procedure is reported in the current section.[11] The synthetic procedure for the preparation of the photosensitive modified azobenzene, already described in the experimental section, is depicted in the Scheme 2.1 reported below.

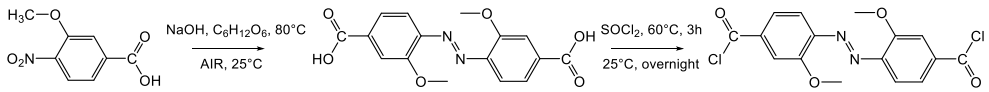

Scheme 2.1 Synthetic steps for the preparation of ortho-substituted azobenzene.

The azobenzene modified with two electron donating groups has been obtained via reduction of nitro compounds using glucose as a carbohydrate reducing

agent. The 3-methoxy-4-nitrobenzoic acid was easily solubilized in a 15% wt solution of NaOH and, when glucose was added dropwise, the reaction rapidly started, resulting in a change of colour; the reduction should lead to hydroxylamine as a reaction intermediate, as proposed by Gowda et al in 2003;[12] the hydroxylamine is then modified into an azo-dicarboxylic acid via further oxidation provided by bubbling air. In order to increase the yield of the final pure product, we slightly modified the existing procedure. It is, indeed, very important to control that the source of bubbling air is positioned in the middle of the reaction system, in order to obtain a homogeneous oxygenation and, thus, a high yield. To guarantee a complete and homogeneous oxidation, we also increased the permanence time of the flux of air into the system from 24 to 48h. The pure product was obtained and isolated through a first precipitation over acetic acid, non-diluted and added dropwise, and a second re-dissolution of the solid in a concentrated NaOH solution (15% wt); the product indeed, can precipitate in highly acidic (pH 1-2) or highly basic (pH 13-14) solutions while it dissolves in water. The pH of the reaction system was constantly checked via pH indicator. To avoid the dissolution of high percentages of the final product, the cleaning of the final product with high volume of water was eliminated. The yield of the obtained light orange precipitate is 49% which results to be higher if compared with previous reported strategies of synthesis. Figures 2.7 and 2.8 show the ^{1}H- and ^{13}C-NMR spectra of the azobenzene-2,2′-dimethoxy-4,4′-dicarboxylic acid in its E configuration with the corresponding assignments.

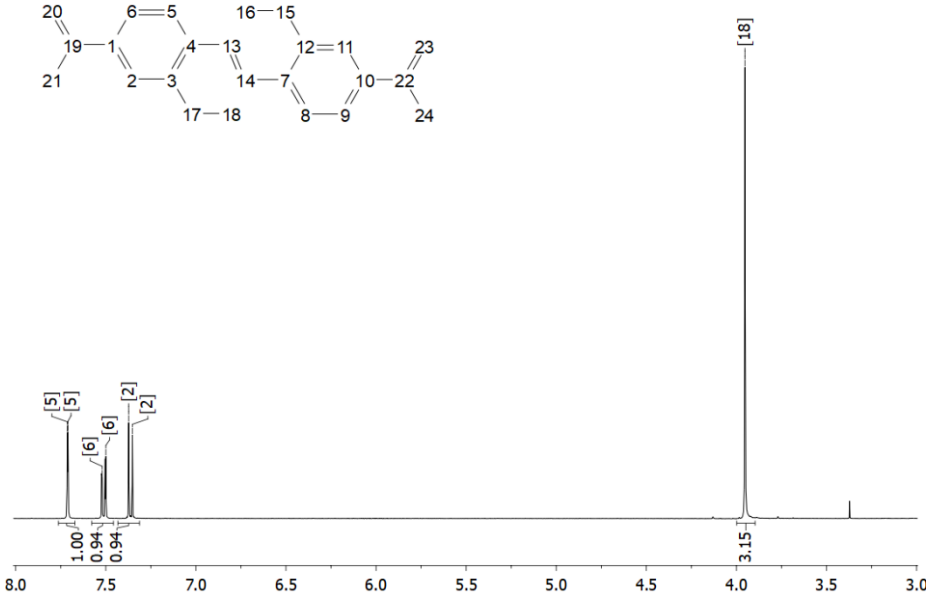

Figure 2.7 ^{1}H-NMR spectrum of azobenzene-2,2'-dimethoxy-4,4'-dicarboxylic acid.

The spectrum shows the typical peaks related to the methoxy group around 4 ppm and the peaks related to the aromatic protons between 7-8 ppm. The small peak at 3.33 ppm is characteristic of the residual water in d-DMSO.

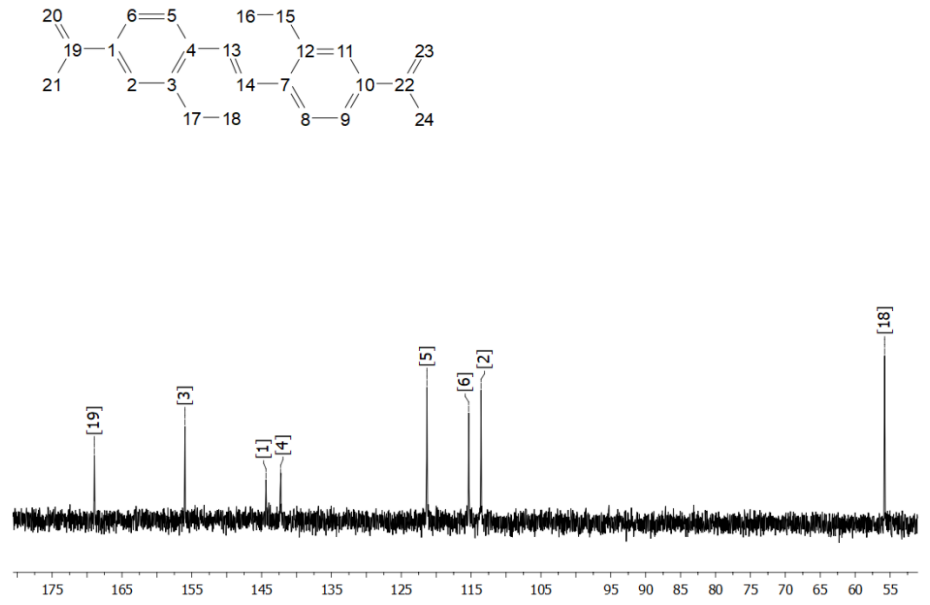

Figure 2.8 ^{13}C-NMR spectrum of azobenzene-2,2'-dimethoxy-4,4'-dicarboxylic acid.

The ^{13}C-NMR spectrum of this compound also shows its high purity and confirms the expected structure. The carboxylic carbon, as expected, falls around 170 ppm while the aromatic carbons appear in the broad range 140-110 ppm; the carbon from the methoxy group appear at 56 ppm.

Considering that the modified azobenzene inserted into the polymeric chain is a specie that contains both acidic and basic groups, special attention should be paid during procedures of precipitations and purification. The azobenzene-2,2'-dimethoxy-4,4'-dicarboxylic acid has a good solubility for intermediate values of pH ($3<pH<12$) while it precipitates at very high or very low values of pH. The strict control over pH, the precipitation of the molecule into both acidic and basic environments and the elimination of the rinsing with neutral water, results in an increase of the yield.

The subsequent conversion of the dicarboxylic acid into the acylic chloride is propaedeutic for the preparation of photosensitive polymers and microcapsules which will be analysed in the next chapters. The previously synthesized dicarboxylic acid was dried carefully and, once all the residual water was eliminated, it was dissolved in thionyl chloride. Thionyl chloride acts both as the solvent and the main reactant. Triethylamine was employed as a base, to neutralize the hydrochloric acid produced during the reaction of chlorination, facilitating the reaction to proceed to completion. The yield obtained for this reaction was 92%.

The NMR spectra of the azo-dichloride show the same peaks relative to the dicarboxylic acid; due to its instability and the ease of hydrolyzation of this molecule it was not further characterized, but the reaction was checked via FT-IR. In the Figure 2.9 the spectra of the modified azo-dicarboxylic acid (A) and of the corresponding obtained dichloride (C) are reported together to prove the completion of the chemical reaction.

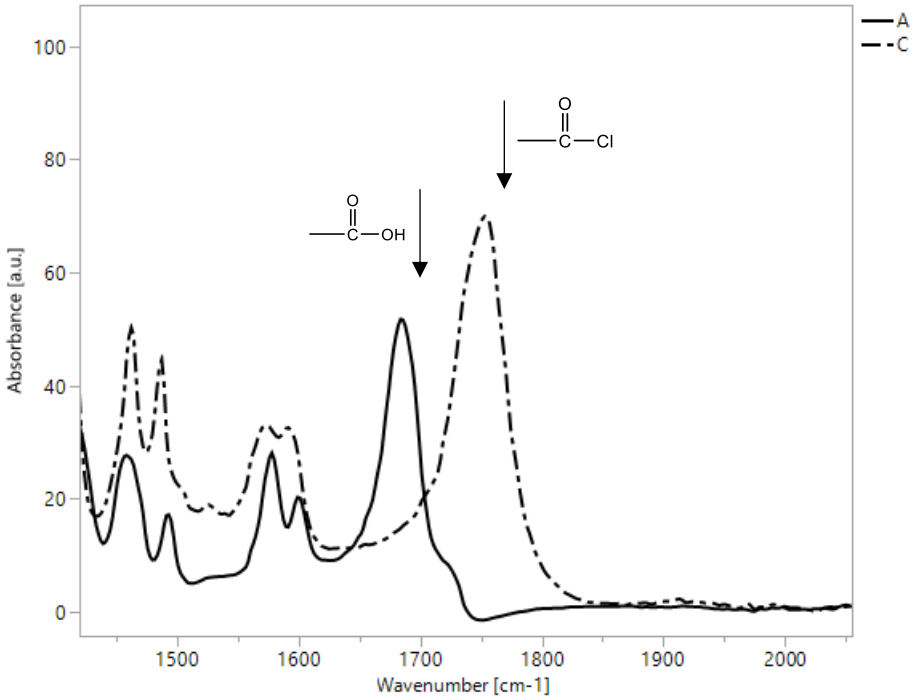

Figure 2.9 FT-IR spectra of A) azobenzene-2,2′-dimethoxy-4,4′-dicarboxylic acid and C) 4,4′-bis(chlorocarbonyl)-2,2′-dimethoxy azobenzene.

The carbonyl stretching (C=O) absorption is one of the strongest IR absorptions signal and, in the case of carboxylic acid, it is expected in the range 1780-1700 cm^{-1} as a singlet. In our case study, the peak relative to the C=O stretching appears at 1690 cm^{-1}. This peak is shifted at lower wavenumbers, if compared to what expected, due to the nature of the substituents to the carboxylic group; in the case of the molecules analysed in this study, the azobenzene-2,2′-dimethoxy-4,4′-dicarboxylic acid and the corresponding chloride, due to the aromatic ring linked to the C=O double bound, the inductive effect shifts the absorption to lower wavenumbers[12]. The second spectrum, C, indicated with the dashed black line, is characteristic of the azo-dichloride and, in this case, the peak relative to the carboxylic acid disappears leading to a new signal at 1760 cm^{-1}, characteristic of the C=O stretching of the acid halides, thus proving successful chlorination.

2.2.2 Simulation

A considerable number of computational studies have been devoted to the un-substituted azobenzene molecule with regards to its photoisomerization. [13–15] The *E-Z* photo-isomerization process can occur via two routes: excitation to a "symmetry forbidden" *n-π** state (S_1) that shows up in the visible region, or excitation of the system in the near-UV region to a *π-π ** state (S_2) revealing a large absorption intensity. It is interesting to notice that, in azobenzene, the quantum yield of the interconversion, is higher in S_1 (~0.3) than it is for S_2 (~0.2)[16], meaning that the probability to have interconversion is higher when the system gets irradiated to a *n-π** state. It is important to remember that the isomerization can follow two different reaction coordinates pathways: the dihedral torsion (CNNC) or the twisting of one of the rings (NNC) (Figure 2.10). It has been recently discovered[17] that excitation to the S_1 state goes through the rotational mechanism whereas through S_2 the pathway is bifurcated between rotation and a restricted pedal-like motion. When the system is excited to S_2, thus, it may revert to the *E* isomer and this explains the lower quantum yield of S_2.

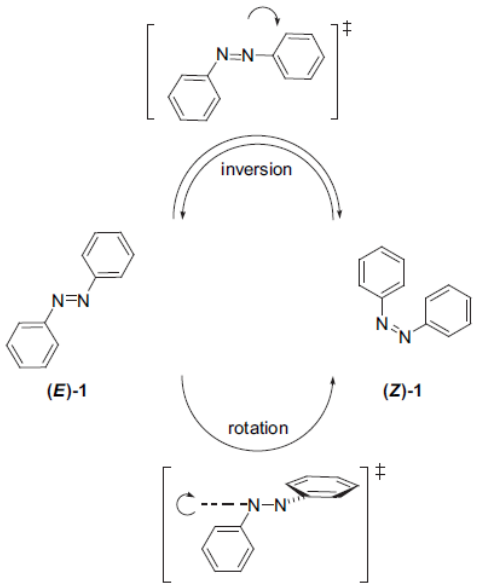

Figure 2.10 Mechanisms of photo-interconversion.

The computational analysis was performed taking as a model the 4,4′-(diazene-1,2-diyl)bis(3-methoxy-N-methylbenzamide) (A) as it can be seen from Figure 2.6. This molecule has been selected as representative repeating unit of the ortho-substituted azobenzene into a polymeric chain or network. In this case we used the molecule (A) obtained by reacting the Azo-chloride with amines; simulation studies on small molecules are, indeed, easier than simulation studies on polymers. Moreover, we decided not to run simulation studies on the Azo-acid to avoid hydrogen bonding interactions. The *Z* and the *E* forms of the molecule A have C_2 (planar structure) and C_{2h} (non-planar conformation) point group symmetries, respectively. As expected, the optimized minima of energy for the special configuration of the molecule, clearly show that there is a disparity in the chain lengths of each structure. This can be measured approximately by the distance between the distal carbons in each isomer. In the *E* form of A this value is 16.8 Å whereas in the *Z* form is 10.1 Å (Figure 2.11 a).

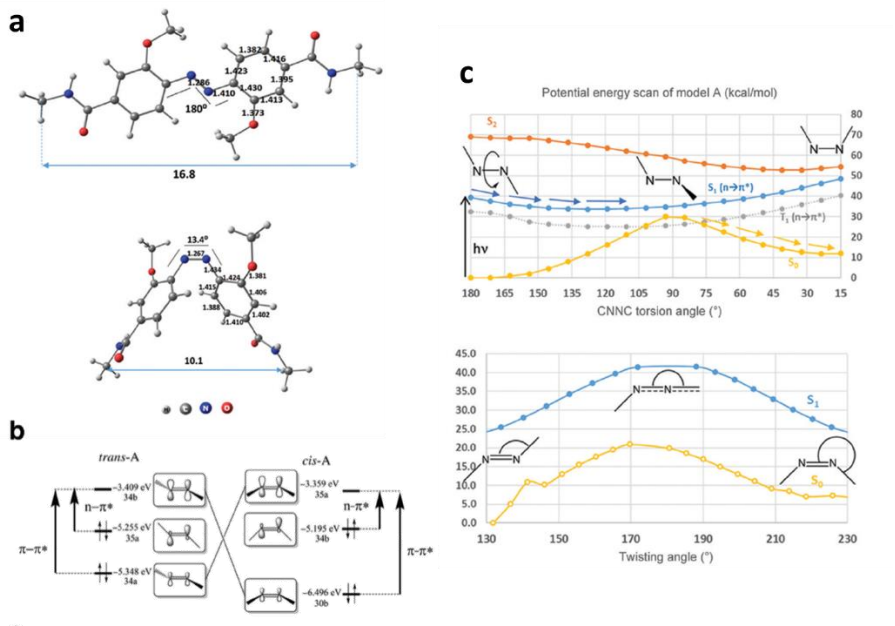

Figure 2.11 (a) Energetically optimized structures of E (above) and Z (below) 4,4′-(diazene-1,2-diyl)bis(3-methoxy-N-methylbenzamide) (A); (b) Kohn-Sham orbital energies and molecular orbital correspondence between both stereo-isomers; (c) potential energy surface scan as a function of the CNNC dihedral (above) and NNC angle (below) for the S_0, S_1 and S_2 states.

Moreover, it has been calculated that, for model A, the HOMO-LUMO gaps are larger by 10 meV for the *E* isomer than for the *Z* structure; a similar trend is also present in azobenzene and this reinforces the evidence that E isomer is more stable than the Z (Figure 2.11 b).

To obtain a good understanding of the isomerization pathways and energy requirements for structural transformations for model A, a reaction coordinate potential energy surface (PES) scan[18,19] was performed on the ground S_0, first excited states S_1 and S_2.

The photochemical excitation of S_0 to S_1 allows for an easy (CNNC) dihedral angle rotation as the S_1 potential energy surface is quite shallow (Figure 2.11 c) based on the weaker π bond, allowing the system to relax into the *Z* form. The S_2 surface is shaped as a reversed 'S' and goes downhill from the *E* geometry into a minimum at approximately (CNNC)=45º from which point it will decay radiatively. At (CNNC)=90º there is a conical intersection from the S_1 surface to S_0 and the system undergoes a non-radiative decay to the *Z* form. In addition, the electron may also undergo a transition radiatively from S_2 to the S_1 curve, cross over to S_0 and thermally relax either to the *Z* or *E* isomers. Considering the (NNC) angle twisting or inversion mechanism it may seem from the PES that the straightforward photochemical process is not possible via the S_1 surface since, like S_0, it requires thermal activation.

Pursuing the (NNC) reaction coordinate through the S_1 curve causes the (CNNC) dihedral to loosen; the distinction between the geometries start to become confused and the difference between the PES associated with a *Z* or *E,* decrease. It means that the twisting coordinate may take part to the interconversion, but only if it is associated with the dihedral rotation coordinate at some point during the isomer switching reaction; only if this happen it can become energetically viable.

From TDDFT single point calculation it is possible to obtain interesting information; the absorption intensities of the *E*-isomer are larger in the visible region since this transition is allowed by symmetry. Moreover, the energies of the thermal interconversions show that the inversion barrier is energetically preferred over the rotational one (respectively 26 kcal/mol and 33kcal/mol); the photochemical activation is thermally more favourable through the rotation

mechanism (whether through S_1 or S_2) whereas the inversion mechanism always requires a greater vibrational stimulus in the form of heat to operate.

The simulation study reported in this chapter, developed in collaboration with Prof. Bandeira from the University of Lisbon, was published, by our research group, in a recent paper.[11]

2.2.3 Photosensitive behaviour

The absorption spectrum of the azobenzene-2,2′-dimethoxy-4,4′-dicarboxylic acid dissolved in DMSO and kept in the dark, is analysed via UV-Visible spectroscopy and reported in the Figure 2.12. The isomer is in its *E* configuration. The UV–Vis absorption spectra exhibit two characteristic and well separated absorption bands. The first characteristic absorption band, related to the strong π–π^* transitions of E isomer, is present around 315 nm. The absorption originating from the forbidden symmetry of n–π^* transitions, is present around 400 nm. Through spectroscopic measurements it is possible to develop a theoretical calculation for the study of the kinetics of photoisomerization and thermal relaxation, as also reported by Jerca et al.[20]

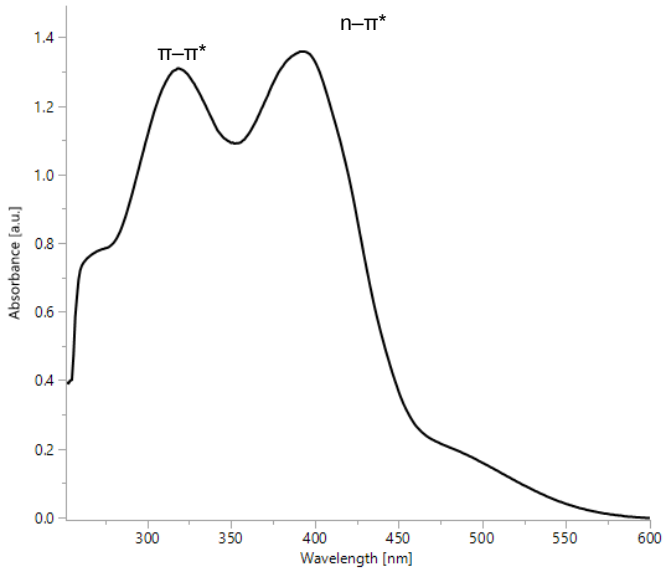

Figure 2.12 UV-Visible spectrum of the ortho-substituted azobenzene in its E configuration.

The sample in solution was irradiated for 5 minutes and the spectrum was recorded again. This process was repeated until the photo stationary state was reached. Every switchable sample in fact will reach, under illumination, an

equilibrium, called photo-stationary state, associated with a steady-state *E-Z* composition. Such composition depends on the competing effects of photoisomerization, quantum yield, thermal relaxation, and *Z* reconversion upon light absorption. The steady-state composition is unique for each system. The spectra recorded for the *E*-to-*Z* isomerization with white light are reported in Figure 2.13. As it is possible to see from the graph, under white light irradiation both bands are slightly red-shifted and, while the intensity of the *π*-*π** absorption band gradually decreases with the irradiation time, the *n*–*π** absorption band increases, until the photo-stationary state is reached.

The photoisomerization kinetic of the azo-monomer, obtained by monitoring the absorbance of *π*–*π** absorption band at 394 nm, is reported in the inset in Figure 2.13. As already described in the experimental section, the isomerization was studied assuming a first order kinetic, analysing the experimental data according to Equation 2.5 and reported here for simplicity.

$$In\frac{A_0 - A_\infty}{A_t - A_\infty} = k_i t \qquad (2.6)$$

where *t* is the irradiation time, A_0, A_t, and A_∞ are the *E* form absorbance corresponding to the time 0, t, and pss respectively. As it is possible to notice from the inset in Figure 2.15, the plot of Equation 2.6 has a linear fit, and the obtained photoisomerization constants is k_i equal to 3.1 x 10^{-3} s^{-1}.[20]

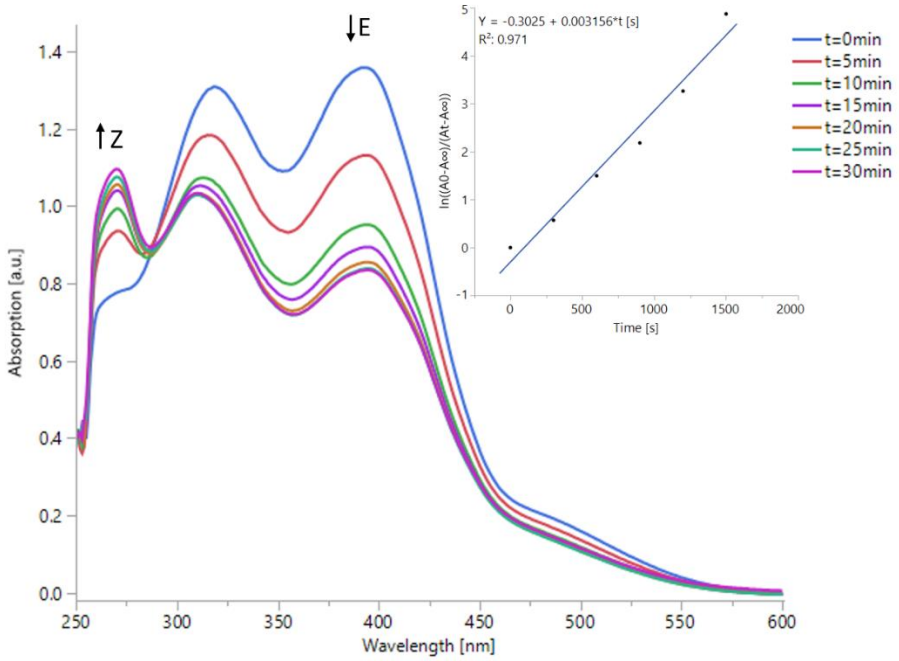

Figure 2.13 Changes in the UV-Visible absorption spectra of the ortho-substituted azobenzene in DMSO at 20°C during E-Z photoisomerization. Inset shows the first order plot for E-Z isomerization.

It is expected that under moderate irradiation, the composition of the pps should be predominantly Z for azobenzenes, mixed for aminoazobenzenes, as it is our case, and predominantly E for pseudo-stilbenes.[21]

With reference to Figure 2.13, the pss of the selected molecule in DMSO, is reached after 30 minutes irradiation; the content of the Z-isomer at the pss was determined using Equation 2.7:

$$Z\%_{UV-Vis} = \frac{A_0 - A_{pps}}{A_0} \qquad (2.7)$$

where A_0 and A_{pps} represent the absorbance at λ_{max} for *E* isomer before and after irradiation with white light, respectively. Given the experimental conditions of complete darkness for the preparation of the analyzed molecule, we assume that the sample is only composed by molecules in *E* configuration.

According to Equation 2.7, the sample obtained at the pss is a mixture that contains approximately 40% *Z* and 60% *E* isomers as it is possible to calculate from the relative intensities of the absorption peaks of the *E* and *Z* isomers.

As for the kinetics of the isomerization, also the thermal relaxation process, can be conveniently studied *via* absorption spectroscopy. The thermal back isomerization was, indeed, studied via UV-Visible spectroscopy at 70 °C. The spectra, recorded every 10 minutes, are reported below in Figure 2.14; in this case the analysis is performed over 50 minutes. Our study on the modified azobenzene isomerization, has been reported in a recently published paper.[11]

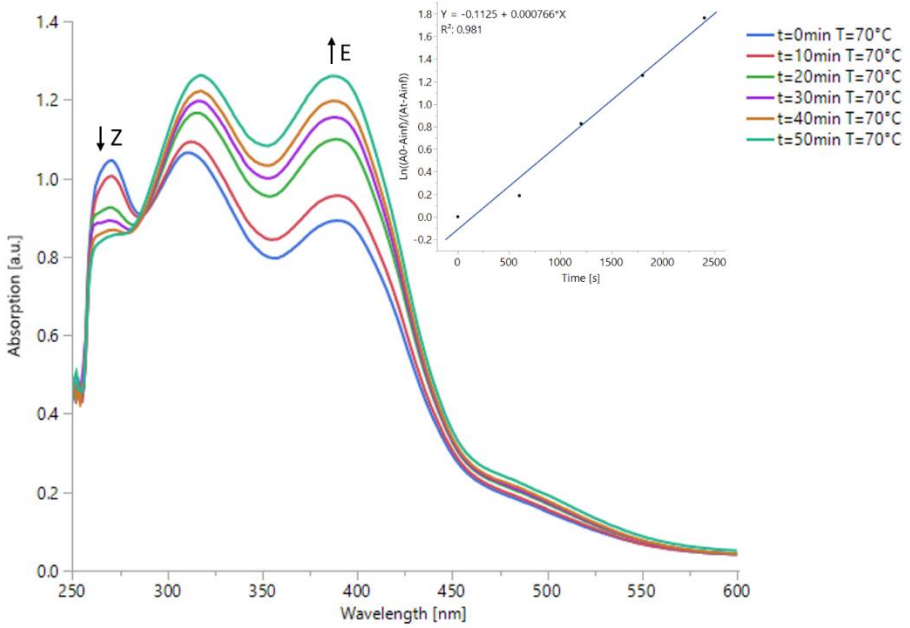

Figure 2.14 Changes in the UV-Visible absorption spectra of the ortho-substituted azobenzene in DMSO at 70°C during Z-E isomerization. Inset shows the first order plot for Z-E isomerization.

The percentage of *Z* isomer in the mixture, after exposure to high temperature, was evaluated taking into account the absorption peak of the *Z* isomer calculated via UV-Visible spectroscopy. Considering the Equation 2.6 for the calculation of the percentage of the *Z* isomer left into the mixture, we found that after 30 minutes of heating at 70°C, 20% of the *Z* isomer is still into the mixture. The kinetic of this process, underlined also in the inset in Figure 2.14, is slow and shows a kinetic constant k_r of 7.66 x 10^{-4} s^{-1}.

In addition, in the following section of this work, the kinetics of thermal back isomerization will also be studied *via* NMR spectroscopy.[22,23] The behaviour of *Z* ortho-substituted azobenzene in solution, kept in the dark, at 30, 50, 60, and 70 °C was studied recording ^{1}H-NMR spectra at each temperature, every 10

minutes, and assuming the isomerization process to have a first order kinetic (Equation 2.8).

$$v = -k\,[A] \qquad (2.8)$$

where, in this case, *v* is the *Z*-*E* isomerization rate at each temperature, k_r is the thermal relaxation kinetic constant and *A* is the area of the ^{1}H-NMR peak selected as reference for the calculation; it represents the concentration of a specific proton in the selected isomer. The same proton in the two isomers, *Z* and *E*, shows the signals at different chemical shifts. It is worth, thus, to report first, the ^{1}H-NMR spectra of the previously synthesized ortho-substituted azobenzene as an overlap between the irradiated and not irradiated sample (*Z* and *E* isomer respectively). From the comparison of the two spectra, it is possible to assign, to each proton, the corresponding peak related to its *E* or *Z* isomer.

In Figure 2.15 it is reported, with a black curve, the ^{1}H-NMR spectrum of the *E* isomer; its chemical structure is also reported in black. In the same figure, the red curve represents the spectrum of the irradiated sample (30 minutes irradiation), whose structure is indeed also schematized in red. As a consequence of the photoisomerization, the peaks relative to the aromatic hydrogens of the *E* isomer duplicate; the peaks of the *E* isomer keep their original positions at around 7.7 (d), 7.5 (dd) and 7.3 (d) but new peaks relative to the same aromatic hydrogens from the *Z* isomer appear around 7.4 (d), 7.2 (dd) and 6.3 (d) ppm. The signal of the methoxy hydrogens splits in two and it shows up at 3.9 ppm for the *E* isomer and at 3.6 ppm for the *Z* isomer.

The inset shows a magnification of the aromatic peaks with the ppm specified for each signal.

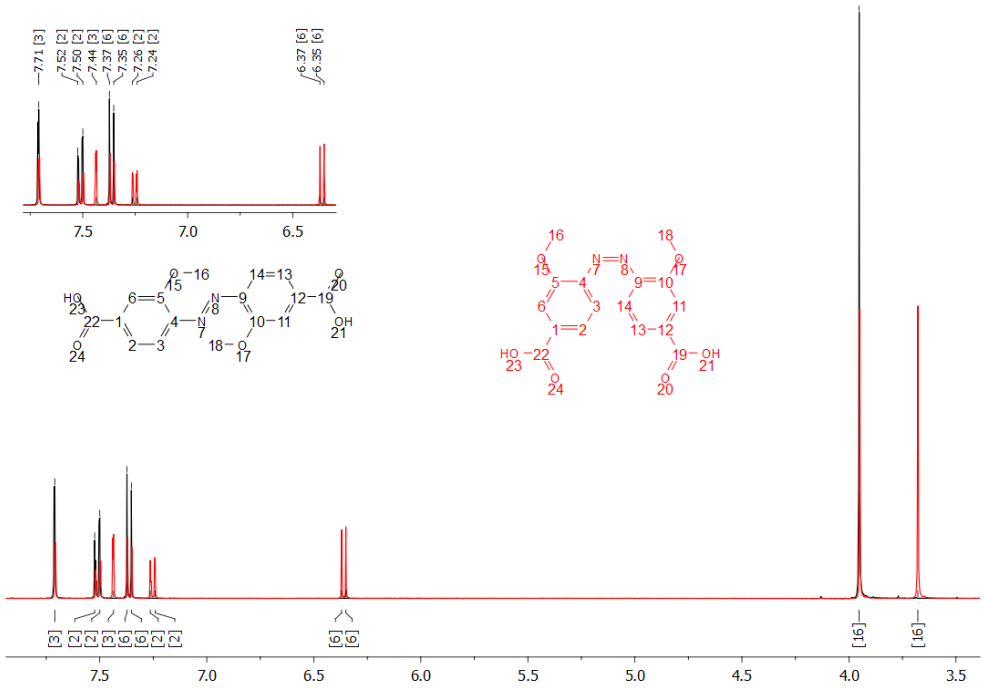

Figure 2.15 ^{1}H-NMR spectra of E- (black) and Z- (red) ortho-substituted azobenzene. In the inset are reported the ppm of the aromatic protons.

To study the kinetic of thermal back isomerization and to calculate the activation energy of the thermal relaxation process, the peak at 3.66 ppm, corresponding to the methoxy group of the *Z* ortho-substituted azobenzene was selected as reference.

At room temperature (20 ± 2 °C), the comparison of the areas of the peaks at 3.93 ppm (A_E) and 3.66 ppm (A_Z) (Equation 2.9), which correspond to the protons of the methoxy group in the *E* and *Z* configuration respectively, shows that after 30 min of sunlight exposure the azobenzene-2,2'-dimethoxy-4,4'-dicarboxylic acid is 50 % in its *Z* form.

$$Z\%_{NMR} = \frac{A_Z}{A_Z + A_E} \qquad (2.9)$$

The experimental data of the thermal back isomerization were analysed considering a first order kinetic[24] and the values for the kinetic constants in d-DMSO were calculated according to the Equation 2.4-2.5 (Figure 2.16). The k_r

values recorded at 70 and 30 °C, ranged between 1.3×10^{-3} and 1.0×10^{-5} s^{-1}, and are in agreement with literature findings.[1,20]

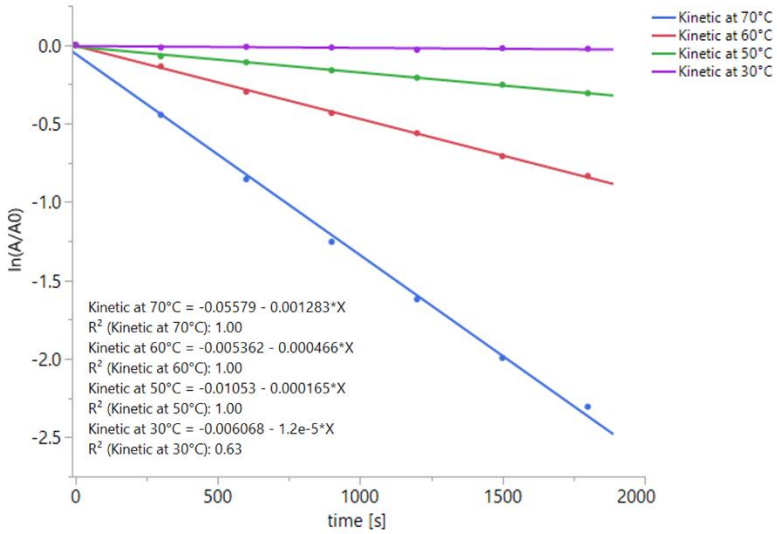

Figure 2.16 Slopes of the kinetics of thermal back isomerization of a 50% E-Z mixture of ortho-substituted azobenzene, at 30, 50, 60, and 70 °C. The A_i refer to the intensities of the ^{1}H-NMR peaks of the methoxy hydrogens of the Z isomer of the molecule.

As expected, the thermal back relaxation at 30° C is very slow and after 30 min only 2.4 % of the *Z* isomer in the starting mixture has reverted to *E*. However, the kinetics at higher temperatures is much more representative of the thermal process as expected: as a matter of example, Figure 2.17 shows the ^{1}H-NMR spectra in d-DMSO of azobenzene-2,2′-dimethoxy-4,4′-dicarboxylic acid recorded in darkness at 70 °C at different times comprised between t = 0 (soon afterwards 30 min sun exposure) and t = 30 min. The inset shows the magnification of the peak at 3.66 ppm which corresponds to the methoxy group of the *Z*-ortho-substituted azobenzene. At this temperature, higher rate of isomerization was found and, after 30 min of heating, only approximately 9% of the *Z* isomer remained in the studied mixture.

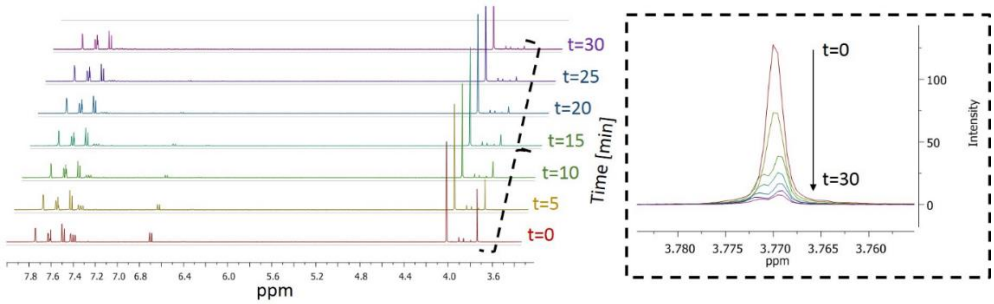

Figure 2.17 Kinetic of thermal back isomerization calculated via ^{1}H-NMR at 70^{o}C starting from a mixture of E and Z isomers of the ortho-substituted azobenzene.

In addition, the activation energy of the thermal back isomerization was determined by measuring the temperature dependence and fitting the data according to Arrhenius equation:

$$k = Ae^{-\frac{E_a}{RT}} \qquad (2.10)$$

where E_a is the activation energy of the thermal process, R is the universal gas constant, k is the constant rate at each temperature T expressed in K. The activation energy E_a exhibited a value of 105 kJ/mol, that is comparable with other values reported in literature.[24,25]

The amount of Z isomer left into the system is higher than the one calculated via NMR analysis where, after 30 minutes heating, only 9% of Z isomer is left. To reach the same percentage of conversion the sample needed to be heated and analysed for additional 20 minutes. The different results obtained for the same process analysed with two different techniques is very likely due to the different experimental conditions; while with the NMR equipment the temperature is kept constant and carefully controlled inside a heating chamber, with UV-Visible spectrophotometer there is no temperature control and the sample was heated in an external oil bath. To measure the absorption spectrum the sample was then removed from the oil bath and kept at room temperature for 10 minutes during each measurement. Due to the absence of temperature control, the system needs longer exposure to high temperature (or higher temperatures of exposure) to reach comparable extent of back isomerization.

2.3 Conclusions

In this chapter we reported the synthesis and characterization of the azobenzene-2,2′-dimethoxy-4,4′-dicarboxylic acid and its subsequent conversion into the corresponding chloride, the 4,4′-bis(chlorocarbonyl)-2,2′-dimethoxy azobenzene; this last molecule is propaedeutic for the preparation of photosensitive linear polymers or crosslinked nets which will be explored in the next chapters. The structure and the purity of the photosensitive di-carboxylic acid was confirmed by means of NMR spectroscopy. As expected, the 2,2′-dimethoxy-4,4′-dicarboxylic acid exhibit *E–Z* photoisomerization triggered by absorption of white light, as demonstrated via UV-Visible spectroscopy and NMR analysis.

Photoisomerization kinetics was studied at 20 °C in DMSO via UV-Visible spectroscopy; the kinetic of *E-Z* isomerization is fast with a rate constant of 3.1 x 10^{-3} s^{-1}. The pps is reached after 30 minutes with 60% of *E-Z* conversion. It is important to underline that 20% of the conversion is reached after only 5 minutes of light irradiation. The kinetics of *Z-E* thermal back isomerization was studied both via ^{1}H-NMR analysis at different temperatures and via UV-Visible spectroscopy at 70 °C. As expected, while the back isomerization at 30 °C is very slow with a rate constant of 1.0×10^{-5} s^{-1}, at 70 °C it is faster with a rate constant of 1.3×10^{-3}. The activation energy for the *Z-E* conversion is 105 kJ/mol.

From simulation studies, conducted in collaboration with the University of Lisbon, we collected information about the geometries of the molecule before and after isomerization; as expected, the optimized minima of energy for each configuration, clearly show that there is a disparity in the lengths of each structure and the distance between the distal carbons in each isomer is 16.8 Å for the *E* form and 10.1 Å for the *Z* isomer. The photosensitive molecule was also computationally analysed with regards to the energy involved in the mechanism of isomerization. We found that the rotation mechanism is the most favourable photochemically, while the inversion mechanism is much more favored in the case of *Z-E* reconversion.

The synthesized molecule, with its capabilities to undergo a fast isomerization associated with geometrical change and possible free volume change, could

therefore be considered as a good candidate to constitute the main building block of the shell of photoactive microcapsules for light-triggered release.

Bibliography

1. Beharry, A. A., Sadovski, O., Woolley, G. A. Azobenzene Photoswitching without Ultraviolet Light. *J. Am. Chem. Soc.* **133**, 19684–19687 (2011).
2. Giamberini, M., Prieto, S. F., Tylkowski, B. *Microencapsulation: Innovative Applications*. Walter de Gruyter GmbH & Co KG, (2015).
3. Zollinger, H. *Color Chemistry: Syntheses, Properties, and Applications of Organic Dyes and Pigments*. John Wiley & Sons, (2003).
4. Jia, S., Fong, W.-K., Graham, B., Boyd, B. J. Photoswitchable Molecules in Long-Wavelength Light-Responsive Drug Delivery: From Molecular Design to Applications. *Chem. Mater.* **30**, 2873–2887 (2018).
5. Forber, C. L., Kelusky, E. C., Bunce, N. J., Zerner, M. C. Electronic spectra of cis- and trans-azobenzenes: consequences of ortho substitution. *J. Am. Chem. Soc.* **107**, 5884–5890 (1985).
6. Sadovski, O., Beharry, A. A., Zhang, F., Woolley, G. A. Spectral Tuning of Azobenzene Photoswitches for Biological Applications. *Angew. Chem. Int. Ed.* **48**, 1484–1486 (2009).
7. Hamon, F., Djedaini-Pilard, F., Barbot, F., Len, C. Azobenzenes—synthesis and carbohydrate applications. *Tetrahedron* **65**, 10105–10123 (2009).
8. Hartley, G. C. The Cis-form of Azobenzene. *Nature* **140**, 281–281 (1937).
9. Kienzler, M. A., Reiner, A., Trautman, E., Yoo, S., Trauner, D., & Isacoff, E. Y. A Red-Shifted, Fast-Relaxing Azobenzene Photoswitch for Visible Light Control of an Ionotropic Glutamate Receptor. *J. Am. Chem. Soc.* **135**, 17683–17686 (2013).
10. Tylkowski, B., Giamberini, M., Underiner, T., Prieto, S. F. & Smets, J. Photo-Triggered Microcapsules. *Macromol. Symp.* **360**, 192–198 (2016).
11. Del Pezzo, R., Bandeira, N. A., Trojanowska, A., Prieto, S. F., Underiner, T., Giamberini, M., & Tylkowski, B. Ortho-substituted azobenzene: shedding light on new benefits. *Pure Appl. Chem.* **0**, (2018).
12. Brand, J. C. D., Eglinton, G. Applications of spectroscopy to organic chemistry. (1965).
13. Biswas, N., Umapathy, S. Density Functional Calculations of Structures, Vibrational Frequencies, and Normal Modes of trans- and cis-Azobenzene. *J. Phys. Chem. A* **101**, 5555–5566 (1997).

14. Zhou, Q., Fursule, I., Berron, B. J., Beck, M. J. Toward Spatiotemporally Controlled Synthesis of Photoresponsive Polymers: Computational Design of Azobenzene-Containing Monomers for Light-Mediated ROMP. *J. Phys. Chem. A* **120**, 7101–7111 (2016).
15. Staniszewska, M., Kupfer, S., Łabuda, M., Guthmuller, J. Theoretical Assessment of Excited State Gradients and Resonance Raman Intensities for the Azobenzene Molecule. *J. Chem. Theory Comput.* **13**, 1263–1274 (2017).
16. Bortolus, Pietro., Monti, Sandra. Cis-trans photoisomerization of azobenzene. Solvent and triplet donors effects. *J. Phys. Chem.* **83**, 648–652 (1979).
17. Casellas, J., Bearpark, M. J., Reguero, M. Excited-State Decay in the Photoisomerisation of Azobenzene: A New Balance between Mechanisms. *Chemphyschem Eur. J. Chem. Phys. Phys. Chem.* **17**, 3068–3079 (2016).
18. Gagliardi, L., Orlandi, G., Bernardi, F., Cembran, A., Garavelli, M. A theoretical study of the lowest electronic states of azobenzene: the role of torsion coordinate in the cis–trans photoisomerization. *Theor. Chem. Acc.* **111**, 363–372 (2004).
19. Steinwand, S., Halbritter, T., Rastädter, D., Ortiz-Sánchez, J. M., Burghardt, I., Heckel, A., & Wachtveitl, J., Ultrafast Spectroscopy of Hydroxy-Substituted Azobenzenes in Water. *Chem. – Eur. J.* **21**, 15720–15731 (2015).
20. Jerca, F. A., Jerca, V. V., Anghel, D. F., Stinga, G., Marton, G., Vasilescu, D. S., Vuluga, D. M., Novel Aspects Regarding the Photochemistry of Azo-Derivatives Substituted with Strong Acceptor Groups. *J. Phys. Chem. C* **119**, 10538–10549 (2015).
21. Mahimwalla, Z., Yager, K. G., Mamiya, J. I., Shishido, A., Priimagi, A., Barrett, C. J. Azobenzene photomechanics: prospects and potential applications. *Polym. Bull.* **69**, 967–1006 (2012).
22. Magennis, S. W., Mackay, F. S., Jones, A. C., Tait, K. M., Sadler, P. J. Two-Photon-Induced Photoisomerization of an Azo Dye. *Chem. Mater.* **17**, 2059–2062 (2005).
23. Beltrame, P. L., Paglia, E. D., Castelli, A., Tantardini, G. F., Seves, A., & Marcandalli, B., Thermal cis-trans isomerization of azo dyes in poly(methyl

methacrylate) matrix: A kinetic study. *J. Appl. Polym. Sci.* **49**, 2235–2239 (1993).

24. Whitten, D. G., Wildes, P. D., Pacifici, J. G., Irick, G. Solvent and substituent on the thermal isomerization of substituted azobenzenes. Flash spectroscopic study. *J. Am. Chem. Soc.* **93**, 2004–2008 (1971).

25. Matczyszyn, K., Bartkowiak, W., Leszczynski, J. Influence of the environment on kinetics and electronic structure of asymmetric azobenzene derivatives — experiment and quantum-chemical calculations. *J. Mol. Struct.* 565–566, 53–57 (2001).

3. Preparation of photosensitive capsules via emulsification and phase inversion precipitation

Benefit agents, such as perfumes, drugs, flavours, vitamins, etc., are expensive and they can be less effective when employed at high levels in compositions. Also, they can be incompatible when in contact with other components in a specific formulation or with the external environment. As a result, the idea is to maximize the effectiveness of such benefit agents via different approaches. One method to protect the active agent is thus, to improve its retention during the preparation of the formulation and during the aging into the finished product (FP) through encapsulation. A protective layer to the active material can thus not only improve the retention of the active, but also prevent it from being lost and wasted during post-applications, improving the delivery efficiency. Encapsulation is an effective way to reach this goal.

In the Procter & Gamble (P&G) company and in many of their consumer good products, microcapsule technology is widely used and, new alternatives for capsule preparation as well as for capsule release mechanism are being currently explored. Since in this work we are interested in perfume encapsulation, we can refer to the obtained system with the acronym PMC, which stands for perfume micro-capsules.

In this chapter we want to explore the possibility to obtain PMC with physical encapsulation methods, which means starting from a pre-existing, previously synthesized polymeric chain. For this objective, first photosensitive oligomers, containing the ortho-substituted azobenzene molecule in the main chain, were synthesized. Indeed, we will explore the preparation of photosensitive polymeric chains *via* reaction of the previously synthesized photo-sensitive 4,4′-bis(chlorocarbonyl)-2,2′-dimethoxy azobenzene and commercially available monomers used as diols spacers.

Polymeric PMCs were prepared *via* emulsification and phase inversion precipitation; the emulsification or droplet formation was explored and proposed through different techniques, namely, flow-focusing and spray gun. In order to reach good mechanical and chemical stability of the PMC, in some cases, a

commercially available polymer, polysulfone, was used in blend with the synthesized photosensitive oligomer.

3.1 Experimental

3.1.1 Materials

The commercial polymer used in this work is the Polysulfon (PSf) provided by Sigma Aldrich as transparent pellets (average Mw ~35,000), while the solvent used are dimethylformamide (DMF), N-methyl pyrrolidone (NMP), dichloromethane (DCM), Toluene, Diethyl ether (98%), all anhydrous and all provided by Sigma Aldrich, with purity 99.8%. Voyager Zen, the encapsulated perfume, was prepared and supplied by the P&G Company. 1,8-octanediol (98%), resorcinol (99%), 1,4-cyclohexandiol (99%), dimethylamino pyridine (DMAP) (>99%), sodium hydroxide (NaOH) (98%) were provided by Sigma Aldirich as fine solid powders. Pyridine (Py) (98%) and benzyltriethylammonium chloride (99%) were provided by Sharlabs.

3.1.2 Methods

3.1.2.1 Synthesis of photosensitive linear oligomers based on ortho-substituted azobenzene monomeric units.

The design of the synthesized polymer was intended to incorporate a light sensitive moiety into a polymeric chain. The light-sensitive monomer to be incorporated, was synthesized with a two-step procedure reported in Chapter 2, that yields 4,4'-bis(chlorocarbonyl)-2,2'-dimethoxy azobenzene, an azobenzene derivative. The synthesis of the photosensitive oligomer was conducted using also one linear monomer, the 1,8-octanediol, and two different bent spacers to generate, thus, polymer P1, when resorcinol was used as bent monomer, and polymer P2 containing the 1,4-cyclohexanediol. The two repeating units are reported in the Figure 3.1.

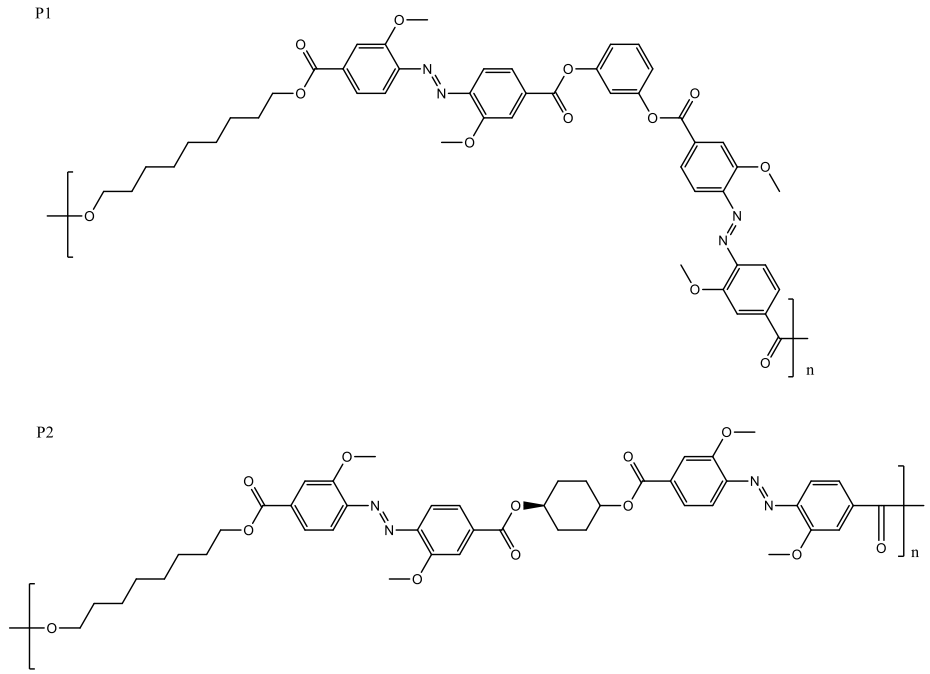

Figure 3.1 P1 (with resorcinol) and P2 (with 1,4-cyclohexanediol) repeating units of the photosensitive polyesters based on ortho-substituted azobenzene molecules.

The oligomers were prepared according to the procedures reported below.

3.1.2.1.1 Liquid–liquid interfacial polyesterification

First, we tried to obtain the polyester formation *via* liquid–liquid phase-transfer-catalyzed interfacial polyesterification.

The -OH group/chloride ratio was kept at 1:1 in an attempt to get high molecular weight. 5.0 mmol of OH terminated monomers were selected and split as follows: 1.5 mmol of the bent monomer, corresponding to 0.165 g when resorcinol was used and to 0.174 g when the cyclohexane-4,4'-diol was used, and 3.5 mmol of the linear spacer, 1,8-octanediol (0.511 g), so that the ratio between the bent and the linear monomer used is always 3:7. The total amount of OH-terminated monomers was solubilized into 20 mL of 0.5 mol/L aqueous sodium hydroxide solution. The mixture was then added into an open reactor containing 31 mL of ice-cold water, 47 mL of 1,2-dichloroethane and 1.0 mmol of benzyltriethylammonium chloride (0.35 g) as a phase-transfer catalyst, stirred at 500 rpm. After 10 minutes of stirring, a solution of the photosensitive chloride (1.83 g, 5.0 mmol) in 31 mL of 1,2-dichloroethane, was added dropwise to the system. The reaction was performed at room temperature, stirring at 400

rpm for 72 h and was monitored using thin-layer chromatography on silica plate with a mobile phase composed by hexane/propylene glycol/dichloromethane in proportion 2.5/5/2.5. The scheme of reaction is reported below in Scheme 3.1.

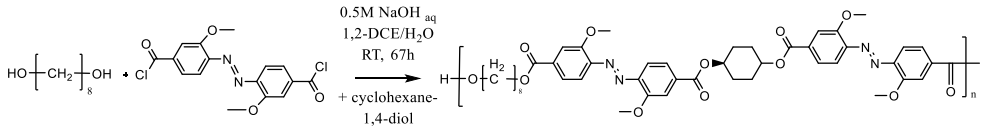

Scheme 3.1 Scheme of polyesterification reaction via liquid-liquid phase transfer catalyzed mechanism.

The organic phase was precipitated in methanol and dissolved again in chloroform; the procedure of purification was repeated 3 times. The product was finally vacuum-dried; with this first attempt of polymerization only 400 mg of product were obtained with a yield of 16%.

3.1.2.1.2 Single-phase polyesterification

With a second different approach of polymerization, the esterification in a single-phase reaction was performed. First the solubility of the monomers involved in the polymerization, was tested in different solvents. All solubility tests are performed solubilizing 5,0 mg of sample in 3 mL of solvent.

Also in this case the ratio between the bent and the linear OH terminated spacers was 3:7 and the stochiometric ratio between the dichloride and the dihydroxy spacers was 1:1. The scheme of reaction is reported below in Scheme 3.2.

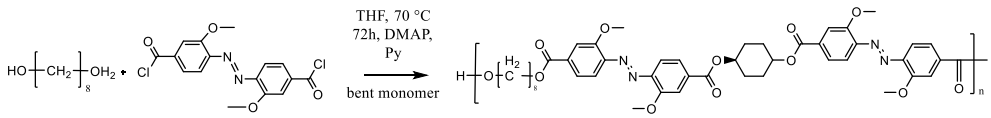

Scheme 3.2 Scheme of polyesterification reaction via single phase mechanism.

1.64 mmol of the bent OH-terminated monomer (0.180 g for resorcinol and 0.190 g for cyclohexane-4,4'-diol) were dissolved in the dry selected solvent (dichloromethane (DCM, bp 40°C), tetrahydrofuran (THF, bp 66°C), Toluene (bp 111°C), N-Methyl Pyrrolidone (NMP, bp 202°C) were used as solvents), together with 3.8 mmol of 1,8-octanediol (0.559 g). Dissolution proceeded under stirring at room temperature in a three-necked 250 mL flask equipped with argon flux. 50 ml, half of the volume, were used for the dissolution of the hydroxyl species while the second half was used for the solubilization of the

photosensitive dichloride (5.46 mmol, 2,0 g) in a separate closed flask also equipped with argon flux. Once the chloride solution was added dropwise to the reaction system, DMAP (0.1 g, 0.8 mmol) and pyridine (0.864 g, 10.93 mmol) were added, and the system was driven to reflux and kept at reflux for 5 days. The reaction was monitored using thin-layer chromatography on silica plate.
The system was precipitated three times in diethyl ether. It was then filtered, yielding 100-600 mg of polymer. The obtained oligomers were characterized by ^{1}H and ^{13}C NMR spectroscopy in deuterated chloroform (CDCl3) and deuterated d-DMSO. P1: ^{1}H-NMR (400 MHz, CDCl3) δ 13.31 (s, 1H), 7.76 (d, 1H), 7.68 (dd, 1H), 7.65 (d, 1H), 7.18 (m, 1H), 6.82 (m, 1H), 6.80 (m, 1H), 6.77 (m, 1H), 5.35 (s, 1H), 4.35 (m, 2H), 4.08 (m, 3H), 3.64 (m, 2H), 1.80 (m, 2H), 1.59 (m, 2H), 1.48 (m, 2H), 1.44 (m, 2H), 1.40 (m, 2H), 1.37 (m, 2H), 0.82 (s, 1H). P2: ^{1}H-NMR (400 MHz, d-DMSO) δ 7.76 (d, 1H), 7.63 (dd, 1H), 7.51 (d, 1H), 5.63 (s, 1H), 4.32 (m, 2H), 4.02 (m, 3H), 3.63 (m, 2H), 3.35 (m, 1H), 2.20 (m, 2H), 1.86 (m, 2H), 1.74 (m, 2H), 1.73 (m, 2H), 1.41 (m, 2H), 1.35 (m, 2H), 1.33 (m, 2H), 1.29 (m, 2H).

3.1.2.2 Nuclear Magnetic Resonance (NMR)

The polymers synthesized in this work, were characterized with ^{1}H-NMR and ^{13}C-NMR spectroscopy, with a Varian Gemini 400 MHz spectrometer (^{1}H-400 MHz, TMS; ^{13}C-100 MHz, TMS). Measurements were carried out at room temperature using 10-15 mg or 30-40 mg of sample respectively for ^{1}H and ^{13}C analysis; the samples were dissolved in deuterated chloroform (CDCL3) or deuterated dimethylsulfoxide (d-DMSO) according to their polarity. ^{1}H-NMR measurements were obtained with 400 MHz frequency, retention time between consecutive pulses d1 between 1 and 16 seconds while ^{13}C-NMR spectra were recorded with 100 MHz frequency and lower d1, between 0.5 and 0.2 seconds of acquisition time. For all the analysis TMS was used as reference.

3.1.2.3 Size exclusion chromatography (SEC)

The number-average molecular weight (Mn), weight average molecular weight (Mw) and molecular weight distribution were measured by SEC. Polymer molecular weight analysis was carried out with an Agilent 1200 series system equipped with an Agilent 1100 series refractive-index detector. The analysis was performed on the three following column system: 3 μm PLgel MIXED-E, 5

μm PLgel MIXED-D, 20 μm Plgel MIXED-A at a nominal flow rate of 1.0 ml/min and a sample concentration of 0.1 % w/w in THF as solvent (5mg of the polymer in 2 mL of THF). The instrument was calibrated with linear monodisperse polystyrene standards from Polymer Laboratories with molecular weights ranging from 500 to 400.000 $Kg \cdot mol^{-1}$.

3.1.2.4 Microcapsules preparation via Phase inversion precipitation method (PIP)

Microcapsules based on the synthesized photosensitive oligomers and containing Voyager Zen as oily encapsulated phase, were prepared by emulsification and phase inversion precipitation (PIP) method.

Droplet formation for the obtainment of microcapsules was performed by using two different nozzles devices, both working in a semicontinuous process; I) a spray gun (SG) equipped with only one inner channel for the passage and the atomization of one single liquid solution containing the polymer, the solvent and the oil, and II) a flow focusing device (ff) equipped with two different and separate capillaries, one inner and another outer, for the passage of the oily phase internal feed and the shell polymeric solution, respectively. Figure 3.2 shows a scheme of the dispersion setup with both used nozzles. The first device was supplied by Spraying Systems Company and the second by Ingeniatrics. Both nozzles were connected to a compressed air supply valve which works as emulsifier agent, offering the energy required to break up the polymeric solution into microdroplets. In both cases the external nozzle size, through which the polymeric solution exits, was 70 μm; moreover, in both cases the nozzle was fixed to a vertical support and located about 20 cm over a big coagulation bath containing distilled water, so that the outlet flux was perpendicular to the water surface and the microdroplets impacted directly on it. The coagulation bath was kept always under stirring at 100 rpm. After precipitation, the coagulated suspension was filtered with a vacuum filter connected to a pump. Microcapsules were then stored in dark vials.

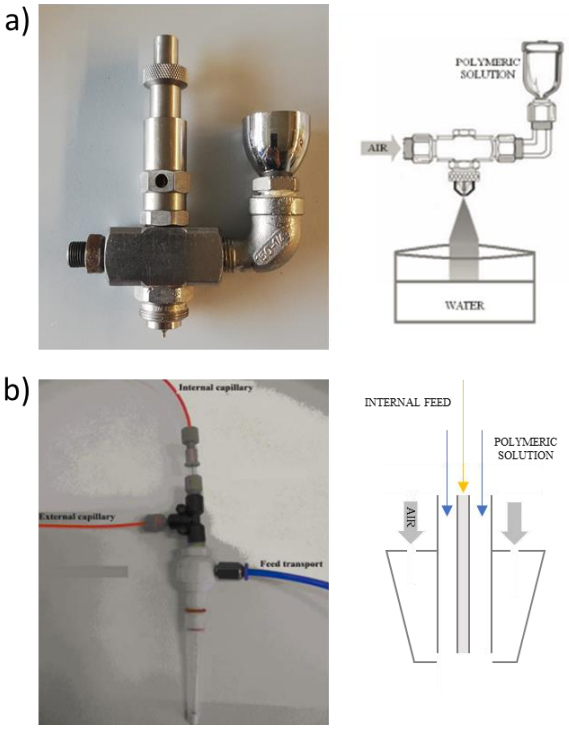

Figure 3.2 Phase inversion precipitation systems: a) Spray gun (SG) b) flow focusing (ff).

The whole procedure of capsules formation, as well as the polymerization steps, was conducted in darkness to ensure that the azobenzene moieties inside the polymeric structures were all in *E* configuration. In order to prepare capsules via PIP, first the polymeric solution was prepared and then, in the case of the SG, was poured into the nozzle just before capsules production; differently, in the case of the ff device, the solution was inserted into a plastic syringe and connected to a syringe pump on one side and to the external capillary conduct on the other side.

For the experiments of capsules formation using only the photosensitive polymeric chain, first the solubility of the photosensitive polyester into Voyager Zen was tested. *Via* repeated addition of 5 mg of Voyager Zen to vials containing 5 mg of polymer, we found that the maximum solubilized concentration of the polymer in Voyager Zen is 7% wt. Therefore, 0.14 g of photosensitive polymer were dissolved in 2.0 g of Voyager Zen and the solution was added to the deposit container connected to the spray gun device.

Capsules were also obtained with a shell formulation composed by a blend of polysulfone and the photosensitive polymer synthesized. For all the experiments a 15% wt solution of polysulfone in dimethylformamide (DMF) was prepared. When the spray gun device was used, in order to assure good solubility of the photosensitive polymer into the perfume, we chose to dissolve 5 wt% of P1 or P2 into the Voyager Zen and, in order to avoid polysulfone precipitation, due to the high amount of perfume, we added the Azo polyester up to 5 wt% respect to the polysulfone (5% P1 or P2 and 95% polysulfone). The final system contains about 50% of oily phase and 50% of polymeric shell. Two different air pressures were tested: 0.75 bar and 2 bar, leading to 100 ±40 μm and 20 ±15 μm capsules diameter respectively.

Capsules with a blended shell and without the incorporation of any oily phase were obtained using, instead of Voyager Zen, THF as solvent for the photosensitive polymer. The shell was composed also in this case by 95 wt% of Polysulfone and 5 wt% of P1 or P2. A 5 wt% solution of the photosensitive polyester in THF was prepared (50 mg of polymer in 950 mg THF) and then added to a 15 wt% solution of polysulfone in DMF (950 mg PSf in 5.38 g DMF). The polymeric solution containing polysulfone needed to be prepared in a closed, dry vial, under stirring, to avoid precipitation of the polymer due to humidity.

When the second device, the flow focusing nozzle, was used, 3 mL of the polymeric solution (0.53 g PSf and 0.03 g Azo-polymer) and 5 mL of the core material were placed in two separate syringes connected on one side to two pumps systems (model KD Scientific), and on the other side to the inner and outer channels of the flow focusing device (Figure 3.3). The operating pressure was 113 mbar, so that pressure had to be reduced by a valve (model Rexroth). The pump connected to the syringe containing the polymeric solution was set to 15 mL/h flow, while the one managing the oily phase was set to 3 ml/h flow; in this case we obtained a volumetric ratio between the active compound and the polymer of 1:1. In a second experiment the internal and the external fluxes were settled at 5 and 3 mL/h respectively leading to a volumetric ratio of 9:1.

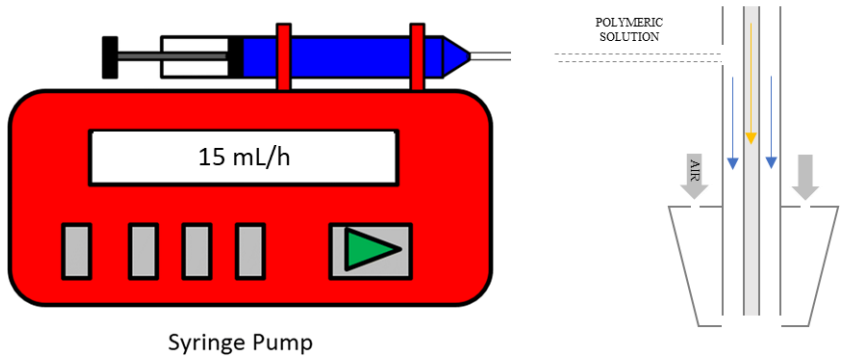

Figure 3.3 Flow focusing device connected to the syringe pump

3.1.2.5 Scanning electron microscopy (SEM)

The surface topography and the morphology of the obtained capsules were investigated tthrough scanning electron microscopy (SEM). In this investigation, SEM analyses were carried out in high vacuum mode, using an accelerating voltage ranging between 15 and 20 kV by means of an ESEM FEI Quanta 600 apparatus. Alternatively, the morphology of the produced microcapsules was studied also by means of a Flex-SEM 1000 VP-SEM provided by the P&G company. The SEM Scios 2 LoVac from Thermo Fisher Scientific was also used, thanks to the collaboration with Ellen Baken, Sr. Applications Scientist, to have a 3D reconstruction of the samples via laser beam sequential cut after Pt e-beam deposition on the capsules surface. The cuts were obtained for 500 µm slices. The 3D reconstruction was obtained via Avizo program.

3.1.2.6 Atomic force microscopy (AFM)

AFM is a high-resolution scanning probe microscopy which helps to measure local properties such as roughness of the surface, magnetism or morphology height, with a probe. The analyzed sample was a millimetric capsule with the shell composed by the polysulfone and the Azo polymer (P1 or P2) blend. The AFM images were recorded with an Agilent 5500 Environmental Atomic Force Microscope (Agilent Technology) equipped with an extender electronics module, which enables phase imaging in Tapping Mode. All the images were recorded in tapping mode using Multi 75 (Budget Sensors) silicon cantilevers (length = 225 µm, width = 28 µm, and thickness = 3 µm) with a force constant

of 3 N/m and a resonance frequency of 75 kHz. The scan rate was typically 0.7−2 Hz. All images were measured at room temperature. The microscope was placed on an active vibration isolation chamber (Agilent Technology) to eliminate external vibration noise.

In these experiments the capsule morphology was analyzed at three different times: 1. Light-irradiated capsule, 2. Previously irradiated capsule after 12 h at 70 °C and 3. Capsule after 2h of white light irradiation. The changes in the capsules external surface morphology before and after white light irradiation were investigated.

3.1.2.7 Thermogravimetric analysis (TGA)

TGA is a thermal analysis in which the changes in weight of a sample are constantly measured over time as temperature changes. Thermal stability studies were carried out on a Mettler TGA/SDTA851e/LF/1100 with N_2 as purge gas in the 30-800 °C temperature range at scan rates of 10 °C/min. This experiment was performed to calculate the activity of the obtained dry capsules. With the term activity we refer to the total amount of perfume encapsulated, expressed as weight percentage to the total weight of the sample analyzed. First, the temperature ramp needs to be set to avoid overlapping of the thermal behaviors of the analysed compounds (core and shell). When the evaporation temperature of the encapsulated active and the degradation temperature of the shell are identified, this technique can be used to evaluate the activity of the capsules and the encapsulation efficiency defined as follow:

$$Encapsulation\ efficiency = \frac{total\ active - free\ active}{total\ active} \qquad (3.1)$$

where *total active* is the weight of active in the initial formulation and the *free active* is the non-encapsulated perfume (also given by the difference between the *total active* and the encapsulated one). The weight percentage lost after the perfume evaporation temperature, represent the encapsulated perfume (*total active – free active*) and thus, correspond to the activity of the capsules.

3.1.2.8 Particle size distribution

The particle size distribution (PSD) measurement were conducted with an AccuSizer 780 AD Autodiluter which leads to information about the mean

particle size and the particles concentration, using sensors based on the single particle optical sizing technique. Since a spherical particle can be always described by its diameter, the scattered light measured by the instrument is always converted into the diameter of a sphere which volume could produce that scattering. After injecting the sample into the mixing vessel, the auto dilution option provides automatic continuous dilution of samples to their optimal concentration for analysis.

3.2 Results and discussions

3.2.1 Photosensitive polyester formation

Light sensitive encapsulates would provide release of perfume in absence of external mechanical forces. Thus, the polymeric shell should be designed properly, with the light sensitive moiety incorporated to help the polyester polymeric shell to release the encapsulated active when exposed to visible light. Instead of functionalizing an existing polymer, a novel polymer was designed with the intention of making capsules with a compacted shell minimizing leakage in presence of surfactants and containing an azobenzene light sensitive moiety into the main chain, in order to obtain control on the release. The polymer was designed as a linear polymeric chain that contains the photosensitive monomer into the main repeating unit, together with a bent and a linear monomer.

The important parameters to consider for the design and the obtainment of the capsules are thus I) the light sensitive behavior of the photosensitive molecule which will be part of the linear polymer, II) the light sensitive behavior of the polymer which will constitute the capsule shell, III) a good flexibility and mobility of the polymeric chain, balanced with a good compactness of the polymer into the shell; in this way the polymer will be capable of undergoing the desired conformational transitions and, in absence of a triggering event, the leakage can be minimized. The final polymer we want to obtain thus contains flexible spacers, to allow a higher compaction of the capsule wall and a good mobility of the photosensitive section, which, otherwise, would be too packed, too tight and inserted in a too rigid random coil. The designed polymer should be linear: we want the photosensitive molecule to participate actively in the spatial disposition and configuration of the polymer as well as to its mobility. This is the

reason why, differently from other photosensitive polymers reported in literature which contains the active species as branched section, we decided to chemically incorporate the modified azobenzene in the main chain. As a flexible spacer, we selected the commercially available 1,8-octanediol and its amount was fixed as 70 wt% of the polymeric chain. Moreover, we selected another spacer to add into the polymeric linear chain, bent and more rigid, which is expected to avoid crystallization of the polymeric structure. Crystallization could actually hinder polymer mobility during isomerization in the presence of light. 1,4-cyclohexanediol and resorcinol were selected respectively as commercially available aliphatic and aromatic bent monomers. The ratio between linear and bent diol was selected as 70/30 to reach a good balance between flexibility and tendency to crystallize.

Several strategies for the obtainment of the photosensitive polyester were considered[1] . As stated also in the experimental part of this chapter, first, we tried to obtain the polyester formation via liquid–liquid phase-transfer-catalysed interfacial polyesterification. The polymerization method is schematically reported in Figure 3.4.

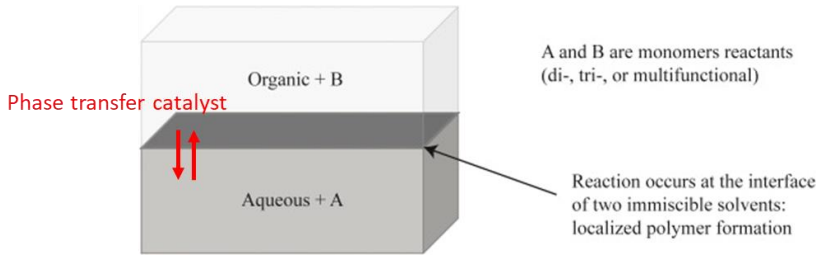

Figure 3.4 Scheme of liquid-liquid phase transfer catalyzed interfacial polyesterification.

Liquid-liquid interfacial polymerization was proposed, in a two-phase system, applying benzyltriethylammonium chloride as phase transfer catalyst and dichloroethane as low-boiling point solvent. The polymer was prepared according to the procedure reported in the experimental section, described before by Jegal and Blumstein.[2] The chlorine/OH groups ratio was fixed at 1/1 in order to maximize polymer molecular weight. The low yield of the polymer is probably due to the scarce solubility of the photosensitive di-chloride into 1,2-dichloroethane and the scarce and slow precipitation of the polymer in methanol. ^{1}H-NMR analysis of the obtained solid showed that there is a consistent amount of azo-dicarboxylic acid and we concluded that the phase

transfer catalyst transports the -OH groups into the organic phase and thus the chloride come into contact with water, causing the hydrolysis of a big percentage of dichloride; the reaction system would then, suffer disproportion, with a lower amount of dichloride if compared with the moles of OH terminated species. The aqueous phase leads to the hydrolysis of the chloride, resulting in low yields.

We tried thus, to obtain polymers in homogeneous phase systems: for this reaction, a mono-phasic Steglich polyesterification, Pyridine (Py) was used in a stochiometric ratio with the dichloride to neutralize the hydrochloric acid (HCl) formed during the reaction and to shift the equilibrium on the product side; 4-(Dimethylamino)pyridine (DMAP) was used in small amount as catalyst (around 1% wt of the solvent used).

In order to increase the molecular weight (Mw) and the yield, several strategies were considered. First the solubility of the azo dicarboxylic acid and of the azo di-chloride, as well as, the solubility of the commercially available monomers used in the polymerization, were tested in different solvents in order to understand which solvent is the most suitable for the reaction. Tetrahydrofuran (THF) and 1, N-methyl pyrrolidone (NMP) were found to be good solvents at room temperature, while the dichloromethane (DCM) and toluene dissolved very easily the monomers when the system got heated. All the solubility tests are performed solubilizing 5,0 mg of sample in 3 mL of solvent. Indeed, this reaction was repeated several times to optimize the used solvent (which determines polarity and temperature of the reaction): dichloromethane (DCM, bp 40°C), tetrahydrofuran (THF, bp 66°C), Toluene (bp 111°C), N-Methyl Pyrrolidone (NMP, bp 202°C). The application of high-boiling point solvents results in an increase of monomers solubility, which should decrease the unbalance between reactants though it did not impact significantly on the polymer yield in our case.

As reported in Table 3.1, polyesterification of the diacyl chloride with the aliphatic 1,4-cyclohexane diol and the 1,8-octanediol showed higher yields when NMP was used as solvent (P2) and the reaction was performed at 100 ºC for 5 days (20% yield). When resorcinol was used as bent monomer the yields obtained were overall higher if compared with the ones of polymers containing the 1,4-cyclohexanediol, even at low temperature reaction; the

higher yield in this case was obtained when DCM (P1) was used as solvent and the temperature of reaction was kept at 37°C (36% yield). Polymers obtained were characterized by ^{1}H and ^{13}C- NMR, SEC, UV-VIS and DSC analysis.

Table 3.1 Characteristics of obtained polymers/oligomers

Polymer	Yield (%)	M_n (g/mol) [a]	M_n (g/mol) [b]	M_w/M_n [a]	X_n [c]	X_n [d]
P1 DCM	36	$2.4 \cdot 10^3$	$1.4 \cdot 10^3$	1.36	2.65	5.82
P2 DCM	10	$2.6 \cdot 10^3$	-	1.20	2.99	6.39
P1 THF	16	$2.5 \cdot 10^3$	-	1.21	2.81	6.15
P2 THF	7	$2.1 \cdot 10^3$	-	1.21	2.38	5.10
P1 Tolu	5	$2.5 \cdot 10^3$	-	1.21	2.78	6.09
P2 NMP	20	$1.6 \cdot 10^3$	$2.6 \cdot 10^3$	1.14	1.79	3.84

[a] From SEC-LS, [b] From ^{1}H-NMR, [c] Degree of polymerization from SEC-LS (O-A-R/C-A), [d] Degree of polymerization from SEC-LS (A-C/R)

For sake of simplicity we show the ^{1}H-NMR spectra of only two polymers representative of the two species synthesized P1 and P2 and reported in Figure 3.5 and 3.6.

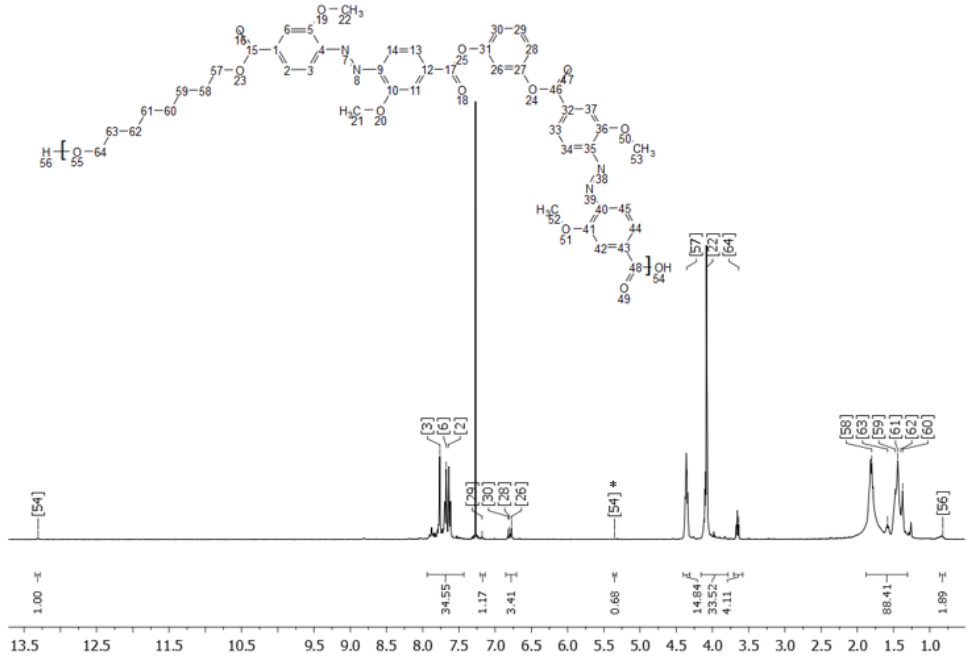

*Figure 3.5 ^{1}H-NMR spectrum of P1. *refers to terminal OH from resorcinol.*

From the spectrum reported in Figure 3.5, we were able to identify the peaks relative to the aromatic hydrogens from the azobenzene moiety between 8 and 7.5 ppm; the peaks relative to the 6 H form aromatic rings give different signals, depending on the terminations of the ortho-substituted azobenzene which can be, hydroxyl terminated, or reacted with 1,8-octanediol or with resorcinol. Similarly, the peaks at 4.08 ppm refer to the methoxy protons from the azobenzene moieties. At 4.4 ppm the signals relative to the proton labeled as 57 into the chemical structure, from the bound termination of 1,8-octanediol, appears. The symmetrical corresponding protons of the 1,8-octanediol moiety from the unbound termination falls at 3.6 ppm indicating the amount of 1,8-octanediol as termination of the polymeric chain. Between 2 and 1.3 ppm, the signals corresponding to the 12 central protons from 1,8-octanediol chain appear; the signals relative to the hydroxyl terminations of 1,8-octanediol, resorcinol and dicarboxylic azobenzene fall respectively at 0.9, 5.3 and 13.3 ppm. From the integrations of the peaks, it is possible to conclude that we are dealing with a mixture of chains which are randomly terminated, as expected. Indeed, there are 6 azobenzene moieties per chain, one of which is a terminal

unit, three 1,8-octanediol units per oligomeric chain, with one of them resulting in a chain termination.

The signals relative to the resorcinol into the structure are very poor in intensity and appears between 7.2 and 6.7 ppm, showing that there is one single monomer per chain, thus lower than expected based on the theoretical stoichiometry. Moreover, from the integrations reported in the spectrum and the identification of small peaks relative to the OH terminations of the chains, it was possible to estimate an average molecular weight for the obtained product which, in the case of P1 in DCM, is 1381 g/mol.

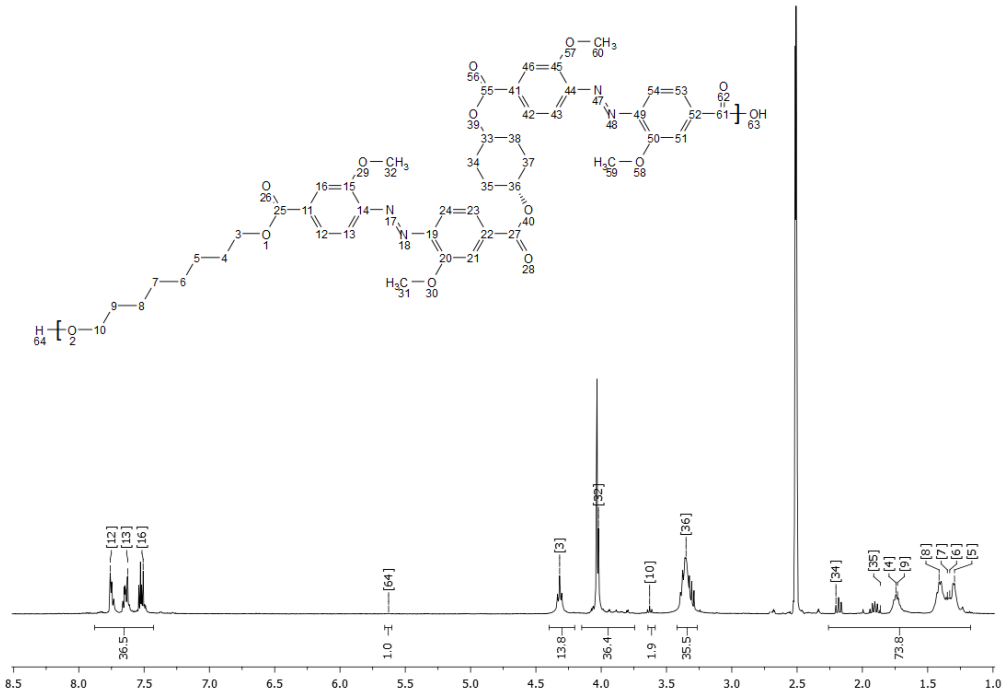

Figure 3.6 ^{1}H-NMR spectrum of polymer P2.

The spectrum reported in Figure 3.6 refers to the oligomer containing 1,8-octanediol and 1,4-cyclohexanediol and dissolved in d-DMSO. It is possible to recognize, also in this case, the aromatic peaks between 8 and 7.2 ppm, and the methoxy hydrogens at 4.1 ppm. The signals of the bound and unbound protons on the 1,8-octanediol terminations fall at 4.3 and 3.6 ppm, while the central atoms of the same moiety fall into the aliphatic range between 2.2 and 1.0 ppm and appear overlapped with the signals of the aliphatic 1,4-cyclohexanediol. In order to identify the amount of 1,4-cyclohexanediol into the

polymeric chain, the signals at 3.4 ppm relative to the symmetrical protons with number position 33 and 36 were considered and integrated. From the identification of the peak at 5.6 ppm, which refers to the hydroxyl terminal of the 1,8-octanediol, it is possible to conclude that, for each chain, there are 6 azobenzene moieties, three 1,8-octanediol and three 1,4-cyclohexanediol, far from the theoretical stoichiometry also in this case. The estimated molecular weight is hence, considering the molecular weights of each single portion, 2569 g/mol approximately.

The molecular weight of the prepared polymers was also calculated via SEC and the results of Mw, polydispersity and degree of polymerization are reported in Table 3.1.

From the degree of polymerization and the calculated molecular weight, it is possible to confirm that all the synthesized species are oligomers and that for each chain there are between 2 and 3 repeating units. Possible reasons for the low extent of polymerization could be the easy hydrolyzation of azo-acyl dichloride, as well as the different reactivity and solubility of the monomers used. In all cases, this can lead to a stoichiometric unbalance between acyl chloride and alcohol functionalities, which ration has a crucial role in determining polyesterification yields and the molecular weight of the obtained polymer.

For the preparation of capsules, the solubility of the synthesized polymers was tested in two different perfumes, Voyager Zen and Abraam. Due to commercial reasons and trends, Voyager Zen was considered the most suitable for further application in detergents. All the tested polymers were found to be soluble into the perfumes, even if in small concentrations (around 5-7 wt%), after vigorous stirring for 24h.

All the polymers were obtained with low yields of 5-40% and low molecular weight. Moreover, they were characterized by differential scanning calorimetry (DSC); only glass transition temperature could be detected, which suggests that they are completely amorphous.

3.2.2 Photosensitive behavior

The isomerization was studied for the obtained oligomers similarly to their parent compound, the ortho-substituted azobenzene. The *E-Z* isomerization of both, the photoactive compound and the resulting polymer, was studied by UV-

Visible spectroscopy of liquid samples kept in the darkness and, thus, supposedly all in *E* configuration. The samples were dissolved in dimethyl sulfoxide (DMSO) and irradiated by a white-light IDual ® bulb which can mimic the emission wavelength of the sun light. The UV-Visible spectra of the olygomer overtime was found to be very similar to the ones of the parent compound; according to the intensities of the peak at 400 nm relative to the absorption of the *n-π** bound overtime, 20% of isomerization is reached after 20 minutes of irradiation, when the pps is also reached. Moreover, the back-isomerization was also monitored by heating the sample for 15 minutes at 70°C showing that the isomerization is almost completely recovered. The calculated k_i for the *E-Z* isomerization process was found to be equal to 3.8 x 10^{-3} s^{-1}, as it is possible to notice from the photoisomerization kinetic in the inset of Figure 3.7, which is slightly higher if compared with the one of the isomerization processes of its parent compound.

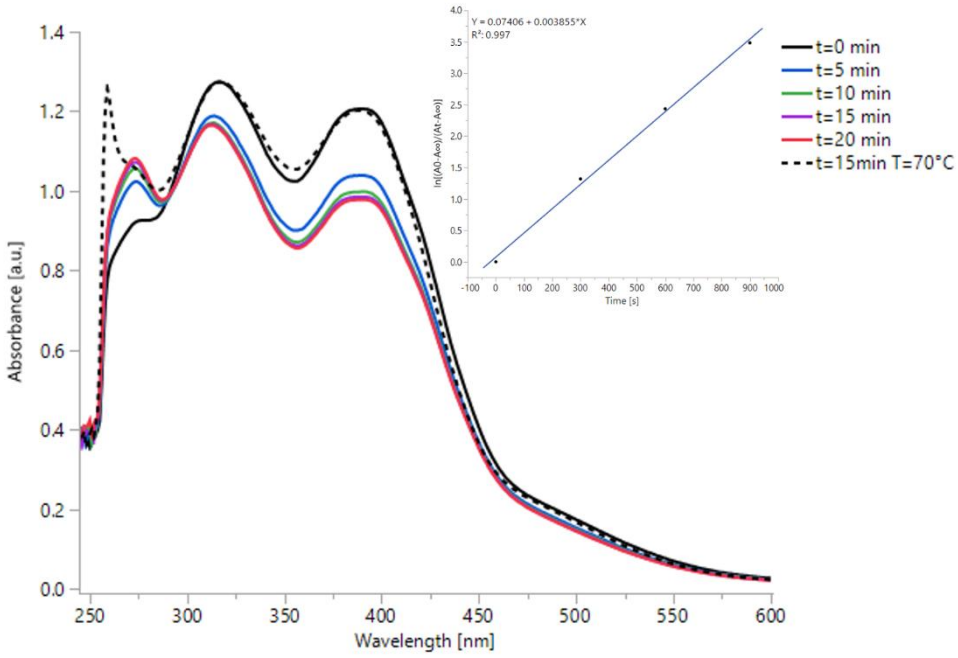

Figure 3.7 UV-Visible spectra of the E-Z isomerization process of the photosensitive polymer P1. The dashed line spectrum represents the recovery of the E isomer (Z-E back-isomerization) after heating at 70 °C for 15 minutes.

3.2.3 Capsules preparation

The goal of this study is the use of photosensitive linear polymers, or its incorporation into a polymeric blend, for the preparation of core-shell perfume capsules. We developed capsules which photosensitive shell was composed by the synthesized polymer itself or by blends comprising the synthesized oligomeric polyesters and the commercially available polysulfone (PSf). As already stated, the method used in this chapter for the preparation of polymeric capsules is the emulsification–phase inversion by solvent diffusion. We need a system composed by three phases: the polymer, a good solvent for the polymer and a non-solvent for the polymer. We used, thus, the synthesized photosensitive oligomer or its blend with the PSf, as polymers, while the non-solvent used is always water. The oligomers P1, P2 DCM and P2 NMP were used for the encapsulation. As encapsulated material, the Voyager Zen was used and, while in the case of the spray gun device it was mixed with the polymeric solution, in the case of the flow focusing device was inserted separately with an internal capillary. As solvent for the polymer we selected the perfume itself, when only the photosensitive oligomer was used, and N,N-dimethylformamide (DMF) for the solubilization of PSf. The emulsification can be obtained by mechanical stirring at high speed or *via* atomization through the implementation of a nozzle. When the spray gun is used, the two inlet channels are used for the polymeric solution, already containing the active to be encapsulated and for the entrance of compressed air which acts as emulsifier agent. On the other hand, when the flow focusing device is used, the presence of a double coaxial nozzle, is used for the feed transport of two immiscible focused fluids; the external capillary with 100 µm diameter carries the polymeric solution for the shell formation while the inner one, with 50 µm diameter, feeds the core with the active to be encapsulated. With this technique, differently from the use of the spray gun device, we can set the amounts of the oily phase and of the polymer concentration independently from each other.

In both cases, however, when the polymeric solution gets in contact with the aqueous coagulation bath, a process of mass transfer starts, the solvent starts to diffuse into the external phase, giving rise to the precipitation of the polymer and the stabilization of the droplets with formation of spheres and capsules. Indeed, after few seconds from the contact, the concentration of non-

solvent increases, leading to a system that is not thermodynamically stable and thus, the polymer is not soluble anymore in the system. When the system gets unstable, it separates in two immiscible phases, one rich and one poor in polymer. The polymer-rich phase is responsible for the shell formation, while the polymer-poor phase leads to the liquid core and to the presence of solvent into the continuous phase/ water. If the active ingredient is incorporated into the polymeric solution, as in most of our cases, the diffusion of the organic solvent leads to the encapsulation of the active as core material. The coagulation bath was kept always under stirring to let the capsules precipitate, during the whole process, in a homogeneous system and to prevent microcapsule aggregation. Since the precipitation of the polymer in contact with water is very fast, the magnetic stirrer was set up at 100 rpm. After precipitation, the obtained suspension was filtered with a vacuum filter connected to a pump so that microcapsules were dried in low vacuum and not aggressive conditions. This method has a high reproducibility, but large volumes of water needs to be removed and the escape of hydrophilic active into the saturated-aqueous phase reduce the encapsulation efficiency. Both the atomization devices used were practical, easy to handle, flexible for the adjustment of parameters and properly used with lab-scale volumes.

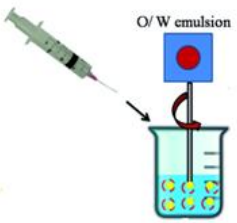

Figure 3.8 Emulsification and droplet formation via syringe dripping.

The first trials of encapsulation were conducted *via* emulsification and phase inversion, forcing the solution of the only photosensitive oligomer in Voyager Zen, dropwise via syringe or pipette into the water coagulation bath as pictured in Figure 3.8.

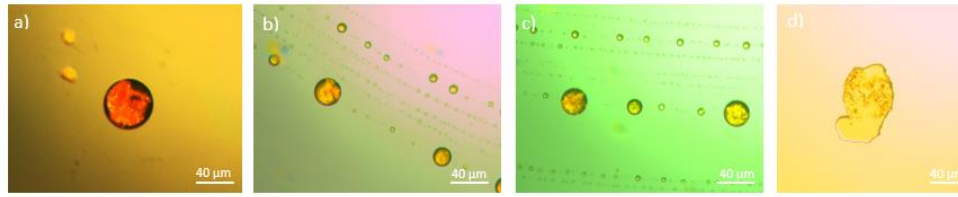

Figure 3.9 Optical micrographs of capsules obtained via PIP in water via syringe dripping.

From the optical micrographs of the resulting capsules reported in Figure 3.9, we can confirm that the mean diameter is around 30 µm while, from the Figure 3.9-d it is possible to see a capsule leaking the encapsulated oil probably due to the instability of the polymeric shell and its consequent rupture.

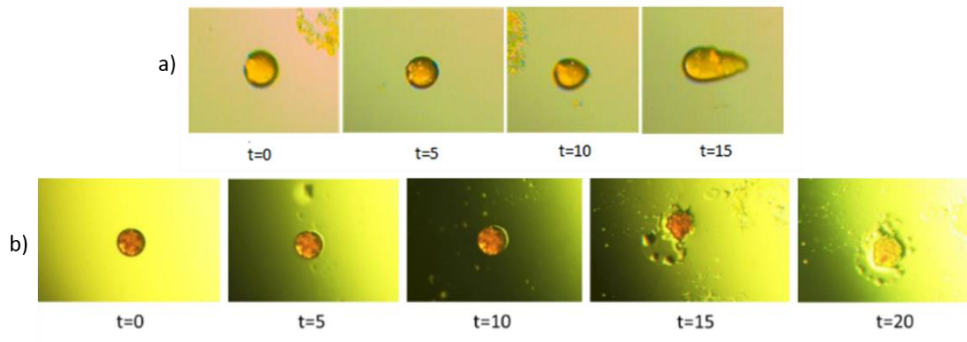

Figure 3.10 Optical micrographs of capsules obtained via SG and irradiated with white light overtime. The two different sequences show capsule deformation a) and capsule breakage b).

The capsules were also observed via OM over time and under white light irradiation as reported in Figure 3.10. After 10 minutes of irradiation the capsule's shape starts slightly to change (Figure 3.10-a) while, after 15 minutes we observe a consistent deformation probably due to the isomerization into the polymeric shell which leads to morphological and geometrical visible changes. We also observed that, on increasing the irradiation time, the capsules get to complete brakeage (Figure 3.10-b). The rupture may be due to the isomerization of the shell, as well as to the drying of the support surface; in both cases this is considered as proof of the low mechanical properties of the shell, which is directly connected to the low Mw of the synthesized polyester.

We couldn't observe the formation of a stable solid shell when encapsulation was performed only using the solution of photosensitive polymer.

In order to strengthen the shell, blends of the synthesized oligomeric polyester with the PSf were used for the obtainment of stable shells. This approach would lead to an increase of the mechanical properties of the system, while keeping the photosensitivity. PSf is a polymer highly used for the preparation of microcapsules and membranes thanks to its good chemical and mechanical properties and mechanical stability.[3,4] It is also considered a biocompatible polymer and, therefore, suitable for medical applications.[5–7]

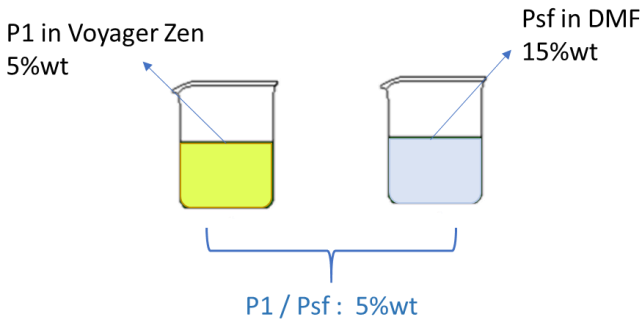

Figure 3.11 Schematic procedure for the obtainment of blended photosensitive capsules.

The possibility of making core-shell capsules out of PSf shell *via* solvent evaporation or phase inversion method, has been already deeply studied.[8,9] As we can see from Figure 3.11, the blend was obtained mixing a 5 wt% solution of Azo-oligomer in Voyager Zen together with a 15 wt% solution of PSf in dimethyl formamide. The percentage of photosensitive polymer in the blend is settled as 5% wt. With this proportions the fixed ratio core:shell is equal to 1:1. The polymeric solution was forced into the aqueous bath *via* pipette, syringe or microneedles. In this study we tried first *via* pipette, obtaining macrocapsules of 5 ± 1.0 mm diameter as proof of concept. From the sphere's section reported in Figure 3.12, we can confirm a core-shell morphology and also that the porosity of the wall increase going towards the center of the sphere.

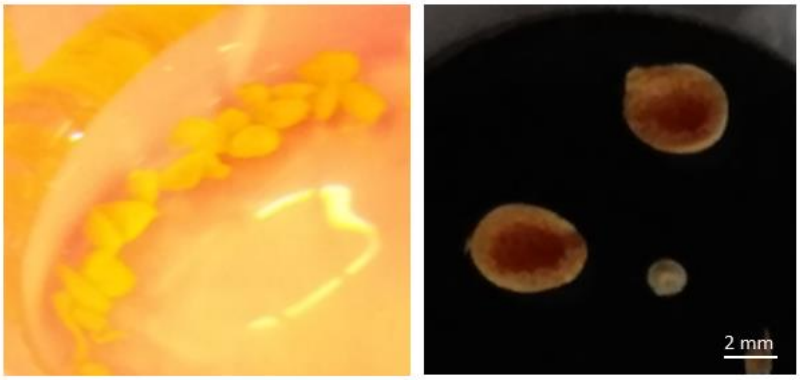

Figure 3.12 Millimetric capsules obtained via pipette emulsion and PIP in water. On the right the porous section of the cut sphere.

With the implementation of the spray gun, it is much easier to control the mean size of the obtained capsules. For the blended system previously described, we obtained 100 ±40 µm capsules, applying an air pressure of 0.75 bar (Figure 3.13), and 20 ±15 µm capsules with an applied air pressure of 2 bar, resulting in a fine powder.

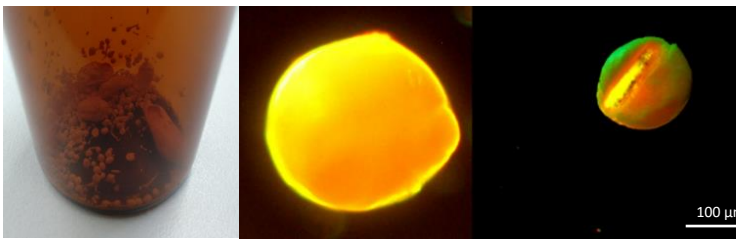

Figure 3.13 Capsules obtained via SG at 0.75 bar air pressure.

Optical micrographs of the capsules obtained at low air pressure values were useful to have a preliminary proof of the core-shell morphology. Below some SEM images are shown from blended capsules obtained by spray gun, with air pressure of 2 bar and cryogenically cut (Figure 3.14). The mean diameter was confirmed to be around 20 µm, while the shell thickness was found to be in the range of 4-10 µm. The high values of shell thickness are due to the core:shell ratio used in these experiments, equal to 1:1.

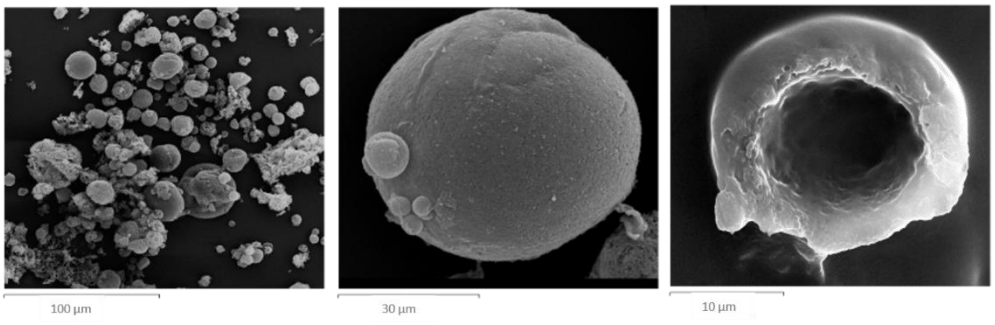

Figure 3.14 SEM images of the blended capsules obtained via SG with 2 bar air pressure.

Also in this case, as described previously, the capsules were analysed via OM over time. From Figure 3.15 it is possible to see how the active encapsulated is evaporating from a ruptured capsule over time and at high temperature, as proof that, when the capsule is formed, the perfume is inside the capsule itself.

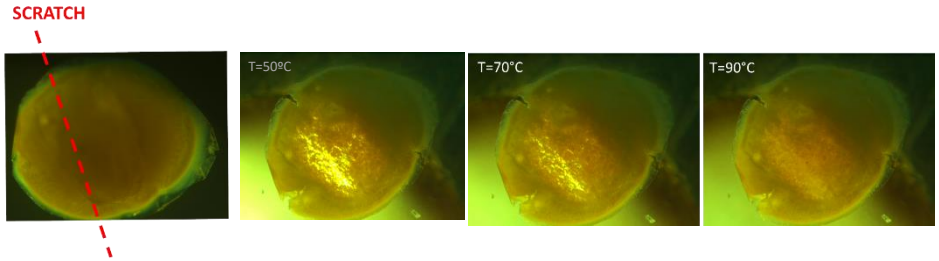

Figure 3.15 Optical micrographs of a ruptured capsule overtime and at high temperature.

Changing the core:shell ratio and get closer to the one used for the polyacrylate commercially used capsules, which is 9:1, turned out impossible with this technique: either decreasing the amount of PSf or increasing the amount of active, does not lead to the formation of particles and the blended system precipitates as a membrane on the water bath surface. The flow focusing seems to be, in the field of blended systems, the only way to increase the ratio oil:polymeric shell. Actually, it was possible to obtain spherical particles with both the ratio oil:polymeric shell 1:1 and 1:9. The resulting SEM images for the morphological characterization of all the blended capsules, obtained via spray gun and flow focusing, are reported below.

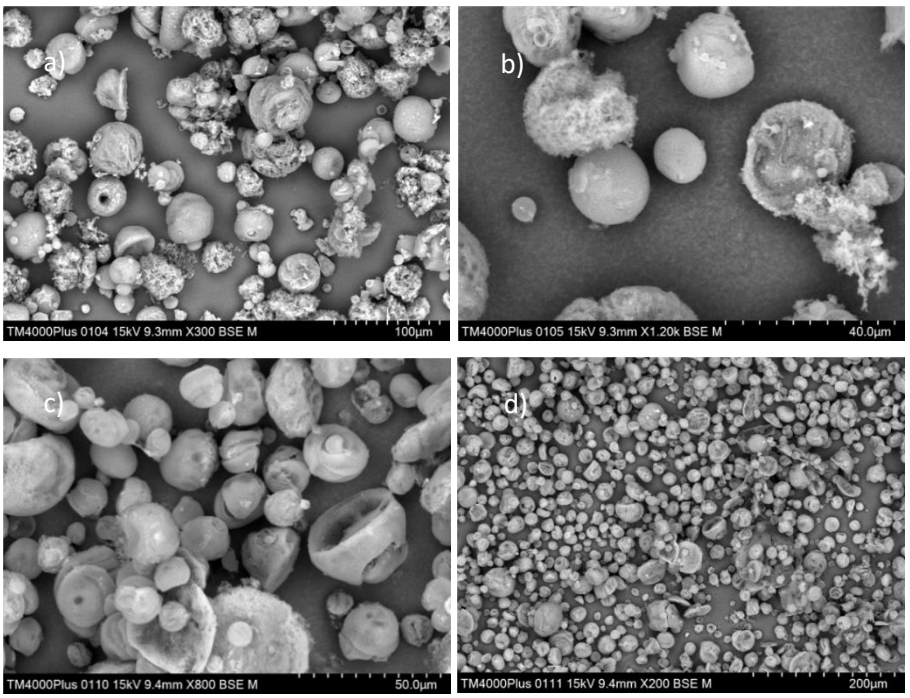

Figure 3.16 Spray gun (SG) 1:1 blended capsules obtained with THF and no oil.

From the SEM micrographs in Figure 3.16, relative to capsules obtained by using THF instead of Voyager Zen as core, it is possible to notice the presence of nicely formed round-shape capsules together with some amorphous precipitates which are present in all the micrographs. The presence of broken capsules in Figure 3.16-c demonstrates that some core-shell capsules were formed with a thick and porous shell. The surface of the capsules does not look highly smooth but characterized by homogeneous roughness and presence of porosity. The same batch of capsules was also analyzed by a SEM Scios 2 from Thermo Fisher; the resulting cross section, together with a 3D reconstruction are reported in Figure 3.17. They not only confirm the porosity of the shell thickness, but also demonstrate that not all the capsules obtained, as in this case, without the use of the oily phase, have a core-shell morphology, since some of them are characterized by a matrix structure. The capsule reported in Figure 3.17 was covered by platinum Pt deposition and cut in slices of 5 µm by means of a Gallium Ga laser beam, in order to see the internal

structure. The 3D reconstruction shows in blue all the voids and in yellow the solid components.

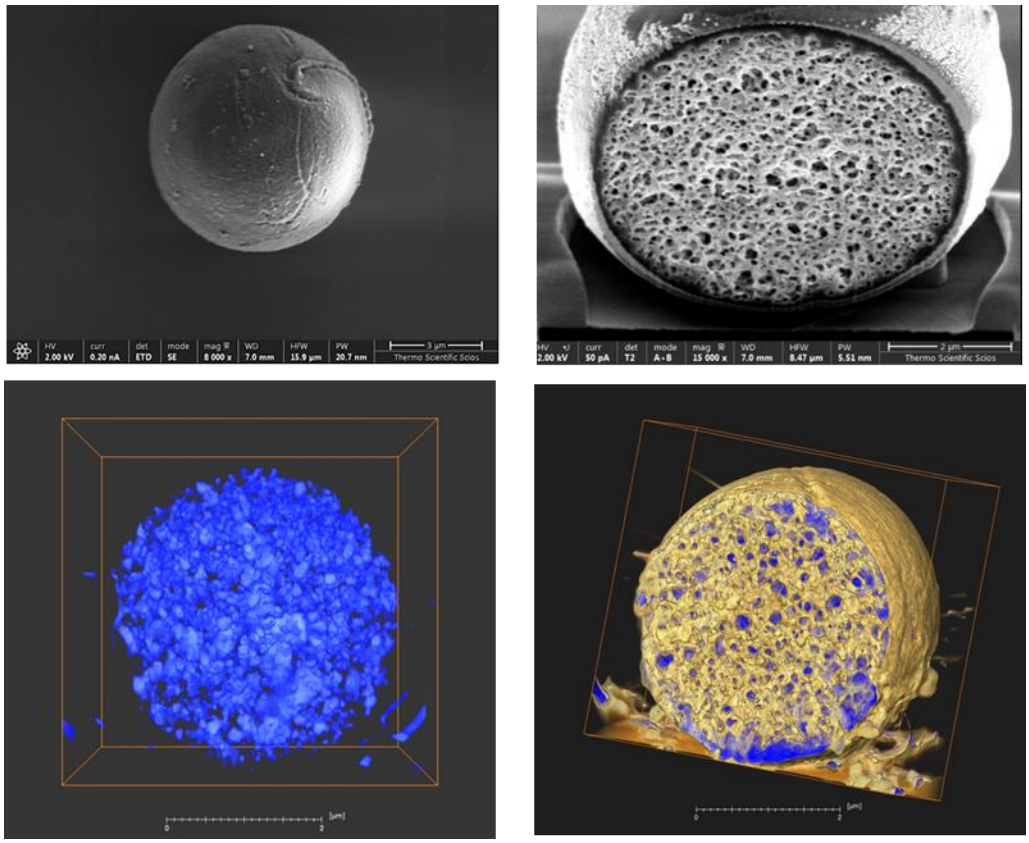

Figure 3.17 3D reconstruction of the blended 1:1 capsules obtained via SG with THF.

We used then, the same approach for the obtainment of capsules containing VZ, which replaces the THF for the solubilization of the photosensitive oligomer. The SEM micrographs are reported in Figure 3.18.

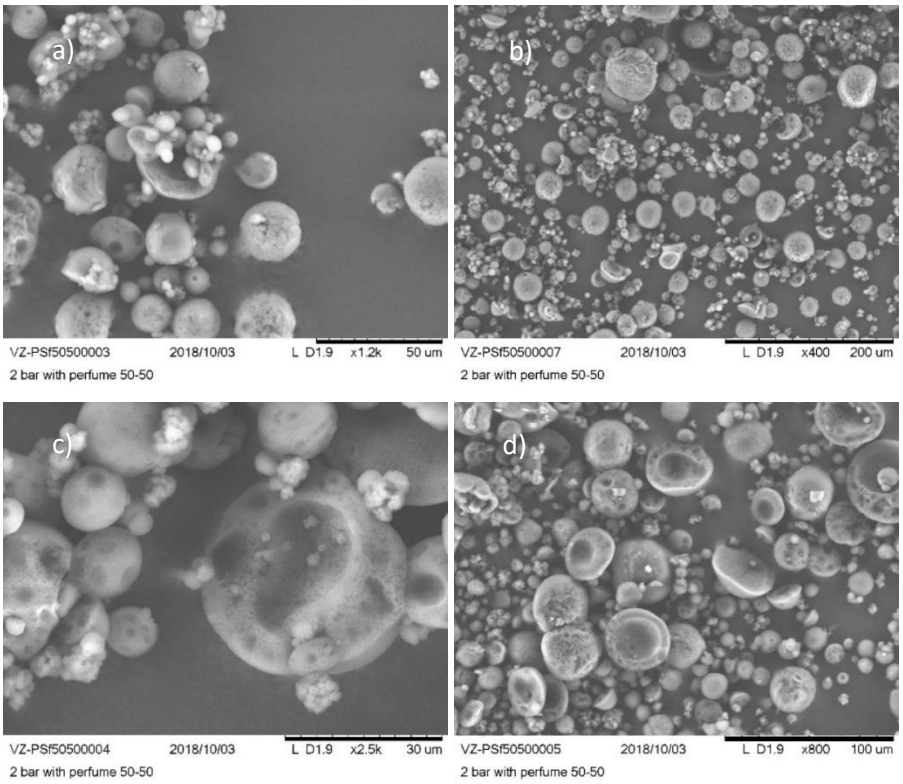

Figure 3.18 Spray gun (SG) capsules, blend 1:1, Voyager Zen encapsulated

As for the previously reported capsules, also in this case it is possible to notice, from SEM images, that the formed particles are affected by a certain porosity which increase starting from the outer surface. From ruptured capsules in Figure 3.18-c,d it is possible to see that, with the use of the oily phase as core material, which is completely insoluble and immiscible with the water from the coagulation bath, we obtained a mixture of core-shell and multi-core structures. The capsules resulting from encapsulation *via* flow focusing with a core shell ratio 9:1 are reported in Figure 3.19, while Figure 3.20 shows the capsules obtained by the same technique with 1:1 core:shell ratio.

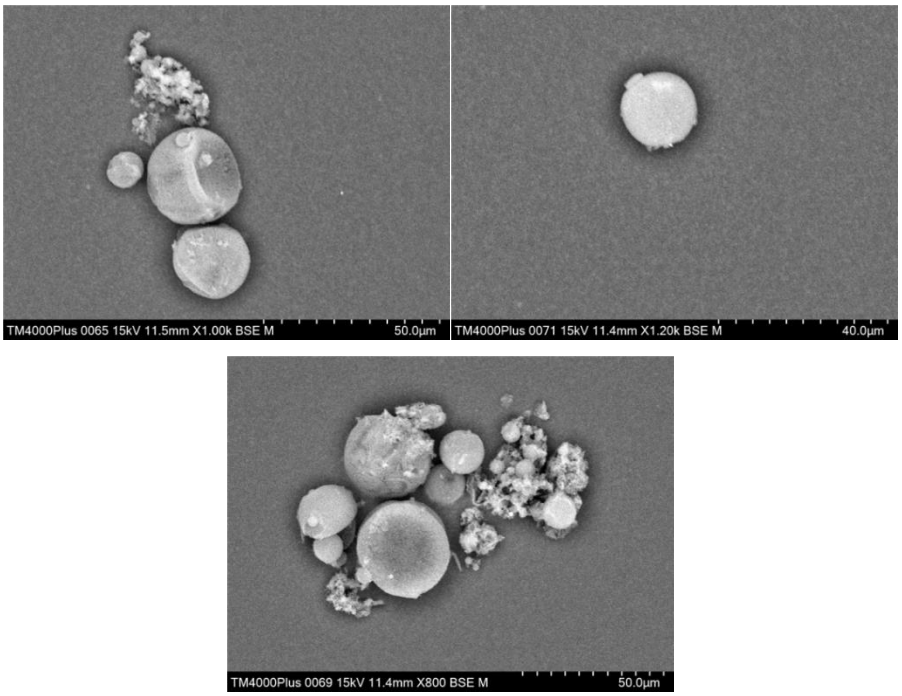

Figure 3.19 Flow focusing (ff) blended 9:1 core shell ratio capsule.

The external surface shown in Figure 3.19 appears much smoother if compared with capsules obtained via SG, and also with capsules obtained with ff but core/shell ratio 1:1 (Figure 3.20); the presence of amorphous precipitates in between the spherical capsules was also detected in this last case.

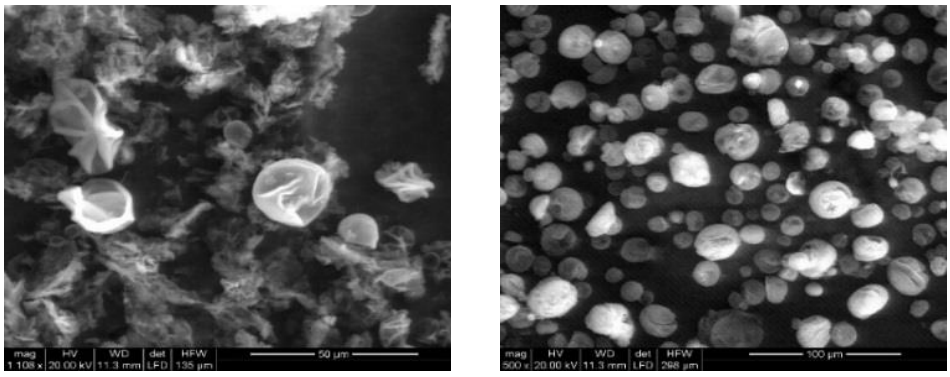

Figure 3.20 Flow focusing (ff) blended 1:1 core shell capsules.

In the case of both systems used, SG and ff, porosity was already evident from capsules surface. We know from literature that the extent of porosity depends on the polymer precipitation rate which can be adjusted by properly varying the

composition of the coagulation bath.[10,11] Actually, the addition of a certain percentage of DMF to the coagulation bath would lead to decrease of the shell porosity; nevertheless, we decided that the leading criteria was to minimize the use of solvent in the microencapsulation process, and thus we didn't go through this experimental part.

3.2.4 Encapsulation efficiency of the blended capsules. Spray gun and flow focusing comparison.

Capsules' activity is defined as the weight percentage of active encapsulated and can be evaluated with different techniques. In this work we used thermogravimetric analysis (TGA) to gain knowledge on the amount of the oil encapsulated into the polymeric capsule; TGA has the advantage of being a fast technique which provides a good estimation of the activity of the capsules; it is also more suitable for the analysis of dry capsules versus the capsules in the form of slurries which are usually analyzed with techniques based on gas chromatography – mass spectroscopy. However, we need to take into account that, since TGA is based on the weight loss of the sample, it is not possible to come out with information about the composition of the system, the concentration of each perfume raw materials (PRMs) and the possible presence of residual solvents used for the preparation of the capsules.

TGA response curves of the pure components, the active and the shell material, are needed for a comparison with the response profiles of the formed capsules. This correlation is used to determine the temperature range where only the mass loss of the encapsulated active occurs. Once the correct temperature range is identified, it is possible to estimate the mass of the encapsulated active as the weight loss of the capsules in that temperature range. In Figure 3.21 we can see the blue line representative of the thermal behaviour of the shell material, the PSf, which represents 95% of the shell and, for this reason, can be considered as its main component; it is stable until temperatures higher than 450°C. The orange line instead, is representative of the active compound (core), the Voyager Zen, which has totally evaporated at 230°C.

In our analysis we found, then, a good distinction between the evaporation temperature of the active and the degradation temperature of the polymer. Therefore, we could choose a temperature included in this range, for the calculation of the encapsulated active, which affected the result with a

negligible error. The temperature we chose for the activity calculation in this experiment was 250°C. The other curves in Figure 3.21, the green, yellow and grey, show the behavior at high temperatures of three different capsules samples: the analyzed capsules were obtained via SG and ff, at different core:shell ratio, and are reported together for comparison. The green, yellow and grey curves refer respectively to capsules made via ff with a 1:1 core:shell ratio, via SG with a 1:1 core:shell ratio and via ff considering a 1:9 core:shell ratio.

The encapsulation efficiency (EE%), can be now defined and calculated as the mass of encapsulated active compared to the mass of the active added to the initial formulation, with the formula presented already in the experimental paragraph and reported here for simplicity:

$$EE\% = \frac{active\ in\ the\ capsule}{Total\ active} \tag{3.2}$$

where the *active in capsule* is the result of the TGA measurements.

The EE%, calculated at 250°C, is respectively 27, 72 and 70%. These values were calculated according to the weight percentage loss at 250 °C for each curve, which is respectively 24%, 36 % and 35 %, and which corresponds to the activity of the capsules analyzed, and to the initial amount of perfume used in the formulation.

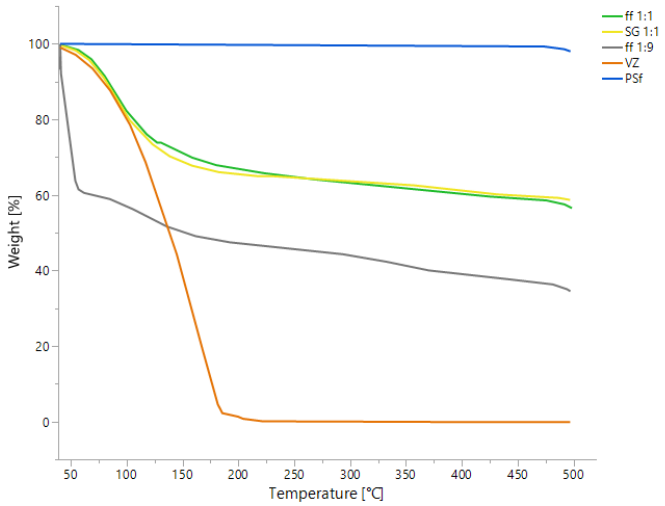

Figure 3.21 TGA measurement on PSf, VZ, SG capsules and ff capsules for the measurement of the EE%.

Concerning the thermal curve of the capsules obtained via ff with a 9:1 core:shell ratio, it is possible to notice a considerable loss of weight below 100 ºC. It can be attributed to the loss of water and residual oil entrapped onto the shell/wall material and was subtracted from the weight loss due to the evaporation of the encasulated oil which is used for the calculatoin of the EE%. Flow focusing technique resulted definitely a more efficient proccedure as far as EE is concerned; neverthless, despite encapsulation of perfume was successful, the obtained values of EE are not competitive with the ones from commercially used capsules. Therefore, the stability of the capsules overtime, in the white base detergents used in the P&G company, was not evaluated.

3.2.5 Photosensitive behavior of the blended capsules

The photosensitive behavior of the capsule shell containing the photosensitive Azo polyester in a concentration of 5 wt% in the shell, was studied *via* Atomic Force Microscopy (AFM) analysis on a small portion of the surface of a capsule shell. The AFM analysis was conducted to prove the light-inducted change in the morphology of the capsules' shell and with the aim of understanding if morphlogical changes can be caused by light/ dark exposure conditions.

Thus, this study was performed on the surface of a millimetric capsule obtained with the same technique and strategy used for the obtainment of the micrometric capsule, but using, for the droplet formation, a pipette. The surface

of the capsule was analyzed in three different conditions: I) light irradiated capsule (thus probably, in partial *Z* configuration), II) kept into darkness and heated for 24h at 70 °C and III) irradiated again for 2h. For each scenario, AFM measurements were performed in 5 different points at room temperature and then the mean of the values of roughness, skewness and kurtosis were obtained. The three topographies with the respective Fourier transform are reported below in Figure 3.22.

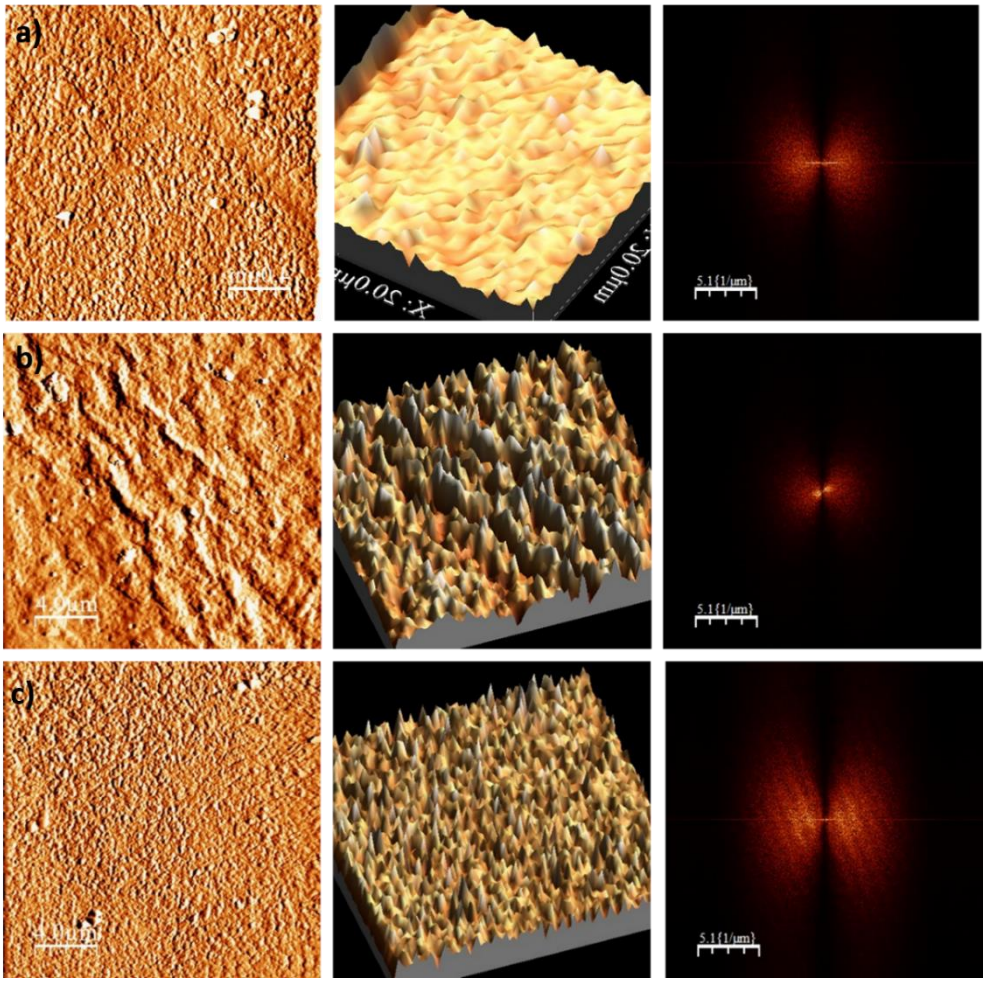

Figure 3.22 AFM topographies and Fourier transform of the surface of a photosensitive millimetric capsule. a) irradiated sample, b) heated sample kept in darkness, c) irradiated sample after b).

It can be observed that in the absence of light irradiation (b) the surface look less rough, compared to the irradiated one. From the topographies it is possible

to see that the morphology is first changing when temperature is applied in darkness (b), and then, with a second light irradiation, is going back to the initial configuration, as expected.

A quantitative characterization of the capsule surface properties was performed by means of a set of standardized roughness parameters,[12] which are listed in Table 3-2. These values are averages calculated from several images acquired in different regions of the membrane/shell surface. Even if the results of average roughness shown in Table 3.2 show a flat behavior, from the Fourier transform it is possible to see that the distance between two points in the real space is first increasing when the sample is not irradiated (b) and then decreasing again after light irradiation (c) showing that the surface morphology is actually affected by light and temperature.

The skewness and the kurtosis of the surface (Table 3.2), which indicate the symmetry of the peaks and valleys (sharpness and asperity), also show an oscillating behavior between irradiated and non-irradiated samples, as it is possible to observe from Figure 3.22 and Table 3.2. We repeated the same experiment also on a capsule obtained, with the same technical conditions, but using only PSf; the results from light irradiated and then heated sample, reported in Figure 3.23 a) and b) respectively, do not show significative differences, thus suggesting that the trigger for the morphological change is the presence of the photosensitive oligomer.

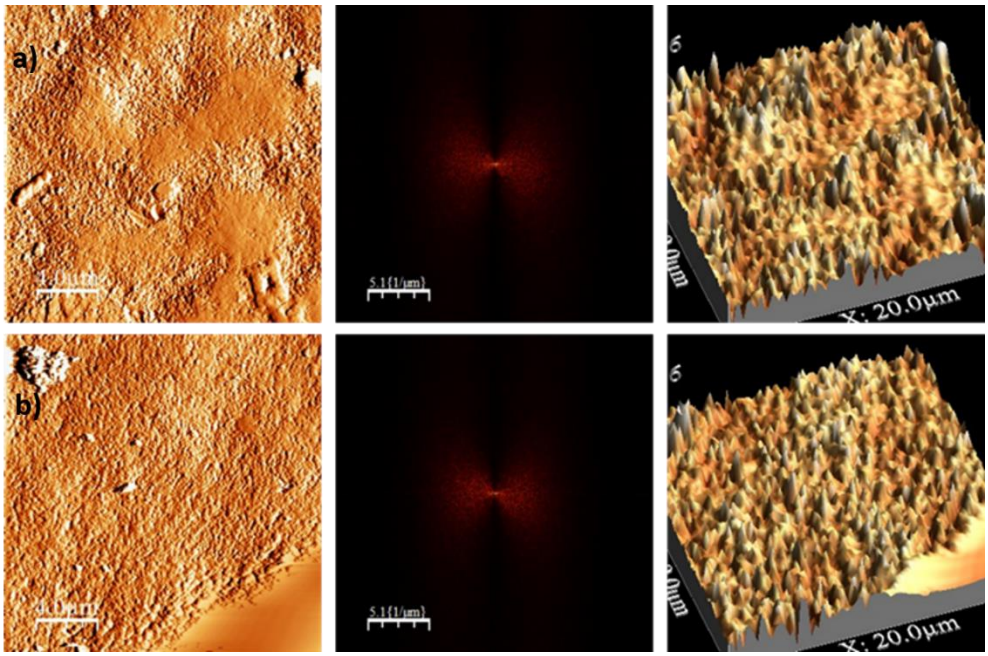

Figure 3.23 AFM topographies and Fourier transform on the surface of capsules obtained with only PSf as shell material; light irradiates capsule a) and heated capsule b) after a).

Table 3.2 AFM parameters for the characterization of surface morphology of the capsule.

Symbol and Name	Irradiated sample (I)	Darkness, 70ºC	Irradiated sample (II)
Rms (roughness)	0.11 ± 0.02	0.16 ± 0.04	0.17 ± 0.03
S_{sk} (surface skewness)	-0.10 ± 0.09	0.08 ± 0.05	-0.06 ± 0.06
S_{ku} (surface kurtosis)	2.15 ± 0.25	2.76 ± 0.31	2.36 ± 0.21

From Table 3.2, one can observe that the root mean square (rms) roughness, considered as a standard deviation of height, shows a flat trend and is not affected by photoirradiation. The surface skewness (S_{sk}), which depicts the asymmetry of the height distribution, changed from a negative value, for the irradiated sample, to a positive one, after darkness and temperature increase. These values may be associated to the absence or the presence of porosity into the shell but, most important, they quantitatively represent a change triggered by light exposure.[13] Furthermore, surface kurtosis (S_{ku}), which value illustrates the sharpness of the surface height distribution, increases with

darkness and temperature exposure and decreases again after light exposure. S_{ku} values smaller than 3.0 generally indicate a broad (heterogeneous) height distribution, whereas values larger than 3.0 refer to a surface with almost quantized height values. Therefore, AFM results confirmed that *E-Z* isomerization of the photosensitive blended moiety can efficiently happen into the shell and is not hindered; moreover it is proven to have an influence on the shell morphology, smoothing the membrane surface when no light is applied (moiety in *E* form) and increasing the heterogeneity of the peaks and dips after light irradiation (*Z* form).

3.3 Conclusions

One of the challenges of this project was the definition of the process conditions in order to obtain core-shell encapsulates that meet required success criteria in final industrial applications. The capsules needed to be obtained with the selected materials and each material would require diverse process conditions. In this chapter several approaches were considered, in order to obtain dense shells that not only are able to encapsulate the perfume Voyager Zen, but also to activate the perfume release when white light is applied, maintaining the benefit agents stable during supply chain and storage.

The general procedure and method used in this chapter for the obtainment of capsules is the phase inversion precipitation method, starting from a pre-existing, pre-synthesized polymer.

The main polymer used was an in-house made photosensitive oligomer; in some cases, also polysulfone blends were used in order to guarantee good stability and good mechanical behavior. Properties of the designed and synthesized light sensitive oligomers were evaluated and the one showing optimized yield and molecular weight, was further used to encapsulate perfume.

In order to form the capsules, diverse drop-formation techniques were used, such as standard emulsification or diverse nozzles to spray the mixtures into the coagulation bath. Underlined advantages of phase inversion precipitation are the easiness of producing capsules at room temperature, enabling the encapsulation of temperature sensitive actives, the good reproducibility provided and the potential to be scaled-up in a continuous process set-up.

Some disadvantages were also defined, especially concerning the morphology of the final capsules: after characterizing the obtained capsules, it was observed that the membranes were forming too fast and therefore they were highly porous, being quite difficult to control the rate of precipitation; additionally, the generation of waste water (due to the precipitation bath) is big and not solvent-free. This not only requires additional processing steps to separate and concentrate the capsules, but also determines the presence of solvents which should be adequately removed and are detrimental to procedure implementation.

Nevertheless, in this chapter we demonstrated that it is possible to obtain blended photosensitive microcapsules *via* atomization of a polymeric solution and PIP method in a water coagulation bath. Indeed, capsules were obtained which photosensitive shell was composed by the synthesized oligomer itself or by blends comprising the synthesized oligomer and the commercially available PSf. The first capsules prepared were composed only by low molecular weight oligomers and, due to the poor solubility of the oligomers into the Voyager Zen, the shell formed was also very thin; these capsules were too unstable as expected on the basis of the low Mw of the shell.

Moreover, we demonstrated that it is possible to incorporate, as core material, into the capsules a certain percentage of perfume (oily phase) and that, with our systems, we obtained an EE of 72 wt%. However, some challenges were identified: high amounts of polymer are required and the solubility and stability of the polymer into the perfume is very poor. The encapsulation efficiency should be improved; on the other hand, porosity should be decreased because it is extremely high and possibly it will lead to high leakage values.

It should be added that, even if the devices and the processes reported in this chapter for the formation of microcapsules belong to the category of discontinuous processes, it is possible to plan a continuous industrial process for an easy and standardized capsule production.

Actually, the capsule size and their PSD may be controlled and adjusted through the implementation of different nozzles with more precise exits or connected to capillaries with a more controlled coaxiality. This is the main reason why the understanding of the PIP technique was at the base of our experimental work.

As final remark it should be considered that a better control over the morphology of the capsules is necessary and may be obtained *via* addition of a solvent to the coagulation bath or the selection of a less water-soluble solvent for the perfume or lower affinity between the non-solvent and the polymer. *Via* PIP is generally possible to form dense shells with certain materials, but it was not with the combination of actives and shell materials we selected for this study. Despite of the difficulty of making a perfume capsule starting from a polymer instead of a monomer, the benefit is that polymer properties can be tuned and adapted before capsule making. Additionally, using polymeric blends might help to balance the photosensitivity of the perfume capsule and manage the overall cost.

Bibliography

1. Tylkowski, B., Bogdanowicz, K. A., Ambrogi, V., Lederer, A., Patroniak, V., Giamberini, M. Synthesis and characterization of a new family of photoactive liquid crystalline polyesters based on α-methylstilbene. *Polym. Int.* **63**, 315–326 (2014).
2. Jegal, J., Blumstein, A. Functional polyesters and copolyesters based on the 4,4′-dihydroxy-α-methylstilbene. *J. Appl. Polym. Sci.* **68**, 387–393 (1998).
3. Pena, B., Gumi, T. State of the art of polysulfone microcapsules. *Current Organic Chemistry*, *17*(1), 22-29 (2013).
4. Guillen, G. R., Pan, Y., Li, M., Hoek, E. M. V. Preparation and Characterization of Membranes Formed by Nonsolvent Induced Phase Separation: A Review. *Ind. Eng. Chem. Res.* **50**, 3798–3817 (2011).
5. Wenz, L. M., Merritt, K., Brown, S. A., Moet, A., Steffee, A. D. In vitro biocompatibility of polyetheretherketone and polysulfone composites. *J. Biomed. Mater. Res.* **24**, 207–215 (1990).
6. Zhao, C., Liu, X., Nomizu, M., Nishi, N. Preparation of DNA-loaded polysulfone microspheres by liquid–liquid phase separation and its functional utilization. *J. Colloid Interface Sci.* **275**, 470–476 (2004).
7. Sivaraman, K. M., Kellenberger, C., Pané, S., Ergeneman, O., Lühmann, T., Luechinger, N. A., Nelson, B. J. Porous polysulfone coatings for enhanced drug delivery. *Biomed. Microdevices* **14**, 603–612 (2012).
8. Yin, J., Chen, R., Ji, Y., Zhao, C., Zhao, G., Zhang, H. Adsorption of phenols by magnetic polysulfone microcapsules containing tributyl phosphate. *Chem. Eng. J.* **157**, 466–474 (2010).
9. Ozcan, S., Tor, A., Aydin, M. E. Removal of Cr(VI) from aqueous solution by polysulfone microcapsules containing Cyanex 923 as extraction reagent. *Desalination* **259**, 179–186 (2010).
10. Mulder, J. *Basic Principles of Membrane Technology*. Springer Science & Business Media, (2012).
11. Barzin, J., Sadatnia, B. Correlation between macrovoid formation and the ternary phase diagram for polyethersulfone membranes prepared from two nearly similar solvents. *J. Membr. Sci.* **325**, 92–97 (2008).

12. Peltonen, J., Järn, M., Areva, S., Linden, M., Rosenholm, J. B. Topographical Parameters for Specifying a Three-Dimensional Surface. *Langmuir* **20**, 9428–9431 (2004).
13. Gizli, N. Morphological characterization of cellulose acetate based reverse osmosis membranes by atomic force microscopy (AFM) effect of evaporation time (2011).

4. Crosslinked capsules with melamine shell containing 4,4-bis(chlorocarbonyl) azobenzene (Azo chloride)

In the previous chapter the use of azobenzene moiety in polyester perfume capsules was proposed and described; in this chapter, after the obtainment of porous capsules *via* emulsification and polymer precipitation, we tried to obtain novel functional polymeric microcapsules based on modified azobenzene moieties *via* interfacial polymerization. This means that we will move from the preparation of capsules *via* physical methods (pre-existing polymer), explored in the previous chapter, to the preparation of capsules *via* chemical methods (reactive monomers). Through an exhaustive theorical and experimental investigation of the formed microcapsules, we demonstrated that visible light can act as a trigger for release of encapsulated material, as a consequence of *E-Z* isomerization which modifies microcapsule surface topography inducing a "squeezing" release mechanism. We selected interfacial polymerization of an oil-in-water emulsion as encapsulation mechanism for the preparation of core-shell microcapsules; a unique feature of this technology is that the capsule shell is formed at or across the surface of a perfume oil droplet by condensation polymerization of reactive monomers as photo-responsive azobenzene, cross-linkers and diamine. The formation of the shell is thus, associated with a reaction of polymerization between different monomers and not to a phase change transformation, as in the case of the capsules obtained in Chapter 3. Capsules morphology and performances were characterized by means of atomic force microscopy (AFM), optical microscopy (OM), scanning electron microscopy (SEM) and light scattering (LS). In the present work, photo-sensitive microcapsules based on synthesized ortho-substituted azobenzene compound (4,4'-bis(chlorocarbonyl)-2,2'-dimethoxy azobenzene) were prepared; moreover we explored the potential application of azobenzene-based polymeric microcapsules for the active release of their content under the simple action of visible light irradiation and we demonstrated that this novel advanced material can successfully control the release of, for instance, fragrancies, through visible light triggering, as confirmed by an olfactive panel.

Modelling studies were carried out in order to understand the mechanism of encapsulated perfume release and capsule morphology changes after irradiation with light. Polyamide photosensitive microcapsules were prepared by using 1,8-diaminooctane as diamine and 1,3,5-Triazine-2,4,6-triamine (melamine) as crosslinker. The results discussed in this chapter have been recently published.[1]

4.1 Experimental section

4.1.1 Materials

1,8-Diaminooctane (Fluka, 98 %), melamine (Sigma-Aldrich, 99 %), sodium hydrogenocarbonate (Aldrich, 99.7 %), Mowiol (polyvinyl alcohol 18-88, Fluka), 3-methoxy-4-nitrobenzoic acid (Sigma-Aldrich, 99), d-(+)-glucose (Sigma, 99.5 %), sodium hydroxide (Sigma-Aldrich), glacial acetic acid (Sigma-Algrich, 99.5 %), triethylamine (Sigma-Aldrich, 99 %), and thionyl chloride (Sigma-Aldrich, 97 %) were used as received without any further purification. PC1025-2 perfume oil, with a composition described in the US patent application 20130039962[2], was provided by Procter & Gamble Company. All the solvents were supplied by Scharlau and used without previous purification as received.

4.1.2 Photo-sensitive microcapsules preparation

The photo-sensitive microcapsules were prepared by oil-in-water interfacial polymerization method developed and reported in our previous studies and also largely applied for the obtainment of micro and nanocapsules in recent applications.[3,4] According to this protocol, for the obtainment of capsules with a 96/6 core/shell ratio, first the oil phase was prepared dissolving 0.600 g of 4,4-bis(chlorocarbonyl) azobenzene in 25 mL of PC1025-2 perfume oil. Then, to get an oil-in-water emulsion, the oil phase was slowly added dropwise into 50 mL of aqueous solution containing 0.500 g of Mowiol emulsifier (10 g/L) under overhead stirrer set up at 1200 rpm. Obtained emulsion was additionally mixed for 10 min at room temperature for stabilization. To obtain the capsules shell, the interfacial polymerization was initiated by adding to the system 25 mL of aqueous solution containing 0.250 g of 1,8-diaminooctane, 0.290 g of sodium hydrogen carbonate, 0.032 g of melamine and 0.250 g of Mowiol. The reaction was carried out in darkness at room temperature for 3 h. Finally, it was stopped by addition of 50 g of aqueous solution containing 6.00 g of sodium sulfate and

0.35 g of xanthan gum (XG). Formed suspension was mixed for 30 min at 300 rpm in darkness. The XG was used to avoid microcapsules aggregation.

In Table 4.1 the amounts of each component used are reported:

Table 4.1 Chemical composition used for the preparation of photosensitive capsules via interfacial-polymerization encapsulation.

Sol. 1		Sol. 2		Sol.3				
Water (ml)	PVA (g)	Perfume (ml)	Azo (g)	Water (ml)	PVA (g)	Diamine (g)	Crosslinker (g)	$NaHCO_3$ (g)
50	0.50	25	0.60	25	0.25	0.25	0.032	0.29

In Scheme 4.1 the representation of the reaction which leads to the microcapsule walls preparation is reported; melamine is used as rigid cross-linker and 1,8-diaminoctane was used as flexible spacer.

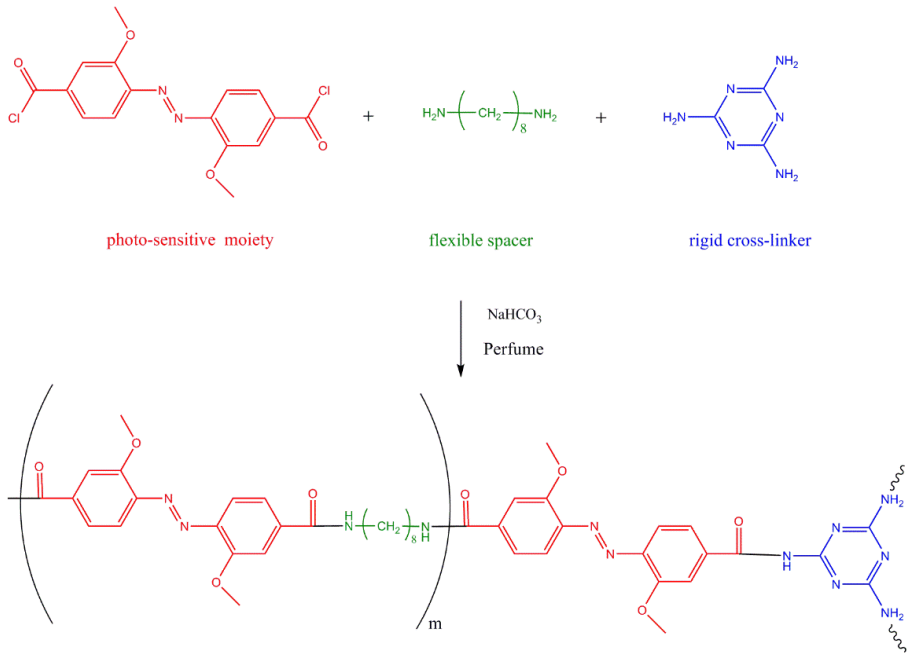

Scheme 4.1 Schematic representation of the interfacial polymerization mechanism for capsules wall formation. Photosensitive azobenzene (red), 1,8-diaminoctane (green), melamine (blue).

4.1.3 Particle size distribution (PSD)

Polyamide microcapsules mean size was determined using a HELOS BR supplied by Sympatec GmbH System Partikel Technik equipped with a R1 cuvette and a Helium-Neon Laser 5mW max output at 632.8 nm. The mean microcapsules size of the microcapsules was measured before and after 1 h of microcapsules irradiation with visible light emitted by a Philips DuraMax 85W

120V bulb. The analysis was carried out in xanthan gum and sodium sulfate water solution as a transport medium. Before the analysis 0.1 g of microcapsules slurry was diluted with 50 mL solution containing 6 g sodium sulfate, 0.35 g of xantham gum and 43.65 g demineralized water. Software setup and sample analysis were performed using Windox 5.8.0.0 software provided with the equipment by Sympatec. In order to verify the effect of visible light on the microcapsule size, the microcapules' average diameters were also measured after 3h of irradiation with the visible light emitted from a Philips DuraMax 85W 120V desk lamp. The distance between the light sources and a quartz cuvette containing dispersed microcapsules was kept constant (around 29.7 cm). During all irradiation processes, cold air was used to keep the whole capsule suspension in a thermostatic environment.

4.1.4 Optical microscopy (OM) and Scanning electron microscopy (SEM)

Microcapsule morphologies were observed by using Nikon Eclipse E600 POL Optical Microscopy equipped with bulb 12V, DC (100W halogen lamp Philips 7724). SEM characterization of the microcapsules was obtained with Cryo-Scanning Electron Microscopy (Cryo-SEM) captured by a Hitachi Model S-5200 Scanning Electron Microscopy equipped with a Gatan Alto 2500 Cryotransfer System (Gatan Model CT2500) to fracture the microcapsules and to get the cross-section structure. The scanning electron microscopy investigations was performed using a low temperature (typically between -100 °C and -175 °C) SEM (Cryo-SEM), due to the SEM microscope chamber and detector contamination caused by the perfume release during the observation at ambient temperature, where the perfume release occurs due to a vacuum condition. The Cryo-SEM involves the freezing of the samples (including liquid filler) and its future examination at low temperature. Before capturing the micrographs, the samples were coated with gold/palladium.

4.1.5 Atomic force microscopy (AFM)

Atomic force microscopy studies were performed by a MultiMode AFM (Bruker, CA, USA) equipped with air probe holder (MMEFCH or similar) using Silicon AFM probes for imaging in air, OMCLAC160TS-W2 (Olympus, Japan) with the following nominal parameters: resonance frequency 300 kHz; spring constant 42 N/m; tip radius of curvature <10 nm, 7 nm. Before the AFM experiments, the

microcapsules were deposited in darkness and dried on Si-wafers; imaging was performed in tapping mode in air.

Scanning was performed in one direction – from top to bottom of slow scan axis. AFM data processing was performed using WSxM software, version 4.0 Develop 5.3 (Nanotec Electronica S.L., Spain). No tilt correction was applied to the images. Profile and Z-measurements on profiles were performed in reference to the same surface features in order to minimize thermal drift effects. A desk lamp equipped with a Philips DuraMax 85W 120V bulb served as the source of exposure for the microcapsules.

The distance between the lamp and the sample was around 30 cm. Light wavelength emitted by this lamp (400–900 nm) was measured by an Ocean Optics USB2000 Miniature Fiber Optic Spectrometer, in a dark room at room temperature 23.0 ±0.5 °C. Temperature of microcapsule surfaces, before and after exposure to light, was measured by an Omega MDSi8 thermometer (Omega Engineering) equipped with a thermocouple.

4.1.6 Gas chromatography mass spectroscopy (GC-MS)

Percentage of total encapsulated perfume in the microcapsule slurries was calculated from the amount of non-encapsulated perfume analyzed by using a Liquid-Liquid Extraction with a n-octadecane as an internal standard, and Gas Chromatographic-Mass Spectrometric Analysis described in the US Patent Application 20130039962.[2]

4.2 Results and discussions

4.2.1 Morphological characterization of photosensitive microcapsules obtained via interfacial polymerization method

The design of the new photo-sensitive microcapsule shell, synthesized by interfacial polycondensation of an oil-in-water dispersion, is illustrated in Scheme 4.1 in the experimental part.

Figure 4.2a shows the results of optical microscopy (OM) of the photosensitive polyamide microcapsules, after their preparation, where the presence of the perfume oil is clearly visible, and they appear separated and spherical. Figure 4.2b offer a first SEM micrograph of the cross-section of a frozen capsule, from which it is possible to notice that the capsule shell obtained via interfacial polymerization is uniformly dense and compacted. The microcapsules appear

well formed and globe-shaped with a dense wall. Wall thicknesses gave a value around 1 µm as expected from theoretical calculations. The Cryo-SEM samples preparation technique involves the immersion of the microcapsule slurry into liquid nitrogen at -210 °C, where the aqueous dispersion phase containing xanthan gum and sodium chloride is frozen and forms the bulk mass. The capsules are visibly coated by an external layer. This can be explained by the presence of xanthan gum in the microcapsule slurries used for their separation.

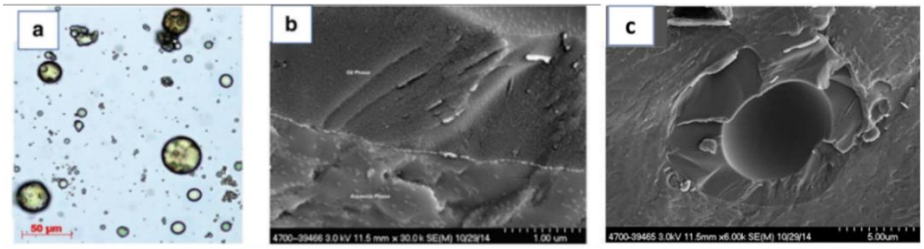

Figure 4.1 Morphological characterization of the obtained microcapsules. a) OM shows that spherical capsules (around 50 µm diameter) are obtained containing perfume, b) SEM of the cross-section shows dense shell, c) SEM micrograph of the fractured capsules immersed into the solid bulk frozen matrix.

GC-MS analysis of free perfume in microcapsules suspension, put into evidence that by using the interfacial polymerization method 99.51 ±0.09 % of perfume oil was encapsulated, which represents a desirable encapsulation efficiency (EE).

The main size diameter of the capsules (62.2 ±0.3 µm) was measured by light scattering (LS) method: 90 % of the capsule diameters were in the range 20–85 µm. This range is comparable with the size of polyamide microcapsules prepared by interfacial polymerization reported in literature.[4]

4.2.2 Photosensitive behavior and shell modification induced by white light irradiation

4.2.2.1 Light induced diameter-size modification

The average size of the capsules before and after irradiation was also measured and it seems to decrease to approximately 16 ±2 % after 3h of light irradiation. In order to evaluate the effect of visible light irradiation on the microcapsules' morphology and size, indeed, the microcapsules were exposed to visible light emitted from a microscopy bulb for up to 1 h and then kept in darkness overnight. Figure 4.2 shows how a single microcapsule shape is changing as a function of time and light exposure.

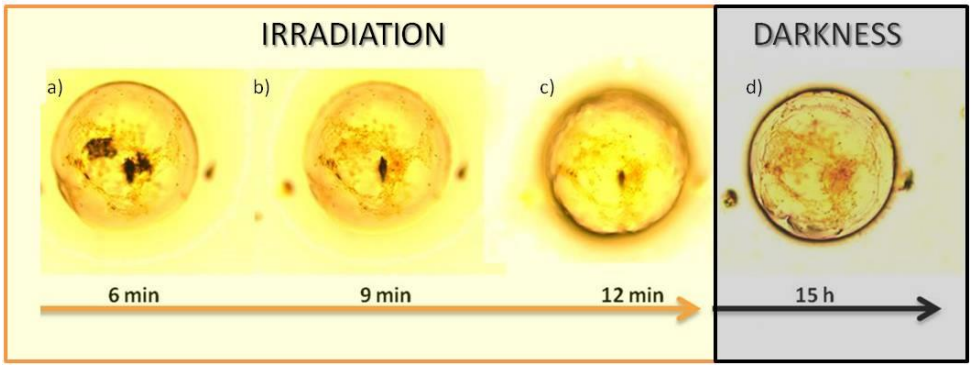

Figure 4.2 OM of a single photosensitive polyamide microcapsule; focus on surface change during irradiation with visible light.

During the first 6 min of irradiation the microcapsule seems to be well formed with a smooth surface.

Then, after additional 3 min of irradiation its surface morphology starts to change, and the microcapsule's diameter decreases approximately 7 %. After 12 min of irradiation the diameter decreases by 11 % from the initial, and its surface appears rough. No further morphological changes were observed between 12 min and 1 h of additional irradiation. The capsule was then kept in darkness for 15 h and its morphology was again observed. As it is shown in Figure 4.2d, its surface has turned back to well defined and spherical, like at the beginning of the experiment. Further, the capsule diameter after keeping in darkness is now only 2 % smaller than the starting capsule prior to irradiation.

To confirm these diameter changes, caused by light, additional experiments were performed. From an aqueous dispersion of microcapsules, mean diameter measurements were taken by light scattering prior to and after 1 h of light exposure to visible light. The measurement was taken again after 15 h in a dark environment. The mean diameter was found to be 62.23 ±0.03, 49.46 ±0.02, and 54.11 ±0.03 μm, respectively. This corresponds to a 21 % reduction in mean diameter after 1 h of irradiation, and a recovery to 87 % of the original diameter after 15 h in the dark in broad agreement with the microscopy results on a single capsule.

Table 4.2 Percentage of encapsulated perfume and microcapsules size after preparation and 3 h of irradiation with visible light.

EE %	Microcapsule mean diameter (μm)	Microcapsule mean diameter (μm) after 3h of irradiation with visible light
99.5 ±0.2	63.3 ±2	52.6 ±2

Then, in order to understand the microcapsule surface topography change occurring during irradiation with visible light, additional computational studies using a BIOVIA Materials studio (Accelrys) platform were performed. By using the Polymer Builder module, surface models containing five chains of polyamide and formed by the five ortho-substituted azobenzene moieties connected by 1,8-diamminooctane, as flexible spacers, were created. This analysis is based on geometry and energy optimization of the photo-sensitive polymer shell topographies and configurations.

Figure 4.3 visualizes the *E* and *Z* topographies of these surfaces. While the *E* topography is greatly symmetrical exhibiting a planarity, the Z topography is much more geometrically irregular and approximately 20 ±1 % shorter than the one formed by the polymers in E configuration. This simulation suggests that the *E-Z* photo-isomerization of the ortho-substituted azobenzene moieties incorporated in the main chain of the polymer which forms microcapsule shell, leads to the capsule squeezing and consequent release of encapsulated active materials. These modelling studies provide a theoretical explanation for the 16 ±2% decrease of mean microcapsule size diameter after 3 h of irradiation with visible light measured with the LS method and the optical micrographs.

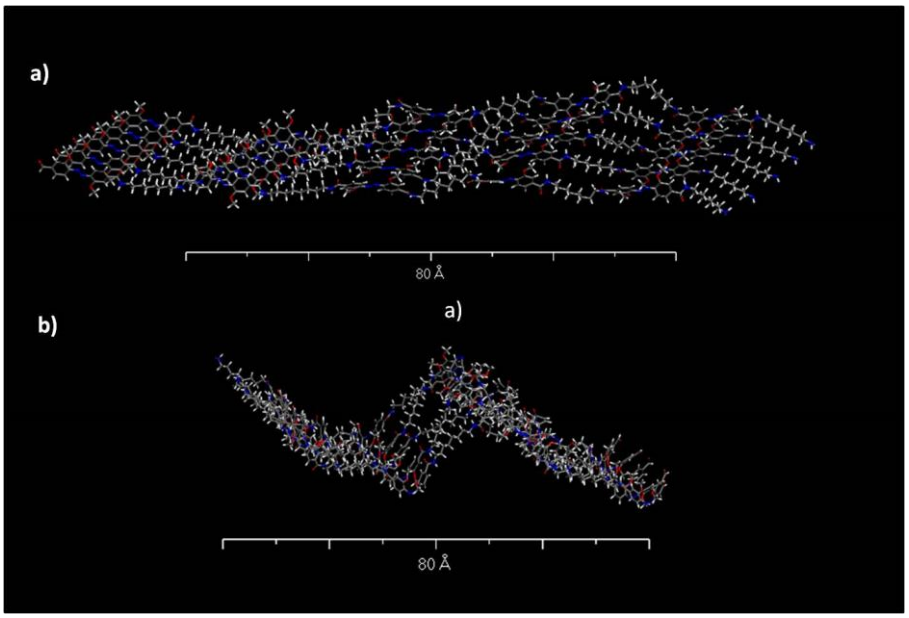

Figure 4.3 Topographies of polymer chains before (a) and after (b) irradiation.

4.2.2.2 Light induced surface changes

In order to understand the morphology changes and the behaviour of the microcapsule shell during irradiation, an exhaustive characterization of the microcapsule surfaces was performed by atomic force microscopy (AFM).[5]

Reported AFM images were recorded at scan size 5×5 μm^2 images at 1 Hz scanning rate. Scanning was performed in one direction – from top to bottom of slow scan axis.

In order to follow the microcapsule's surface topography changes due to light irradiation, AFM topographies were analysed by line profiling routines. Linear scans (x direction) and topographic analyses (z direction) were investigated between two points forming profile 1 and profile 2, at the beginning of the experiments, as well as after 10 and 35 min of irradiation, respectively. As, it can be observed in Figure 4.4, during the first 10 min of light irradiation the *E*-*Z* photoisomerization occurs causing the topographic changes. Then, a prolonged illumination (from 11 to 35 min) causes an unexpected shape-change of profiles 1 and 2. They are similar to the ones measured before sample irradiation. These results suggest a back Z-E isomerization, which according to literature can be driven by sample heating;[6,7] it s well known, indeed, that *Z*-azobenzene can be thermally relaxed back to the *E*-isomer.[8,9]

For this reason, the temperature of the microcapsule surface during the AFM investigation was monitored by Omega MDSi8 thermometer equipped with a thermocouple. Obtained results put into evidence that the bulb emits heat and increases the sample temperature from 22 ±2 °C up to 50 ±2 °C after approximately 25 min of irradiation: this thermal effect could be responsible of the observed topographic variation. AFM device and chamber are indeed, made of metal, and heat emitted by the bulb utilized can influence the sample temperature during analysis. Therefore, to prove a cyclic on-off switching effect of photo/thermal isomerization, the sample surface, initially at room temperature, was submitted to cycles of photo-irradiation/heating to 50 °C and its topographies recorded after each step (Figure 4.4 Cycle II and III).

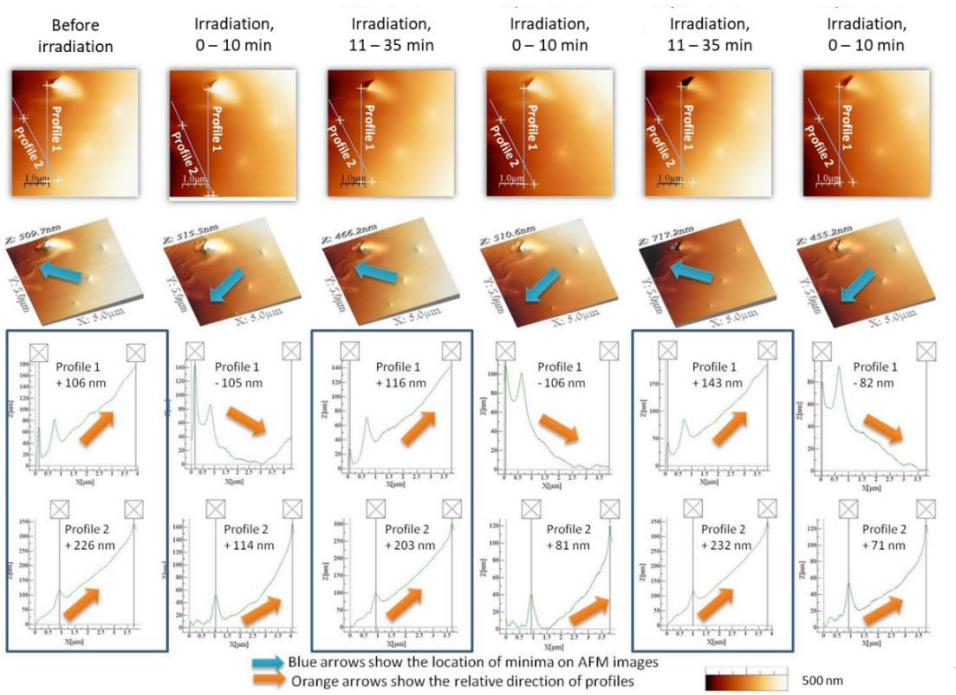

Figure 4.4 AFM topographies of microcapsule surface changes caused by visible light irradiation.

Results demonstrate the switching behaviour of prepared microcapsules and AFM experiments clearly confirmed that the topographic changes depend on *E-Z* photoisomerization, followed by thermal back-isomerization. Indeed, all these changes triggered by light irradiation can be of course driven by the isomerization of the photo-sensitive monomer azobenzene-2,2′-dimethoxy-

4,4′-dicarboxylic acid which was exhaustively investigated by 1H-NMR analysis in the second chapter of this thesis work where we demonstrated that, even short irradiation of the molecule with white light, lead to consistent percentages of *E-Z* isomerization.

4.2.2.3 Panelist smelling test

In order to demonstrate a consumer relevant benefit of photo-sensitive microcapsules application in consumer goods, a tests for the evaluation of the perfume release triggered by light irradiation and a sensory evaluation with perfume experts, were performed according to standard tests reported in the literature.[10] The grading scale utilized by perfume experts is adapted to consumer noticeability: a grade less than 20 is not considered as consumer noticeable in this test.

During this test based on the trained panelists' nose, we compared the release of the perfume from fabrics exposed to daytime light over time. At the beginning of the test, the fabrics were treated with prototypes containing encapsulated or neat perfume. As shown in Figure 4.5 the encapsulated perfume perception over time shows a significant difference, versus the neat perfume one, which is clearly related to a difference in release.

The preliminary results clearly demonstrate that the encapsulated perfume shows delayed release and is noticeable up to 7h, while the non-encapsulated perfume is not detected by the standard consumer after 3h.

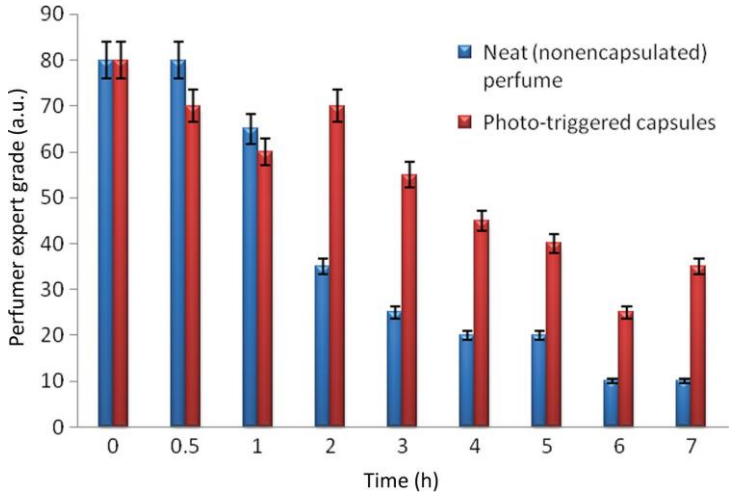

Figure 4.5 Comparison of perfume release noticeability from fabric under visible light irradiation over time, evaluated by perfumer panelist experts.

4.3 Conclusions

In this work we showed that by incorporating 4,4′-bis(chlorocarbonyl)-2,2′-dimethoxy azobenzene (ortho-substituted azobenzene) moieties into polyamide microcapsule shells, it is possible to trigger active components release by simple exposure to visible light. This is due to light-driven E to Z isomerization which modifies shell morphology, as it was first predicted by computational studies and subsequently confirmed by experimental preparation of the photoactive polymeric material. By using interfacial polymerization, we succeeded in encapsulating more than 99 % of active agent in globular shaped and separated, well-formed microcapsules with a compact shell. OM and AFM analyses confirmed that photoirradiation induces a change in capsules surface and morphology, as well as size. Both theoretical and experimental studies suggest that a squeezing effect can be responsible for photo triggered increased release. Moreover, the combination of AFM and ^{1}H-NMR put into evidence that the initial morphology and size of the microcapsules are restored as a consequence of thermal back-isomerization above 50 °C.

Finally, experts' test adapted to consumers and based on perfume perception, showed that after 7 h the encapsulated perfume can be still noticed, while the neat one is not perceived after 3 h. In view of the generated results, the obtained microcapsules can have future potential applications in: consumer goods (household and personal care products), medicine, catalysis,

electronics, textile, chemical industry, and others. Summing up, all these analyses, the whole set of AFM and ^{1}H-NMR experiments, put into evidence that microcapsules' size and surface morphology are strongly affected by irradiation under visible light and they suggest the intriguing possibility of a reversible switching of active compounds release from microcapsules upon combination of visible light and thermal stimuli.

Bibliography

1. Del Pezzo, R., Bandeira, N. A., Trojanowska, A., Prieto, S. F., Underiner, T., Giamberini, M., Tylkowski, B. Ortho-substituted azobenzene: shedding light on new benefits. *Pure Appl. Chem.* 91(9), 1533-1546. (2018).

2. Smets, J., Ganapathysundaram, R. V., Prieto, S. F., Bianchetti, G. O., Combs, M. J., Guinebretiere, S. J., Evers, M. F. T. Encapsulates. *U.S. Patent Application No. 12/984,049*. (2011).

3. Liao, Z., Xue, D., Li, H., Shi, L. Fragrance-Containing Microcapsules Based on Interfacial Thiol-Ene Polymerization. *J. Appl. Polym. Sci.* **133**, (2016).

4. Tylkowski, B., Pregowska, M., Jamowska, E., Garcia-Valls, R., Giamberini, M. Preparation of a new lightly cross-linked liquid crystalline polyamide by interfacial polymerization. Application to the obtainment of microcapsules with photo-triggered release. *Eur. Polym. J.* **45**, 1420–1432 (2009).

5. Horcas, I., Fernández, R., Gomez-Rodriguez, J. M., Colchero, J. W. S. X., Gómez-Herrero, J. W. S. X. M., Baro, A. M. WSXM: a software for scanning probe microscopy and a tool for nanotechnology. *Rev. Sci. Instrum.* **78**, 013705 (2007).

6. Asano, T., Okada, T., Shinkai, S., Shigematsu, K., Kusano, Y., Manabe, O. Temperature and pressure dependences of thermal cis-to-trans isomerization of azobenzenes which evidence an inversion mechanism. *J. Am. Chem. Soc.* **103**, 5161–5165 (1981).

7. Dokic, J., Gothe, M., Wirth, J., Peters, M. V., Schwarz, J., Hecht, S., Saalfrank, P. Quantum Chemical Investigation of Thermal Cis-to-Trans Isomerization of Azobenzene Derivatives: Substituent Effects, Solvent Effects, and Comparison to Experimental Data. *J. Phys. Chem. A* **113**, 6763–6773 (2009).

8. Bushuyev, O. S., Tomberg, A., Friščić, T., Barrett, C. J. Shaping Crystals with Light: Crystal-to-Crystal Isomerization and Photomechanical Effect in Fluorinated Azobenzenes. *J. Am. Chem. Soc.* **135**, 12556–12559 (2013).

9. Titov, E., Lysyakova, L., Lomadze, N., Kabashin, A. V., Saalfrank, P., & Santer, S. Thermal Cis-to-Trans Isomerization of Azobenzene-Containing Molecules Enhanced by Gold Nanoparticles: An Experimental and Theoretical Study. *J. Phys. Chem. C* **119**, 17369–17377 (2015).

10. Meilgaard, M., Civille, G. V., Carr, B. T. *Sensory evaluation techniques*. Boca Raton : CRC Press, (1991).

5. Crosslinked capsules with polyacrylic shell containing bis(2-(methacryloyloxy) ethyl)4,4'-(diazene-1,2-diyl) (E)-bis(3-methoxybenzoate) (Azo acrylate)

In the current chapter we propose the incorporation of small percentages of the modified azobenzene moiety, descried in the second chapter, in a polyacrylate chemistry, which it is known to provide compact and stable shells. With this new approach, we want to test whether it is possible to form compact shells in which the light sensitive moiety has the capacity and the required mobility to isomerize and increase the porosity of the shell.

In the following paragraphs we will discuss thus, new photo-sensitive chemistries for the obtainment of delivery particles. First, the new path for the synthesis of an acrylic ortho-substituted azobenzene will be explored. Then, in-situ polymerization will be investigated as an alternative technique to emulsification and solvent removal, for the obtainment of compact photosensitive shells for perfume encapsulation and subsequent light triggered release.

The chemistry proposed in this chapter was already introduced in a patent from 2015 filed by The Procter & Gamble Company[1] to eliminate or minimize the main drawbacks of capsules and to prevent the typical issues of capsules performances, such as high leakage or poor stability in finish products (FP).

In this work we decided to explore the possibility to incorporate photosensitivity in crosslinked capsules for consumer good products, to provide existing formulations with new additional perfume delivery opportunities. The processes used nowadays in the P&G company to produce PMC and to encapsulate perfumes all belong to the category of the chemical methods;[2,3] one of these approaches, the polyacrylate chemistry for the obtainment of the so-called Poly Acrylate Capsules (PAC) with in-situ polymerization and an inside-out approach, will be used in this chapter. First, the synthesis of the ortho-substituted azobenzene molecule was performed, following the procedure reported in the experimental part of Chapter 2. Then, the modification of the ortho-substituted azobenzene with methacrylic groups is conducted,[4] followed

by its subsequent incorporation into the polymeric network which constitute the shell, via in-situ polymerization.

In polymer chemistry, in situ polymerization means "polymerization into the mixture": this process consists of an initiation step followed by a series of polymerization steps, which result, in this case, in the formation of a polymeric crosslinked network. The characteristic of in situ polymerization is that all the reactants are included in one single phase, in this case the dispersed one, and PMCs result in an oil droplet covered by a crosslinked polymeric shell which provides high protection from the external environment and in liquid detergents for the final application. Melamine formaldehyde capsules were the first PMC launched on the market by P&G, while the PAC started to be utilized only recently. Acrylates, which are the only monomers used to prepare PACs, are the esters of acrylic acid and its derivatives. The acrylate ion contains the vinyl group which is susceptible to polymerization and the carbonyl carbon which can be conveniently functionalized. These monomers are, thus, of great interest because they are considered as bifunctional and can be suitable for many applications. More often it is possible to refer to the acrylic and methacrylic monomers as the family of esters obtained from the reaction between an alcohol and the acrylic acid or its derivatives in the presence of a catalyst. Acrylic acids are numerous, and a wide variety can be taken into account for the production of acrylates. The possibility to react a wide variety of acrylic acids, or their derivatives, with a wide variety of alcohols leads to acrylic monomers with several and different properties which can be then transferred to the resulting final polymer; this versatility of the acrylate chemistry, is exactly what justifies their wide applicability in the industrial field.

For a full and complete characterization of capsules there are a few parameters to consider. We need to take into account that when we talk about a system composed only by capsules, we refer to dry capsules which shows as a powder; it is possible to obtain dry capsules *via* spray drier, fluidized bed coating, phase inversion followed by filtration, or other techniques which require treatment under vacuum and/or at high temperature. It is obvious that in many cases such treatments can damage the capsule system affecting the capsules shape, morphology and encapsulation efficiency.

When capsules are obtained *via* other techniques as, for example, *via* in-situ polymerization, the presence of the continuous phase needs to be taken into account and we refer to capsules by meaning the slurry. Inside the slurry there are many components as: the capsule shell, sometimes unreacted monomers, the encapsulated perfume, the free and not-encapsulated perfume, the water and an emulsifier as well as other stabilizers. The slurry can be then inserted into the FP to test the performances of the capsules in real-life usage conditions; in this case, the capsules get in contact with the additives of the FP and, in particular, with a certain percentage of surfactants which are used as detergents, wetting and foaming agents, emulsifiers and dispersants in the FP. Surfactants incentivise the perfume inside the capsules to leak out and this is the main reason why it is very important to study the stability of the capsules in this aggressive environment.

When analyzing a slurry, it is important to study the capsules size and their distribution, the triggered release, the surface chemistry, the non-encapsulated oil and the activity of the total batch; the performances of the capsules inside the slurry can be studied by determining percentages of leakage, mechanical properties and performances under usage conditions.

5.1 Experimental

5.1.1 Materials

All the solvents used, dry Tetrahydrofuran (THF) (≥99.9%), dry dioxane (99.8%), THF (98%), methanol (99.8%), chloroform (99.5%), deuterated chloroform (99.8%) and dimethylsulfoxyde (DMSO) (99.9%), were provided by Sigma Aldrich and used as received without prior purification. $MgSO_4$ (99.5%), pyridine (Py) (99.8%), dimethyl amino pyridine (DMAP) (99%), 2-hydroxyethyl methacrylate, 2-(tert-Butylamino) ethyl methacrylate, 2-Carboxyethyl acrylate, isopropyl myristate, polyvinyl alcohol (PVA) (85,000-124,000 g/mol) were provided by Sigma Aldrich. CN975 was provided by Sarton Americas and the Soluplus (polyvinyl caprolactam polyvinyl acetate-polyethylene glycol graft copolymer (PCL-PVAc-PEG)) was provided by BASF. The Freesia PAC 60 was supplied by Procter & Gamble.

5.1.2 Methods and characterization techniques

5.1.2.1 Synthesis of bis(2-(methacryloyloxy) ethyl)4,4'-(diazene-1,2-diyl) (E)-bis(3-methoxybenzoate) (Azo acrylate)

The final objective of this synthesis work is the obtainment of the bis(2-(methacryloyloxy)ethyl)4,4'-(diazene-1,2-diyl)(E)-bis(3-methoxybenzoate), the so called Azo-methacrylate, a bifunctional photosensitive methacrylate which will be incorporated into the crosslinked net of PAC. The synthesis of this molecule follows a multi-step procedure; the first step is the synthesis of the azobenzene dicarboxylic acid, followed by its conversion into the corresponding photosensitive Azo-dichloride,[5] as reported in the experimental section of Chapter 2. Then, the chemical modification of the Azo-dichloride with a commercially available methacrylate is conducted.

The reaction takes place between the previously synthesized azobenzene dichloride, the 4,4′-bis(chlorocarbonyl)-2,2′-dimethoxy azobenzene, and the 2-hydroxyethyl methacrylate, in inert atmosphere of N_2. In a first procedure, the solvent utilized for this reaction was the dry dioxane, which was then substituted by dry tetrahydrofuran (THF). Considering a stoichiometric amount (molar ratio of 1:2) of dichloride to the methacrylate, 2.13 g (16.4 mmol) of 2-hydroxyethyl methacrylate were dissolved in 10 mL dry THF; the reactor system was inserted in a bath of ice and cold water to keep the temperature low and close to 0 °C. Pyridine (Py) (8.2 mmol, 0.65 g) and catalytic dimethyl amino pyridine (DMAP), were added to the reaction mixture and, subsequently, a solution of 3.0 g (8.2 mmol) of Azo-dichloride in 20 mL of dry THF was added dropwise to the reaction mixture. The reaction was monitored and followed via thin layer chromatography (TLC) in methanol. The reaction was conducted at 0 °C for 1h and then it was allowed to warm up to room temperature (rT) and kept at rT for an additional hour.[6]

After two hours of reaction, the liquid mixture was precipitated into distilled water and purified through three cycles of extraction in chloroform. The resulting organic phase was dried over $MgSO_4$, filtered and concentrated *via* rotavapor. The structure of the obtained compound is reported in the results section together with the schematized procedure of synthesis.

The purity of the compound was evaluated via NMR spectroscopy. The photosensitive behavior of the azobenzene acrylate under white light irradiation was studied via UV-Visible spectroscopy. Yield 80%. ^{1}H-NMR (400 MHz,

CDCl3, TMS, d ppm) δ 7.75 (s, 1H), 7.66 (dd, 1H), 7.62 (dd, 1H) , 6.14 (s, CH2), 5.59 (s, CH2), 4.59 (m, 2H), 4.52 (m, 2H), 4.06 (m, CH3), 1.94 (s, 3H), and ^{13}C-NMR (100 MHz, CDCl3) δ 167.8, 167.1, 156.7, 136.2, 135.9, 126.2, 124.4, 123.1, 122.2, 114.8, 63.1, 62.2, 56.6, 18.3.

5.1.2.2 Nuclear Magnetic Resonance (NMR)

The mechanistic understanding of NMR spectroscopy has been already reported and explained in detail in Chapter 2. In this paragraph we will report only the parameters used for the investigation of the chemical species synthesized in this chapter.

The acrylate molecules synthesized were, indeed, characterized by ^{1}H-NMR and ^{13}C-NMR spectroscopy, with a Varian Gemini 400 MHz spectrometer (^{1}H-400 MHz, TMS; ^{13}C-100.4 MHz, TMS). Measurements were carried out at room temperature using 10 - 15 mg or 30 - 40 mg of sample respectively for ^{1}H and ^{13}C analysis; the samples were dissolved in deuterated dimethyl sulfoxide (d-DMSO). ^{1}H-NMR measurements were obtained with retention time between consecutive pulses d1 between 1 and 16 seconds for the accumulations, while ^{13}C-NMR spectra were recorded with 100.4 MHz frequency and lower d1 between 0.5 and 0.2 seconds. For all the analyses tetramethyl silane (TMS) was used as reference.

5.1.2.3 Ultraviolet-Visible spectroscopy (UV-VIS)

The isomerization of the new synthesized photosensitive methacrylate was studied via UV-Visible spectroscopy. UV-Vis spectrophotometer was used to measure the ultra violet or visible light absorbance of the irradiated Azo-acrylate and, in this case, to obtain a fast screening of the absorption spectrum of the Azo-acrylate in order to move on to capsules preparation.

The technical understanding of UV-Visible spectroscopy has already been reported and explained in detail in Chapter 2. In this paragraph, we will report only the parameters used for the investigation of light-sensitive behavior.

The UV-Visible spectrophotometer used, is a Shimadzu UV-1800 and the samples, in DMSO solution (0.9 – 2 g/L), were irradiated with white light from an IDual bulb Adaptative LED (11 W). The light source of the equipment, a combination of tungsten/halogen and deuterium lamps, provides the visible and near ultraviolet radiation covering the 200-800 nm range.

First, a 0.1% wt solution of the Azo-acrylate (0.05 g) in DMSO (25 mL) was prepared and placed in a quartz cuvette. The solution, kept in the dark, was first analysed at time t=0 then, to induce the isomerization, it was irradiated for 5 minutes and analysed again over the UV-Visible spectrometer. The process of analysis was repeated until the pps was reached.

Differently from its parent compound, the 4,4′-bis(chlorocarbonyl)-2,2′-dimethoxy azobenzene, only the *E*-to-*Z* isomerization was studied, mainly to compare the isomerization path of the Azo-acrylate and its isomerization kinetics, with the ones from its parent compound.

5.1.2.4 Poly Acrylate Capsules preparation

Polyacrylate capsules (PAC) were prepared through the chemical method of in-situ polymerization encapsulation; this technique is performed following the procedure reported in patent US20150071977[1].

With this approach the droplet formation is associated to the preparation of an oil in water (O/W) stable emulsion, while the droplet stabilization is associated with the completion of the polymerization of the involved monomers, at the interface between the said two phases. It is first necessary, thus, to prepare two immiscible phases; an aqueous phase which will be also called continuous phase, and will contain a certain amount of polyvinyl alcohol (PVA) as emulsifier agent, and an oily phase, also called discontinuous or dispersed phase, which contains the oil/perfume/active to be encapsulated and all the reactive monomers involved in the polymerization reaction. Different initiators, with a different activation temperature, are involved in the reaction; the initiators are solubilized in both the continuous and the dispersed phase.

We will refer to the oil encapsulated as the core material; by shell we mean the crosslinked polymer formed by reaction of three different acrylic monomers and the initiators. In the procedure reported in the patent the core:shell ratio is 90:10 and three different monomers are involved: two commercially available monofunctionalized monomers, the 2-(tert-Butylamino)ethyl methacrylate and the 2-Carboxyethyl acrylate, and the CN975 which is a mixture of monomer 6- and 3- functionalized and act the as main monomer for the shell formation. The two monofunctional acrylates constitute together the 4.4% of the shell and the CN975 constitute the 95.6% left. The isopropyl myristate (IPM) is added to the dispersed phase to facilitate the precipitation of the polymeric shell; is will, most

probably, become part of the core material. The compositions of the continuous and dispersed phase are reported below in Table 5.1, where the percentages of all the raw materials (RM) used are expressed as percentage in weight. In order to obtain a stable emulsion, in all the experiments, the ratio in weight continuous phase : dispersed phase is 60:40.

Table 5.1 Composition of the dispersed phase.

RM name	%
Voyager Zen	59.84
2-(tert-Butylamino)ethyl methacrylate	0.24
2-Carboxyethyl acrylate	0.19
CN975	9.36
2,2'-Azobis(2,4-dimethylvaleronitrile)	0.83
2,2'-Azobis(2-methylbutyronitrile)	0.19
IPM	29.89

For the dispersed oily phase, indeed, the data are reported in Table 5.2.

Table 5.2 Composition of the continuous phase.

RM name	%
Water	97.67
Selvol 540	1.95
4,4'-Azobis(4-cyanovaleric acid)	0.37

In order to obtain photosensitive capsules, a modification of the reported procedure is necessary; the incorporation of the light-sensitive molecule requires a specific new design.

The target percentage of photosensitive Azo-acrylate into the shell is 10 wt% but, in some of the experiments, the percentage needs to be adjusted according to need.

In all the experiments the disperse and the continuous phase were prepared separately. In order to prepare the dispersed phase, a certain amount of Azo-acrylate was first solubilized into the desired amount of perfume (or perfume plus solubilizer); the solution was gently stirred for 24h and only when it reached

complete dissolution the other components, such as the initiators and the remaining acrylates, were also added into the system and solubilized under continuous stirring *via* the use of a magnetic stir bar.

Similarly to the dispersed phase, also for the preparation of the continuous phase first a 2% PVA solution was obtained; then, the initiator was added and solubilized with the help of a high speed T25 digital Ultra-Turrax at 3000 rpm. Once all the components of the two phases were dissolved, leading to homogeneous systems, they were emulsified together with the preferred emulsification equipment. In these experiments the emulsification was obtained mixing with an overhead stirrer Eurostar 200 digital from IKA. Stirring, in order to obtain fine drops and a stable emulsion, was conducted at 1200 rpm for 30 minutes. Once the O/W emulsion was ready and stable, the system was transferred to a reactor connected to heating system where the polymerization and the curing of the polymeric network took place. As a final result, we obtained a slurry of solid capsules dispersed into the aqueous phase. For not photosensitive capsules a big reactor with a capacity of 500 mL, double walls and connected to a thermoset for the temperature control, was used; the stirring in this case was guaranteed using an anchor stirrer at 200 rpm. The volume considered for the reaction into this reactor was 250 mL. For the obtainment of the photosensitive capsules smaller volumes were considered, due to the small amounts of in-house synthesized Azo-acrylate available; a smaller reactor of 50 mL was used and, in order to control the temperatures, it was inserted in an oil bath with thermometer control. The maximum reaction volume considered in this case was of 25mL. The schematic representations of the two reactors used, and just described, are reported below in Figure 5.1, together with their real images.

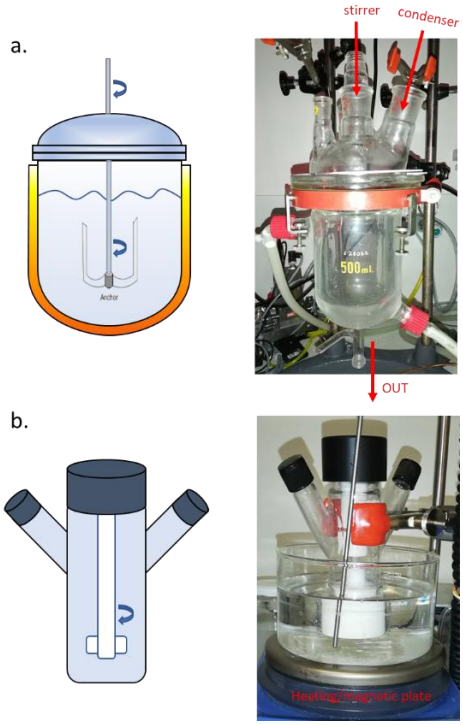

Figure 5.1 Schematic representation of the reactor used for the polyacrylate crosslinking encapsulation process (in-situ polymerization). a) 500mL reactor with heated double walls, equipped with reflux condenser and overhead stirrer, and b) 50mL small closed reactor equipped with an internal magnetic stir bar, placed in a heating oil bath on a heating stirring plate.

In both cases, the temperatures reported in Table 5.3 were subsequently applied, for the corresponding time ranges:[7]

Table 5.3 Temperature ramp for the microcapsules formation

Temperature [°C]	Time [min]
40	15
60	75
75	270
90	480

The compositions of all the performed experiments are reported in Table 5.3. In some cases, a certain percentage of Soluplus®, is added which is the commercial name for (polyvinyl caprolactampolyvinyl acetate-polyethylene

glycol graft copolymer (PCL-PVAc-PEG) provided by BASF and which chemical structure is reported in Figure 5.2. it is an amphiphilic polymer with outstanding solubilization properties.

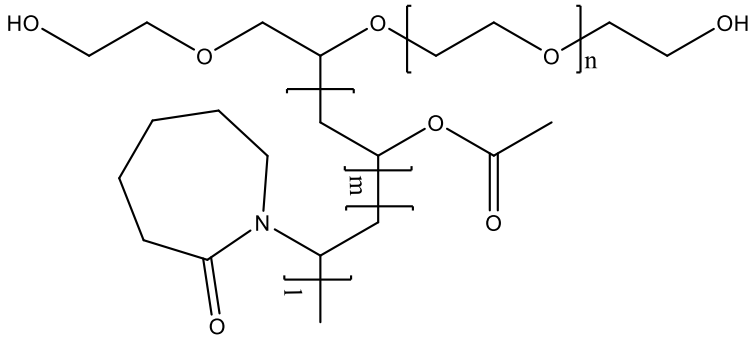

Figure 5.2 Chemical structure of Soluplus®.

The Table 5.4 below, summarizes the encapsulation experiments performed in this work with the corresponding core:shell ratios, compositions, percentage of Azo acrylate into the shell and percentage of Soluplus® in the dispersed phase. All the experiments are performed in a 50 mL reactor except for the C1 batch where the big 500 mL reactor was used.

Name of slurry	Core:shell	Reactor	CN975 (g)	2-(tert-butylamino) ethyl methacrylate (g)	2-Carboxyethyl acrylate (g)	Azo-acrylate (g)[a]	Soluplus (g)[b]
C1	90:10	500 mL	7.487	0.189	0.156	-	-
C2	90:10	50 mL	0.936	0.024	0.019	-	-
C3	90:10	50 mL	0.979	-	-	-	-
C4	90:10	50 mL	0.881	-	-	0.098 (10%wt)	-
C5	90:10	50 mL	0.881	-	-	0.098 (10%wt)	1.00 (10%wt)
C6	90:10	50 mL	0.979	-	-	-	1.00 (10%wt)
C7	90:10	50 mL	0.936	0.024	0.019	-	1.00 (10%wt)
C8	90:10	50 mL	0.881	-	-	0.098 (10%wt)	-
C9	90:10	50 mL	0.930	-	-	0.049 (5%wt)	0.50 (5%wt)
C10	95:5	50 mL	0.448	-	-	0.050 (10%wt)	-
C11	90:10	50 mL	0.838	0.043	-	0.098 (10%wt)	1 (10%wt)
C12	90:10	50 mL	0.887	0.043	-	0.049 (5%wt)	0.50 (5%wt)
C13	95:5	50 mL	0.426	0.022	-	0.050 (10%wt)	-
C14	90:10	50 mL	0.940	-	-	0.039 (4%wt)	-
C15	95:5	50 mL	0.478	-	-	0.020 (4%wt)	-

Table 5.4 Experiments for PAC (photosensitive and non-photosensitive) preparation.
[a] weight percentage of the shell.
[b] weight percentage of the discontinuous phase.

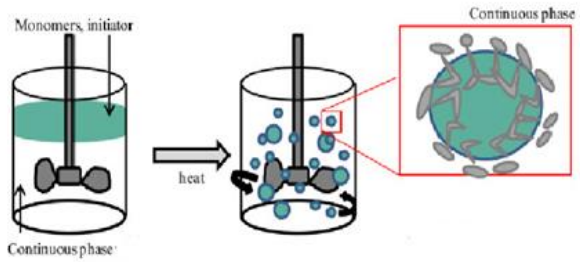

Figure 5.3 In-situ polymerization microencapsulation scheme.

5.1.2.5 Optical Microscopy (OM)

In order to obtain a first and fast insight of capsules morphology, size and loading, optical micrographs were obtained via an Axio Imager light microscope from Zeiss. The microscope was used in transmitted light mode at room temperature.

5.1.2.6 Environmental Scanning Electron Microscopy (ESEM)

Surface and morphology of microcapsules were investigated by means of an ESEM FEI Quanta 600 apparatus and a Flex-SEM 1000 VP-SEM. The investigation was carried out in high vacuum mode, using an accelerated voltage ranging between 15 and 20 kV.

5.1.2.7 Gas Chromatography – Mass spectroscopy (GC-MS)

The technique of gas chromatography – mass spectroscopy (GC-MS) was used for the study and the characterization of capsule's performances.

5.1.2.7.1 Leakage tests

The stability of capsules in the FP, over time and in specific conditions of temperature and humidity, were studied via Headspace GC-MS in a leakage experiment designed by P&G. In the mentioned leakage test, a certain amount of capsules, in the form of slurry with known activity, was added to a Heavy-Duty Liquid (HDL) and then analysed *via* Headspace GC-MS. The activity is defined as the percentage in weight of active material (perfume) respect to the total weight of the sample. The samples were prepared with a final 1.0% activity of the perfume in the FP, starting from the known initial activity of the slurry. We analyzed samples stored for several days at room temperature and samples stored for the same time at 35°C in a 60% humidity room. The leakage profile overtime was obtained through this test.

The procedure for analysing samples is the following: small aliquots of the sample (FP + slurry) were analysed by fast headspace GC-MS approach. 0.1 g of the sample was transferred to 25 mL headspace vials. The samples were equilibrated for 3 hours at room temperature. The headspace above the FP was sampled *via* solid-phase microextraction (SPME) (50/30µm DVB/Carboxen/PDMS) approach for 1 minute at ambient temperature. The SPME fiber was subsequently thermally desorbed into the GC. The analytes were analysed by GC/MS in full scan mode. The amount of free perfume in headspace has been calculated vs a reference corresponding to 100% free perfume.

5.1.2.7.2 Total oil

The total oil analysis is a test performed to evaluate the activity of the slurry, and the content of the active encapsulated into the shell. A certain amount of sample, in the form of capsules slurry, was transferred to a vial, weighted, dispersed with some water and diluted in ethanol. For the extraction of the perfume, the sample was heated up to 60°C for 30 minutes. After spiking with an internal standard, the perfume was analyzed by GC-MS with a chromatograph Agilent 6890 with split/splitless injector and MSD detector. As a reference, the same perfume encapsulated in the analyzed capsules was used, i.e. PAC 60 Freesia. It was also analyzed *via* GC-MS and the resulting peaks were compared to the ones relative to the sample, to obtain its final concentration.

5.1.2.7.3 Free oil

In order to calculate and quantify the free, and thus unencapsulated, perfume present into the capsules slurry, a new method, based on GC-MS was proposed by P&G and applied in this study. The quantification of the free unencapsulated perfume from a microcapsule slurry requires the extraction of the perfume under precise conditions, yielding high recovery but not inducing leakage. It is critical to control the mixing and extraction time to ensure reproducible and sufficient mixing to yield quantitative results.

This method requires the dilution of the slurry with a surfactant solution, followed by liquid - liquid extraction. An Agilent GC6890 equipped with Agilent 5973N mass spectrometer, capillary column operation, quantization based on extracted ion capability and an autosampler were used.

The internal standard solvent mixture is constituted by a well-mixed solution of 0.1g tetradecane diluted in 4L hexane. The perfume standard is obtained weighting 0.050 g of the desired perfume oil into a 50mL volumetric flask. For the sample preparation, first the confirmation that the slurry is well mixed, is required; then, 0.3 g of slurry were weighted into a 10mL vial and the final weight is recorded. At this point, 1µl injection with a split ratio of 10:1 up to 30:1 is suitable. The calibration curves are generated from the perfume standard for each perfume raw material (PRM) and used to calculate the individual PRM weight %.

5.1.2.7.4 Dynamic Head Space (DHS)

Release experiments of the encapsulated perfume from microcapsules were performed diluting the samples, in the form of capsules slurry, in distilled water. 100 µL of the well mixed and homogeneous diluted sample with a 0.1% wt activity (amount of perfume) was sampled on a filter paper 3x2cm and placed in a 250 mL closed glass jar. In some experiments only one jar per sample was prepared and the amount of perfume released was measured at time t=0 in dark conditions and after a certain range time of light irradiation. In other experiments instead, two jars, A and B, containing the same sample, were prepared in order to quantify the perfume release with (A) and without (B) white light irradiation, thus eliminating the error provoked by the perfume released due to the leakage. Since the use of this method for the measurement of photosensitive release is novel and not jet optimized, we needed to adjust the settings of each experiment as we go along: the exposure time thus, changed according to the experiment. In most cases there is an alternation of irradiation and darkness time ranges in order to study the possibility of cyclic perfume release from photosensitive PAC. Usually the cycle of measurements and dark/light exposure was: analysis at (I) time 0, (II) after white light exposure (5, 10, 20 minutes), (III) after darkness exposure (30 minutes to 1h) and, finally, (IV) after second irradiation with white light (5, 10,20 minutes).

In this study, Tenax® TA sorbent traps were chosen; the sorbent tube was placed into the closed jar, introduced from a hole in the lid, in the middle of the head space volume, the volatiles were adsorbed for 10 minutes with a flow of 20 mL/min and, after 10 minutes, the traps were transferred to the thermal

desorption unit (TDU) and the analytes thermally desorbed. The analytes were finally introduced to the GC/MS system as a narrow band leading to improved peak shape and separation as well as increased sensitivity.

5.1.2.8 Olfactive sensory test

Sensory tests were performed in the BIC facilities of sensory laboratory. In order to explore the possibility to utilize photosensitive capsules slurries in sprays for the dry cleaning of carpets and/or curtains, olfactive tests were performed with the help of expert panelists. 0.1% activity samples made by slurries diluted in milliQ water, were sprayed on curtains by a spray dispenser, inside the home care rooms (21 °C (± 1.7 °C), 45% RH (± 5% RH)). Olfactive assessment by external panel was used to investigate the influence of the photosensitive molecules in PAC on the scent experience. The assessment was performed at four different moments: fresh, 2h, 24h, after weekend.

5.2 Results and discussions

5.2.1 Synthesis of bis(2-(methacryloyloxy)ethyl)4,4'-(diazene-1,2-diyl)(E)-bis(3-methoxybenzoate) (Azo acrylate)

New methacrylic monomers containing the azobenzene light sensitive structures as main unit, have been prepared by reacting azobenzene assemblies possessing acylic chloride terminations, with 2-hydroxyl methacrylate. The synthetic route utilized in this work is described and reported in the scheme below (Scheme 5.1).

After the design of the photosensitive methacrylic monomer, the synthesis of bis(2-(methacryloyloxy) ethyl)4,4'-(diazene-1,2-diyl) (*E*)-bis(3-methoxybenzoate) (Azo-acrylate) was successfully achieved following a procedure reported by Evans et al. in 1990[6]. First, the photosensitive di-chloride was synthesized as described in chapter 1; its subsequent esterification with the commercially available 2-hydroxyethyl methacrylate was conducted in the presence of pyridine (Py) and dimethyl amino pyridine (DMAP), leading to the desired Azo-acrylate. The reaction was conducted at 0 ºC for the first hour to prevent the polymerization of the methacrylic groups. Py is added to neutralize the HCl formed after the condensation reaction and to shift the equilibrium of the reaction, allowing the maximum of conversion; DMAP acts as a catalyst.

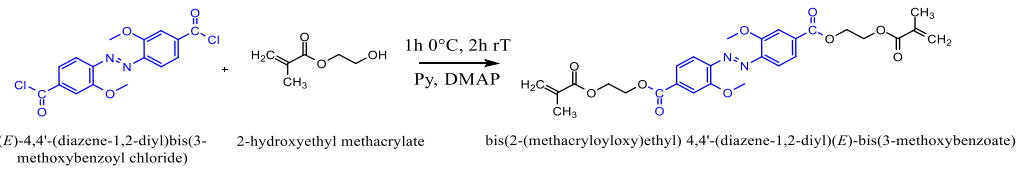

(*E*)-4,4'-(diazene-1,2-diyl)bis(3-methoxybenzoyl chloride) + 2-hydroxyethyl methacrylate → bis(2-(methacryloyloxy)ethyl) 4,4'-(diazene-1,2-diyl)(*E*)-bis(3-methoxybenzoate)

Scheme 5.1 Schematic representation of the esterification reaction leading to the Azo-acrylate.

The purity and the yield of the novel azobenzene derivative, containing the methacrylic terminations, were studied via ^{1}H-NMR analysis. The final yield of the Azo-acrylate was found to be 80%. From the spectrum reported in Figure 5.4 it is possible to identify the peaks related to the novel synthesized compound.

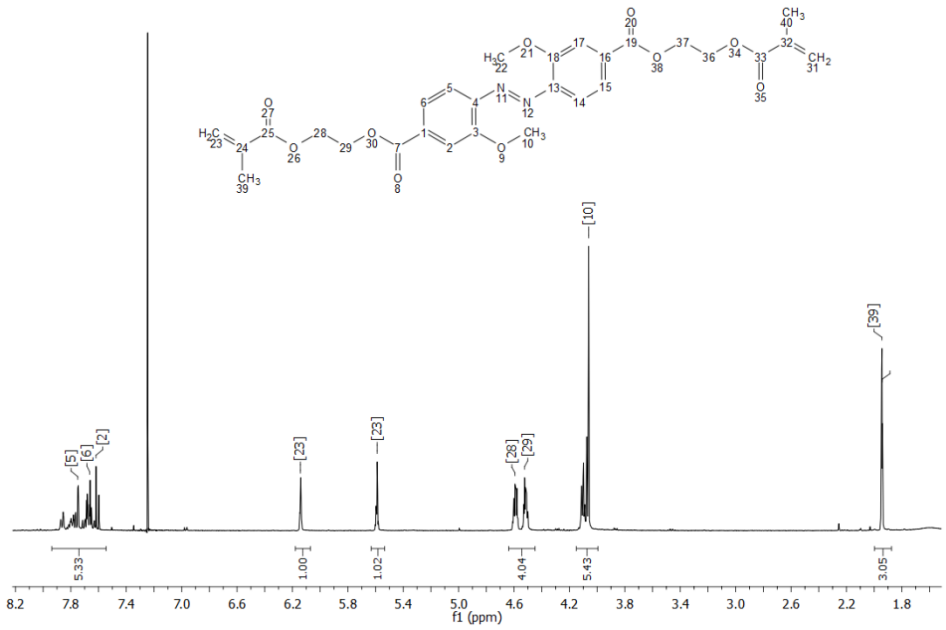

Figure 5.4 1H NMR spectrum of the Azo-acrylate in CDCl3 in THF.

Starting from the ^{1}H-NMR spectrum reported above, we can do some considerations.

What is important to notice is that, the multiplets relative to the aliphatic hydrogens of the unreacted 2-hydroxyethyl methacrylate, at 4.31 and 3.88 ppm, disappear leading to new signals at 4.60 and 4.53 ppm; this shift is due to the formation of the new bond with the ester group. Moreover, by integrating and comparing those peaks we can conclude that the unreacted methacrylate represents the 3% of the final obtained compound and thus, can be considered

negligible. The area between 7.92 and 7.56 ppm is characteristic of the aromatic protons of the azobenzene section, while the peaks at 6.13 and 5.59 ppm are related to the acrylic CH_2. As already explained, the two peaks at 4.60 and 4.53 ppm refers to the hydrogens of the acrylate, when it is bonded to the azobenzene segment. Around 4 ppm there are the signals of the CH_3 from the methoxy group and, at 1.95 ppm, the ones of the CH_3 from the methacrylic acrylate. From the integrations of the peaks relative to the CH_3 from the methacrylic acrylate (1.95 ppm, labeled 39), and the ones relative to the CH_3 from the methoxy group (4 ppm, labeled 10), we can notice that there is one methacrylic termination for each azobenzene section, meaning that, most probably, we have only monofunctionalized acrylate.

5.2.2 Photosensitive behavior of the Azo-acrylate

UV-Visible spectroscopy has been used to study the *E-Z* isomerization of the photosensitive compound and to demonstrate whether the absorption wavelength of this new compound falls in the visible region or not. The sample was irradiated via an IDual bulb Adaptative LED white light for 30 minutes and measurements were registered every 5 minutes in a range of 30 minutes. As its parent compound, also this methacrylic molecule can undergo *E-Z* (Figure 5.5) and *Z-E* (Figure 5.6) isomerizations when irradiated with white light or driven to higher temperature, respectively. The spectra overtime also show that the pps is reached after 15 minutes irradiation, which is a range of time slightly shorter than the one required to its parent compound. We started analyzing the photosensitive behavior of a system synthesized and kept all the time in the dark and, for this reason, expectedly composed only by molecules in *E* configuration. After the first 5 minutes of irradiation already 87% of the total allowed conversion was reached, with a content of *Z* isomer, calculated by Equation 4.1, of 28%.

$$Z\%_{UV-Vis} = \frac{A_0 - A_{pps}}{A_0} \qquad (5.1)$$

where A_0 and A_{pps} represent the absorbance at λmax for E isomer before and after irradiation with white light, respectively.

After 30 minutes of irradiation, at the pss, the 32% of *Z* isomer is present in the mixture. The calculated photoisomerization constant is 6.9 x 10^{-3} s^{-1}, as it is possible to see from the inset in Figure 5.5.

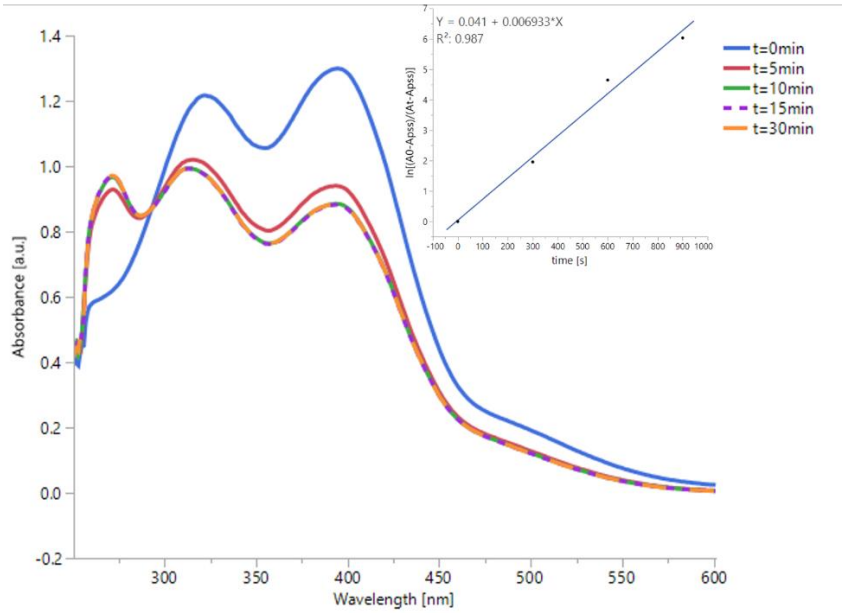

Figure 5.5 UV-VIS spectra of the photosensitive Azo-acrylate in DMSO solution during continuous irradiation with white light for 30 minutes.

In order to confirm the occurrence of thermal back isomerization, the sample was heated for 30 minutes at 70 ºC. The spectra were recorded after 5 minutes and after 30 minutes. As it is possible to see from the comparison of the blue and the dashed lines in Figure 5.6, the initial state is almost completely recovered and, indeed, only 6% of the *Z* isomer remains into the mixture.

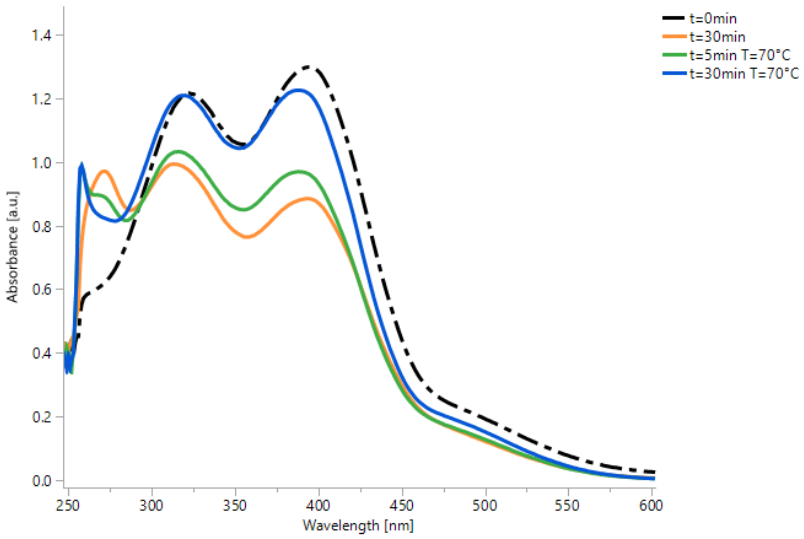

Figure 5.6 UV-Vis spectra depicting the thermal back isomerization of the Azo-acrylate at 70 ºC.

5.2.3 Radical polymerization mechanism

Acrylic monomers are pretty reactive thanks to the presence of the acrylic double bond and can easily lead to polymerization especially in the presence of light, temperature or suitable catalysts; radical polymerization is highly utilized in industrial applications because it is very fast, it may not require the presence of solvents, which can be undesired for the specific final application, and it ensures high percentages of conversion and therefore low presence of unreacted monomers. The main drawback of this approach is the poor control over the polymer growth and the chain length; however, it is possible to drive longer chain formation through the control of polymerization settings as time, temperature or monomer concentration.

The mechanism of free radical polymerization through double bound breakage was defined by Khararsh in 1937 and utilized by Flory to demonstrate the three phases of the radical polymerization which are: starting, propagation and termination.[8]

For the description of the three polymerization steps we will use, as an example, an azo-based initiator and as a monomer the Azo-acrylate.

5.2.3.1 Starting

Each molecule of initiator can decompose with temperature, light or other external stimuli according to its nature, and leads to two separate and identical

radicals. The organic molecules suitable for the radical formation and for the beginning of a radical polymerization should be stable at room temperature and capable of fast decomposition in the presence of the specific trigger. According to the strategy of decomposition, the initiators can be classified as: I) thermic, when the absorption of heat can stimulate the initiator decomposition and free radical formation, II) photosensitive, if the absorption of light can stimulate the initiator decomposition, III) redox, when the electron exchange between two species can lead to initiator decomposition and free radical formation.[9]

In this study only thermic initiators will be used. The two most used thermic initiators families are the organic peroxides and the azo-based initiators, which give rise to radicals according to the mechanism reported in Figure 5.7.

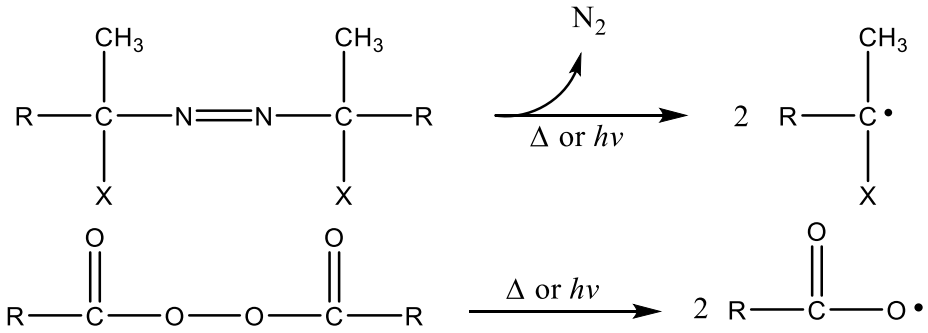

Figure 5.7 Mechanism of radical formation. a) schematic representation of an azo-based initiator and b) schematic representation of peroxide initiator.

In this study we will use azo-based initiators which are described as compounds having an azo group (R-N=N-R'), which decomposes with heat and/or light, to form carbon radicals and nitrogen gas. The formed carbon radical is excellent in reactivity and progresses polymerization of different types of vinyl monomers. According to the azo-initiator chemistry, the decomposition temperature can vary a lot and usually it is much lower than the one needed for the peroxides.

Azo-based initiators are usually selected according to their 10-hour half-life temperature which is defined as the temperature at which, after 10 hours into the selected solvent, the concentration of azo group halved. In this work, we used 4,4'-Azobis(4-cyanovaleric acid), a nitrile-based water-soluble azo polymerization initiator, which has a 10h half-life of 68 °C, the 2,2'-Azobis(2-methylbutyronitrile) an oil-soluble azo -initiator which shows a 10-hour half-life temperature of 60 °C and an excellent solubility in many different organic

solvents. As third initiator we used the 2,2'-Azobis(2,4-dimethylvaleronitrile); the 10-hour half-life temperature of this oil-soluble azo polymerization initiator is the lowest between all the initiators used and equal to 50 °C. Their structures are reported in Figure 5.8.

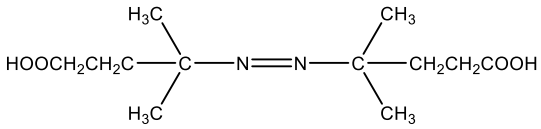

4,4'-Azobis(4-cyanovaleric acid)

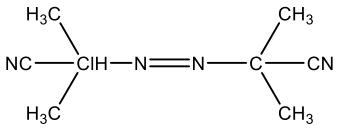

2,2'-Azobis(2-methylbutyronitrile)

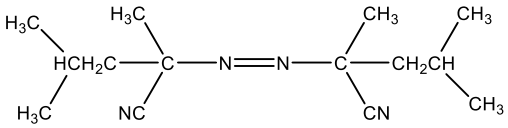

2,2'-Azobis(2,4-dimethylvaleronitrile)

Figure 5.8 Azo-based initiators used for the temperature-activated in-situ polymerization reaction.

As soon as free radicals are formed, they can recombine, or they can react with an acrylic monomer and thus, start the polymerization mechanism. When a free radical reacts with the double acrylic bond of the monomer, a new, longer acrylic radical gets generated, as reported in Scheme 5.2.

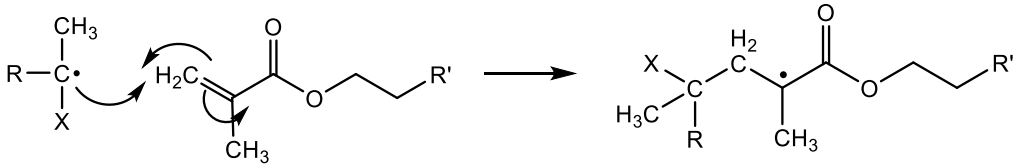

Scheme 5.2 starting step of radical polymerization reaction.

Where R', in the case studied for this work, is an azo based compound:

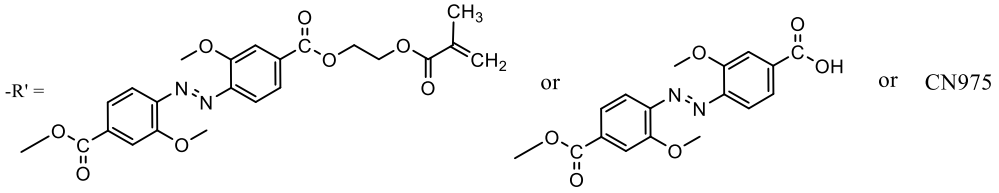

5.2.3.2 Propagation

In the propagation step the new monomeric acrylic radical, obtained during the starting step, reacts with other monomers to increase the polymer molecular weight; this step is accompanied by an increase in the viscosity of the reaction mixture. Usually the higher is the functionality of the monomer, the higher the

polymerization rate. The propagation step is schematically represented in Scheme 5.3.

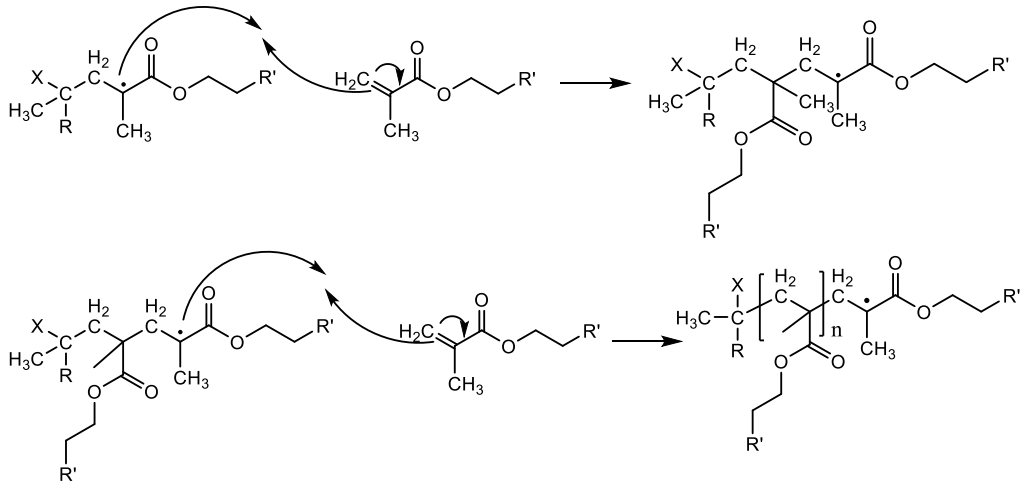

Scheme 5.3 Two propagation steps of the radical polymerization reaction.

5.2.3.3 Termination

To stop the reaction of polymerization and the polymer growth, a reaction between two radicals and the formation of a new chemical species without radicals regeneration is required. It is possible to have termination of the radical polymerization via recombination of two radicals or of a radical and a polymeric chain (Scheme 5.4), or *via* disproportion (Scheme 5.5).[10] In the first case, if two radicals recombine, they can form the starting initiator, but if one radical combines with a growing polymeric chain, a new chemical specie is then formed. In disproportion one radical transfers a hydrogen atom to the other, generating two stable molecules:

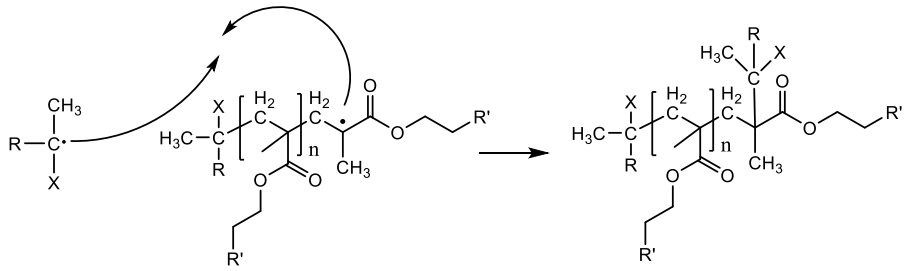

Scheme 5.4 Termination step via recombination of a radical with a polymeric chain.

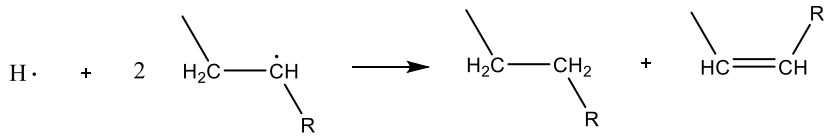

Scheme 5.5 Termination step via disproportion.

5.2.4 Hansen Solubility Parameters (HSP) for the selection of a new active material.

Before reporting the methodology for capsules preparation, it is important to explain why, after encapsulating Voyager Zen as a perfume *via* polymer precipitation in Chapter 3, we decided to focus our attention on encapsulating another perfume, Freesia PAC 60. Due to studies on the trends of customers' satisfaction and rating of different perfumes, indeed, Voyager Zen was discarded for commercial purposes; therefore, since capsules obtained by in-situ polymerization are much closer to the market and have more opportunities to be introduced in commercial formulations, we decided to use, for this procedure, an active ingredient that is also more appreciated by consumers. However, in order to verify that the change of the perfume does not determine a huge change in the microencapsulation process, and therefore that a comparison between the two encapsulation techniques still makes sense, we decided to compare the previously used perfume Voyager Zen with the new selected Freesia PAC 60, as far as their characteristic as solvents are concerned.

We used the Hansen Solubility Parameter in Practice (HSPiP) software, as a powerful set of tools that provides a 3D representation of HSP via a combination of software, datasets and a large eBook. Hansen Solubility Parameters (HSP) have proven to be a powerful, practical way to understand issues of solubility, dispersion and diffusion, characterizing solvents, polymers and/or nanoparticles by just three parameters: the dispersion δD, linked to Van der Waals forces, the polarity δP, related to dipole moment, and δH for hydrogen bonding.[11] These three numbers, which describe how a solvent behaves, together are called HSP. In practice, solvents are represented as points in a three-dimensional space called HSP space. It has been found that perfect HSP matches, between the solvents and the sample to be solubilized, are not

required for complete solubility. However, if many solvents are tested to see whether they are good or bad for a certain compound, it was found that the good ones clump together in a three dimensional plot that forms a sphere in the three dimensional HSP space with the HSP of the compound in the centre; the bad solvents fall outside of the sphere. While these predictions are, of course, not so reliable as the experimental determinations, nevertheless they allow sorting what is promising from what is not.

In addition, we also compared the partition coefficient (logP) of the two perfumes, which defines the ratio of their solubilities in two immiscible solvents; usually octanol and water are used as immiscible phases, but it could be any combination of immiscible fluids. The logP of the two fragrances is 3.1 for the Voyager Zen and 3.4 for the Freesia PAC 60; the two found values are not significantly different, and this can be considered as a first demonstration that the two perfumes could be interchanged without significantly affecting the properties of the final system.

The HSP were calculated and plotted in Figure 5.9 for several species: the Azo-acrylate in green, the CN975 in red, the Voyager-Zen and the Freesia PAC 60 respectively in orange and violet, the isopropyl myristate (IPM) in black. It is possible to do some consideration from the 3D graph below. From experimental tests we know that CN975 is soluble into the Voyager Zen. Therefore, it implies that any compound which falls in the imaginary sphere centred into the CN975 with radius equal to the distance between the Voyager-Zen and the CN975, in the HSP space, is still soluble in Voyager Zen. This, taking into account the positions of Freesia and the Azo-acrylate in the HSP plot, we can deduce that, not only the Freesia should be a solvent for CN975 as good as Voyager Zen, but also that the new synthesized acrylate, should be soluble into both the perfumes. As already stated, the HSP approach represents only a prediction which must be, thus, checked experimentally. We demonstrated experimentally that CN975 is soluble in Freesia perfume and also that the Azo-acrylate can be solubilized in it, though in small amount. As matter of fact, if we plot inside the HSP space, also another point, characteristic of a good experimental solvent for the Azo-acrylate, chloroform (blue point in Figure 5.9), we can notice that the high solubility sphere for the Azo-acrylate has a smaller radius if compared with the one from the CN975.

In any case, due to commercial reasons, we will still consider for the following study the capsules containing Freesia PAC 60 encapsulated into a shell bearing the Azo-acrylate. Given these premises, the solubility of the Azo-acrylate into the selected perfume has been considered a challenge to be addressed with different approaches.

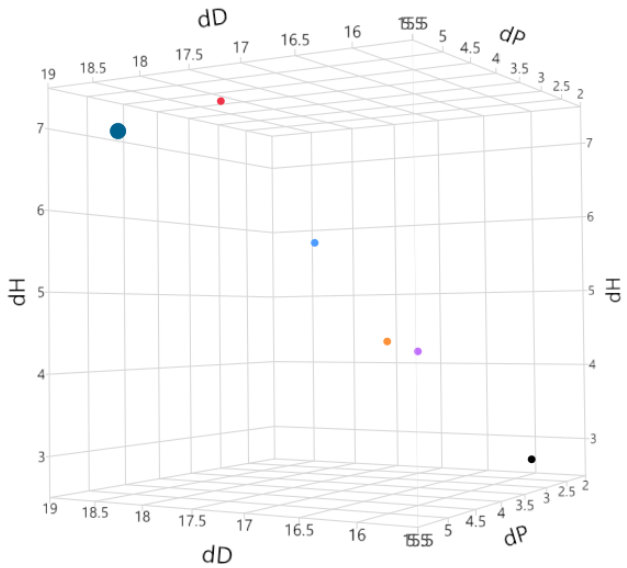

Figure 5.9 HSP space with the representation of: Azo-acrylate (green), CN975 (red), Voyager-Zen (orange), Freesia PAC 60 (violet), IPM (black) and chloroform (blue).

5.2.5 Photosensitive capsules: preparation and characterization

As pointed out in the previous section, the main challenge identified during the preparation of the photosensitive capsules was the solubility of the Azo-acrylate monomer into the perfume used, the Freesia PAC 60; it is indeed, important to remember that the in-situ polymerization encapsulation technique must be solvent free: therefore, several strategies have been pursued.

In most of the cases reported in this chapter, the use of Soluplus®, a polymeric solubilizer with an amphiphilic chemical structure, helped the solubilization of the Azo-acrylate when added in convenient percentages.

The obtained capsules, already listed in the Table 5.4 in the previous paragraph, are reported again in Table 5.5 with the corresponding values of

Encapsulation Efficiency (EE), which is evaluated through the following formula:

$$EE\% = \frac{total\ oil - free\ oil}{total\ oil}\ x\ 100 \tag{5.2}$$

where *total oil* is the amount of active in the initial formulation, calculated *via* total oil extraction, and the *free oil* is the amount of non-encapsulated, free active present in the slurry. As already explained in the experimental section, the percentages of total and free oil, and thus, of encapsulation efficiency, were calculated via GC-MS.

Table 5.5 Total oil, free oil and corresponding encapsulation efficiency for each batch of capsule.

Name of slurry	Core:shell	Composition	EE %
C1	90:10	2-(tert-butylamino) ethyl methacrylate, 2-Carboxyethyl acrylate, CN975	99
C2	90:10	2-(tert-butylamino) ethyl methacrylate, 2-Carboxyethyl acrylate, CN975	98
C3	90:10	CN975	98
C4	90:10	CN975, Azo acrylate	-
C5	90:10	CN975, Azo acrylate, Solupus	68
C6	90:10	CN975, Solupus	72
C7	90:10	2-(tert-butylamino) ethyl methacrylate, 2-Carboxyethyl acrylate, CN975, Soluplus	73
C8	90:10	CN975, Azo-acrylate	92
C9	90:10	CN975, Azo-acrylate, Soluplus	90
C10	95-5	CN975, Azo-acrylate	94
C11	90:10	2-(tert-butylamino) ethyl methacrylate, CN975, Azo-arylate, Soluplus	70

C12	90:10	2-(tert-butylamino) ethyl methacrylate, CN975, Azo-arylate, Soluplus	69
C13	95-5	2-(tert-butylamino) ethyl methacrylate, CN975, Azo-arylate	94
C14	90:10	CN975, Azo-acrylate	95
C15	95-5	CN975, Azo-acrylate	90

In the following sections we will comment the values of encapsulation efficiency reported in Table 5.5 and we will go through a more detailed study of the procedures and of the characterization of the morphology of each capsules' batch. Optical micrographs and scanning electron microscopy images of the obtained capsules were used for the morphological characterization of the systems. Emulsions were analysed mainly via OM to study their stability, size and the presence of un-dissolved material. On capsules, both OM and SEM were used to study the morphology and the size of the particles. Especially the case of optical microscopy is considered as a valid first screening to understand whether solid capsules are formed or not and if amorphous precipitates are present, to determine capsules mean size diameter and to detect the presence of encapsulated oil. This last test can be done by simply scratching the capsules under the microscope light irradiation with a spatula, and breaking the shell allowing the perfume to leak out. In some cases from ruptured shells it was even possible to put into evidence that the structure of the capsules was core:shell. The morphological details discussed with the help of optical micrographs were always confirmed by scanning electron microscopy (SEM). The mean particle size for the systems obtained was around 20 µm in all cases. As first experiment, we performed encapsulation of Freesia PAC 60, *via* in-situ polymerization and polyacrylate capsules formation, in a 500 mL reactor regularly used for laboratory scale up processes (**C1**), using three different commercially available acrylic monomers: 2-(tert-Butylamino)ethyl methacrylate, a monofunctional methacrylate, 2-Carboxyethyl acrylate, a monofunctional acrylate, and CN975, an aromatic urethane acrylate monomer which contains a mixture of monomers with a number of functional groups from 3 to 6; this last acrylate structure is covered by copyright from Sartomer

Americas. This procedure was patented and already optimized for the Voyager Zen fragrance.

Since the production of photosensitive capsules was based on the use of in-house synthesized molecules, we needed to use smaller volumes and, thus, smaller reactors in order to approach different strategies. The procedure just proposed was repeated in a smaller (50 mL) reactor (**C2**) and the two slurries obtained were compared.

Their encapsulation efficiency (**C1** and **C2**) was very high and close to 99%, meaning that almost all the perfume used into the initial formulation was encapsulated. Moreover, we can deduce that the change in the reactor used for the polymerization at high temperatures (**C2**) had a minor impact on the encapsulation efficiency. When only CN975 is used for the shell formation (**C3**), the degree of crosslinking increased, and we still obtained high values of encapsulation efficiency.

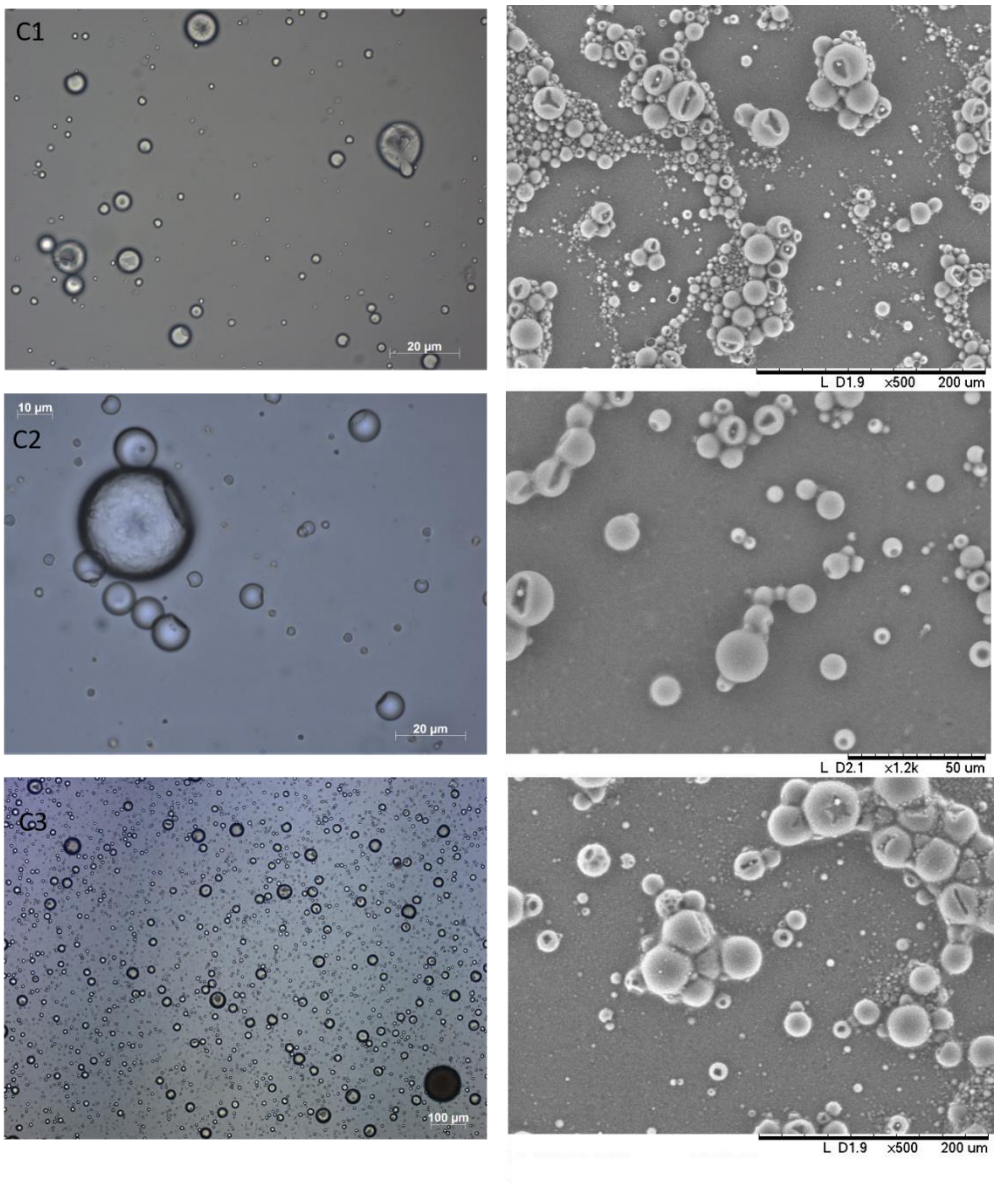

Figure 5.10 Optical micrographs (left) and SEM images (right) of batches C1, C2 and C3.

From the micrographs of the slurries **C1, C2** and **C3** reported above in Figure 5.10, we noticed that it is possible to obtain compact and dense capsules, which can successfully encapsulate the Freesia PAC 60 (top left scratched capsule), *via* in-situ polymerization of the three commercially available monomers both in a big (500 mL) (**C1**) and a small (50mL) (**C2**) reactor. Moreover, also by polymerizing only the CN975 (**C3**), we proved that it is possible to obtain polymeric capsules.

When we tried to replace 10 wt% of the shell composition with the Azo-acrylate (**C4**), we obtained an unstable emulsion and thus, the formation of an amorphous orange precipitate which is not formed by capsules. The selected amount of Azo-acrylate was, indeed, not completely solubilized into the perfume, showing up as a very fine dispersion which did not allow obtaining a stable emulsion. For this reason, we decided to add a certain amount of solubilizer to lead to complete dissolution of the monomer into the perfume. The capsules obtained with 10 wt% of Azo-acrylate into the shell and with 10 wt%, respect to the total dispersed phase, of Soluplus (**C5**), showed low EE, equal to 68%. Optical micrographs and SEM images from the batch C5 are reported in Figure 5.11. They demonstrate that also after introducing the in-house synthesized Azo-acrylate into the shell chemistry, it is possible to obtain capsules and that these capsules contain the oily Freesia encapsulated, even if with a low EE, as shown by the broken capsules in the optical micrograph on the left (Figure 5.11 - a). Figure 5.11 – b) shows instead, that amorphous precipitates were found on the surface of the capsule as well as floating in the dispersed phase; the presence of precipitate is also very clear from the SEM images.

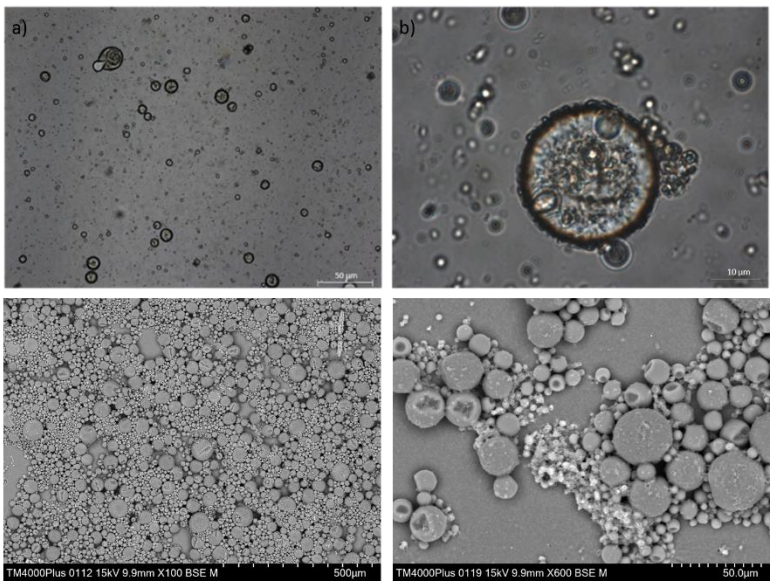

Figure 5.11 Optical micrographs (top) and SEM images (bottom) of the photosensitive batch C5.

In order to understand the reason for the low EE of C5, we performed encapsulation with the systems **C6** and **C7**, in which the shell is constituted only by commercially available monomers (as in the case of batches C2 and C3) and 10 wt% of Soluplus; the encapsulation efficiencies of both systems was found to be around 72% which showed that the main responsible for the low performance is the solubilizer. The preparation of batches C6 and C7 was helpful also to understand the nature of the precipitate in the batch C5, and to check whether it is unreacted Azo-acrylate; they have indeed, exactly the same composition of batches C3 and C2 respectively, but with the additional presence of Soluplus. We can see a clear difference between **C6** and **C7** reported in Figure 5.12, where there is presence of precipitate on the capsules' surface, and the samples C2, C3 (Figure 5.12) which only differ in composition for the absence of Soluplus and do not show precipitates onto the surface which appear, instead, smooth. This suggested that the amphiphilic polymer tends to go to the capsules' interface, mainly depositing on their surface.

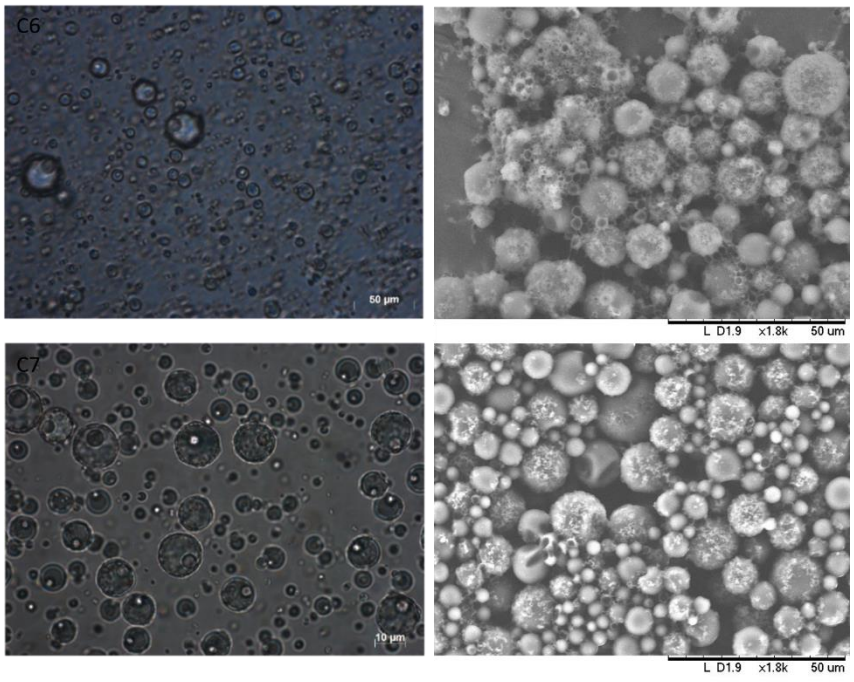

Figure 5.12 Optical micrographs (left) and SEM images (right) of the batches C6 and C7 which contains a certain percentage of Soluplus.

With the batches **C8, C9, C10** we tried different approaches to reduce the amount of Soluplus into the system while keeping a certain concentration of the photosensitive acrylate into the shell. First, we tried to solubilize the amount of Azo-acrylate corresponding to the 10% in weight of the shell into the perfume for three days and, before adding the final components of the dispersed phase, we centrifugated the dispersion in order to eliminate the fine solid content. It was not possible to calculate the accurate weight of the removed solid because it was not completely dry and wetted by perfume but, we can guess that approximately half of the initial monomer was removed; the solubilized phase changed colour if compared with the initial colour of the perfume, meaning that a certain amount of Azo-acrylate is surely solubilized and present into the dispersed phase. For this sample (**C8**), the EE reached again high values, equal to 92%. The same happened for **C9** and **C10** samples: in **C9**, Azo-acrylate in an amount corresponding to the 5 wt% of the shell was solubilized into the perfume containing 5 wt% (of the dispersed phase) of Soluplus (90% EE), while in **C10** we tried, as a different approach, to thinner the shell and to obtain 95:5 core:shell ratio capsules. With this strategy, we expected to have not only more perfume which could act as solubilizer but, also a thinner shell, in which the mobility of the photosensitive acrylate should be enhanced and facilitated (94% EE). Also in this case, 10 wt% of the shell was composed by Azo-acrylate but no Soluplus was used. In Figure 5.13 the OM and SEM images from batches **C8**, **C9** and **C10**, show that the capsules' surface does not seem affected by any precipitate and they appear smooth. No morphological differences could be found even when the capsules shell is thinner as in the case of the slurry C10.

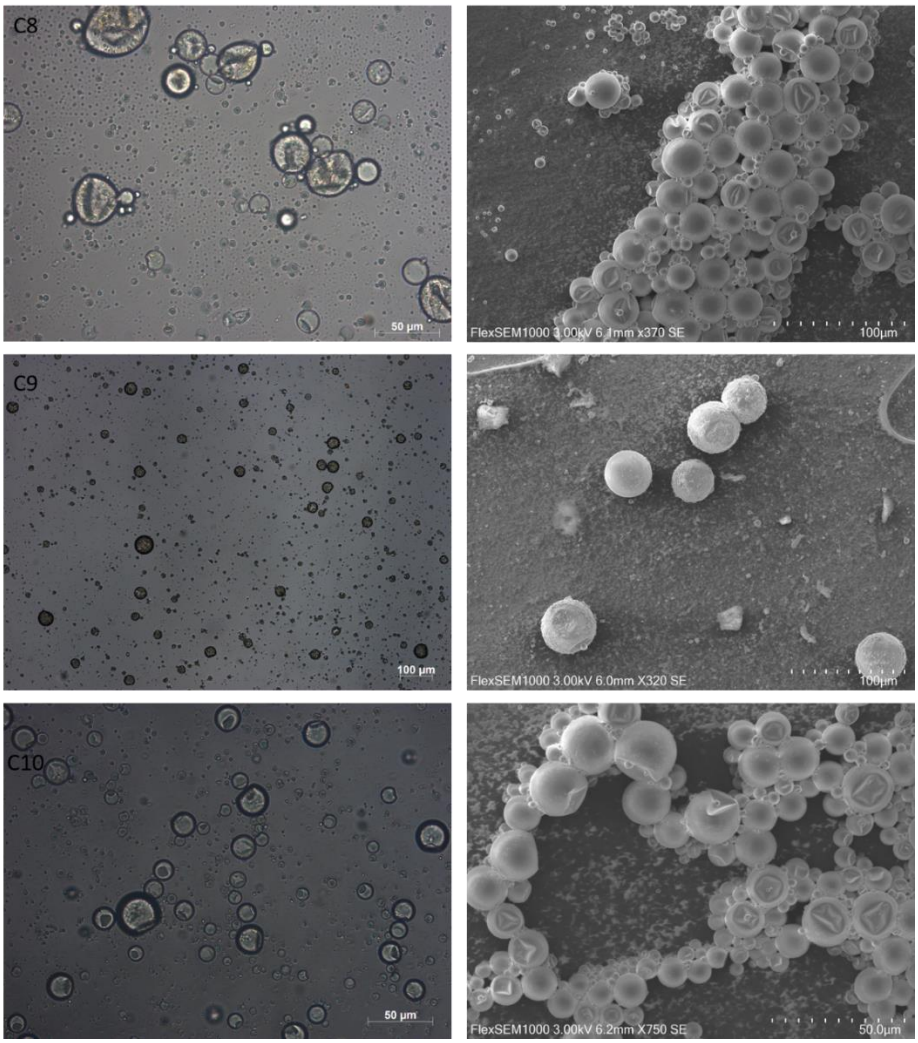

Figure 5.13 Optical micrographs and SEM images of photosensitive batches C8, C9 and C10.

In the case of **C11, C12** and **C13** we obtained capsules with 90:10, 90:10 and 95:5 core:shell ratio, using 10%, 5% and 0 wt% of Soluplus respectively and thus, 10%, 5% and 10 wt% of Azo-acrylate. Since in the previous photosensitive batches we eliminated 4.4% wt of monofunctional acrylates to add, in substitution, 10% wt of a bifunctional acrylate, we decided to reintegrate the 4.4% of monofunctional acrylate into the shell, with the aim of enhancing the mobility of the crosslinked network. Between the two monofunctional acrylates present in C1 and C2 we decided to discard the acrylate and to keep the methacrylate to ensure similar reactivity with the photosensitive monomer.

This last three experiments are more aimed to an enhancement of the photosensitive behaviour but, concerning the EE the behaviour is exactly in the expected ranges: when the Soluplus is added in high amounts, the encapsulation efficiency is low and close to 70% (**C11** and **C12**) but, when the amount of perfume is high enough to avoid the use of the solubilizer, the 94% of the initial perfume got encapsulated (**C13**). Also, concerning the morphological characterization it is possible to notice the same trend of the previous batches when 10, 5 and 0% of Soluplus is applied. The micrographs are reported in Figure 5.14.

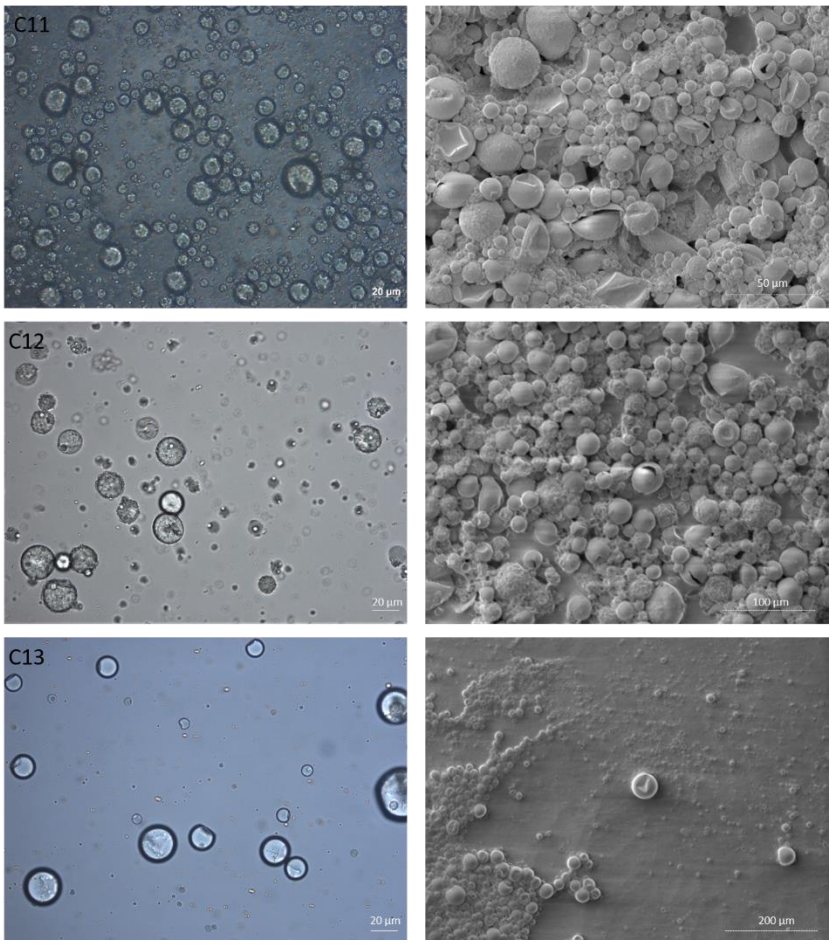

Figure 5.14 Optical micrographs (left) and SEM images (right) of photosensitive batches C11, C12 and C13.

Finally, in the last two experiments from Table 5.4, **C14** and **C15**, we decided to avoid the use of Soluplus in order to study the photosensitive release starting

from systems with a good EE; the two systems are composed by 4 wt% of Azo-acrylate in a 90:10 core:shell ratio capsule or 10% wt Azo-acrylate in a 95:5 core:shell ratio capsule with an EE of 90 and 95% respectively. In Figure 5.15, the morphological characterization of **C14** and **C15** is reported and they demonstrate that capsules were successfully formed.

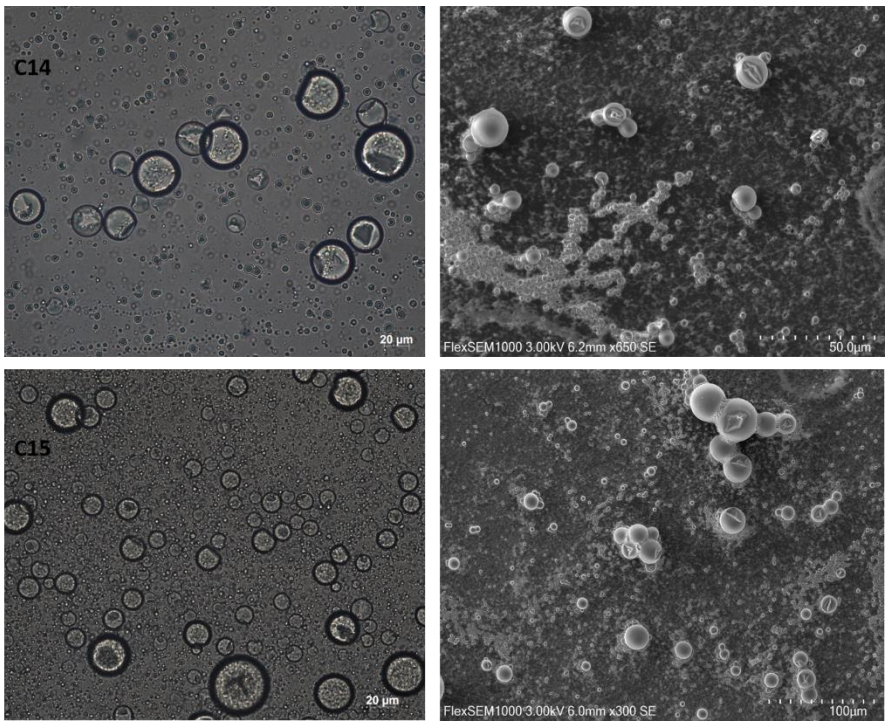

Figure 5.15 Optical micrographs (left) and SEM images (right) of the photosensitive batches C14 and C15.

5.2.6 Capsules performances

The stability of the obtained capsules overtime and in the finished products (FP), such as liquid laundry detergents, fabric enhancers and facial moisturizers, is a crucial characteristic to be tested. Optical microscopy was used for a fast screening, to show the stability of capsules in these products overtime; however, this is not enough to ensure long-term stability. Leakage tests were performed, following a well-defined and validated method based on GC-MS for the detection of perfume loss in the FP. Light sensitive behaviour of the capsules was tested using Dynamic Head Space (DHS) and sensory panel test.

In leakage experiments, samples are prepared by adding a known amount of perfume *via* encapsulates to the FP and mixing it according to standard protocols. Each batch of capsules, indeed, has a certain activity, which corresponds to the totality of the perfume inside the slurry (encapsulated and/or free) and thus, in most cases, to the perfume added into the initial formulation. The sample prepared are stored under controlled temperature and humidity to accelerate aging; tests are performed at time 0, after 1 and after 1 week, at rT and at 35°C and at constant humidity. For the systems reported in this Chapter, stability was studied in Heavy duty liquid (HDL) using standard HS method. The three measurements refer to different phenomena, according to the following:

- The values obtained for the first day, time 0 and at rT, give an idea of the free non-encapsulated perfume or perfume released from capsules that broke during mixing;
- The values after 1 day at 35°C, represent, in extreme conditions, the perfume entrapped in the wall and that diffuses immediately to the product.
- The values after 1 week, represent the stability of the capsule in the FP after 6 months, being indicative of the performances during the shelf life of the product.

Therefore, through these experiments it is possible to obtain the leakage profile overtime. The result of leakage takes into account all the PRMs which constitute the active; each PRMs value gives information about the concentration of that component in the analyzed sample (HS) compared with a standard (the perfume itself into the HDL base).

In the following graphs, the values of fresh leakage (t=0) and of leakage after 1 day (1D) and 1week (1W) are reported.

First, we compared the PAC obtained without the photosensitive acylate and in the two different reactors. From the graphs reported in Figure 5.16 it is possible to notice the ascending behavior of all the leakage profiles, which indeed increase overtime, at room temperature as well as at 35 ºC. Moreover, the capsules obtained in the small reactor (**C2**), show slightly higher leakage then **C1**, both at rT and 35 ºC, with an higher slope, especially at higher temperatures.

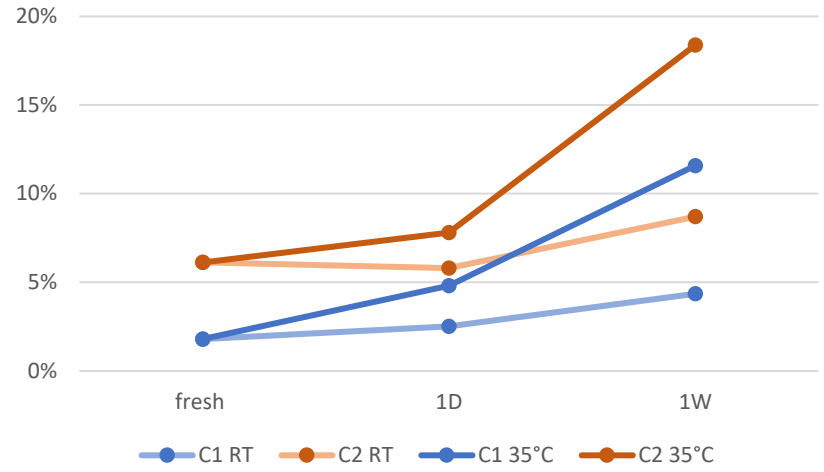

Figure 5.16 Leakage profiles of batch C1 (capsules obtained in the 500mL reactor) -blue- and of batch C2 (capsules obtained in the 50 mL reactor) – red.

The leakage profile of the batch C2 will be reported in all the other graphs and considered as a model behaviour for the comparison of the leakage profiles of all the remaining slurries, which were also obtained in the small reactor.

As we can see from Figure 5.17, the addition of Soluplus solubilizer into the system, has a big impact on capsules performances.

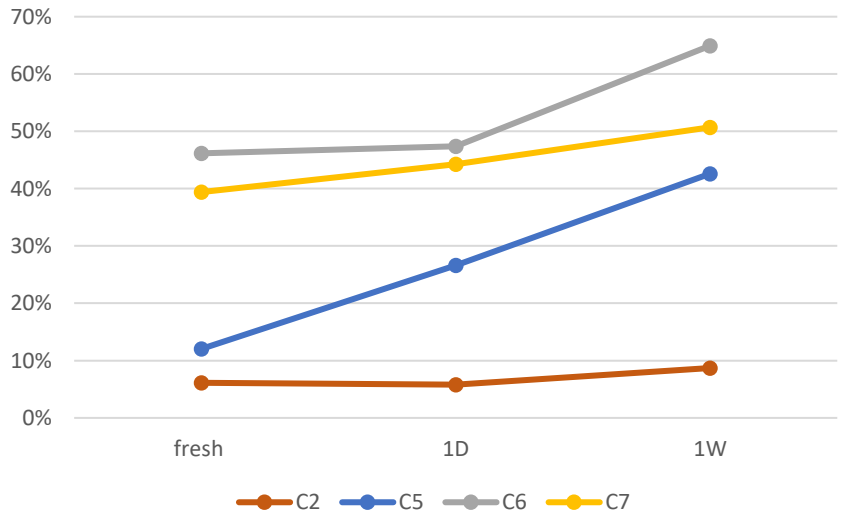

Figure 5.17 Leakage profile overtime at rT for C2, C5, C6, C7.

The addition of 10% of Soluplus into the system leads, after 1 week, to a perfume loss in the range 40 – 65% in weight of the initial perfume

encapsulated, independently from the presence of the photosensitive monomer. These leakage values are considered too high for commercial applications. The strategies adopted in order to decrease the amount of Soluplus and, thus, the leakage, lead to the profiles reported below in Figure 5.18.

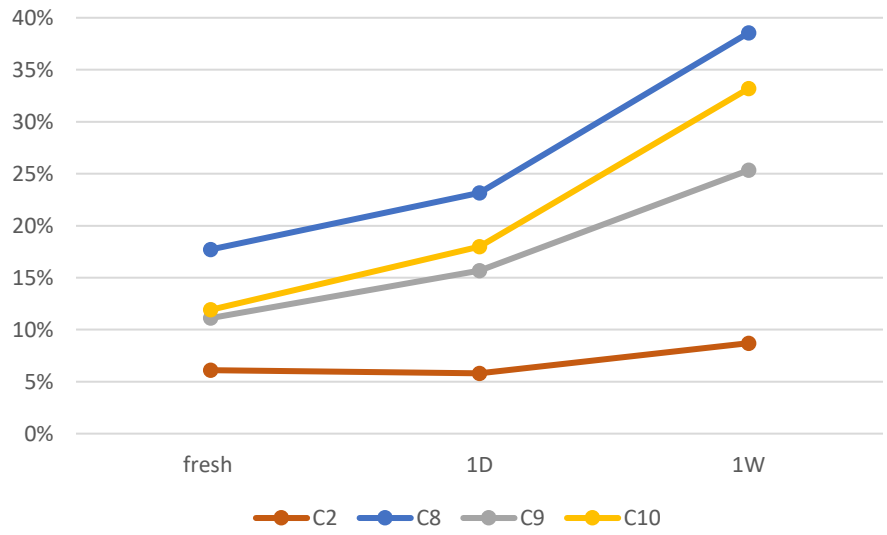

Figure 5.18 Leakage profile overtime at rT for C2, C8, C9, C10.

The reduction of the amount of Soluplus or its complete removal in a 95:5 core:shell ratio capsule (C9 and C10 respectively), allowed reducing perfume loss after one week, giving values in the range 25 – 40%. In the case of centrifugated systems, (C8), we were expecting better performances in terms of stability in the FP but, although leakage is lower if compared with C5, C6 or C7, the values are not meeting the expectations, probably due to the solid dispersed which was not completely removed.

We decided then to study the leakage profiles of the three photosensitive batches of capsules obtained *via* addition into the formulation of photosensitive acylate (10 and 5% wt) and 4.4% wt of monofunctional commercial methacrylate. The leakage profiles are reported in Figure 5.19 but, also in these cases, the leakage has very high values due to the presence of Soluplus.

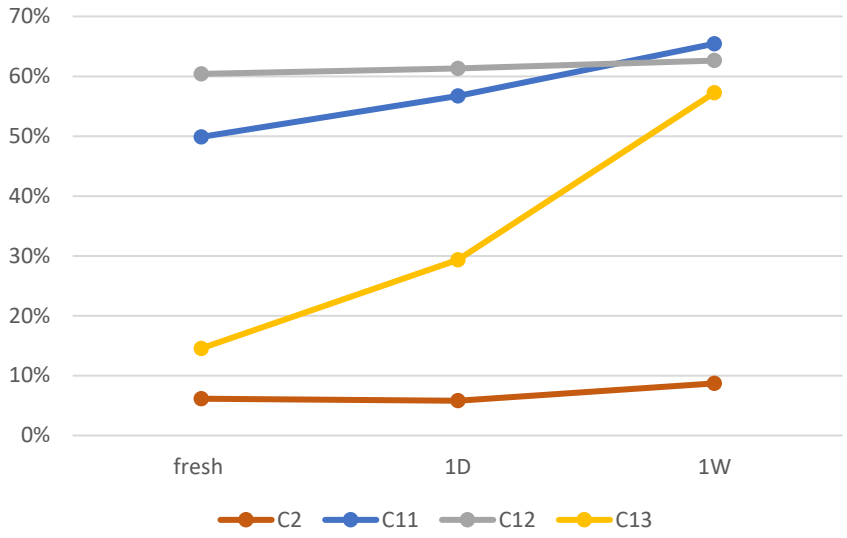

Figure 5.19 Leakage profile overtime at rT for C2, C11, C12, C13.

As final leakage experiments, we report in Figure 5.20 the profiles of two batches obtained without the use of Soluplus and with 4% wt of Azo acrylate: **C14** refers to 90:10 core:shell ratio capsules, while **C15** refers to 95:5.

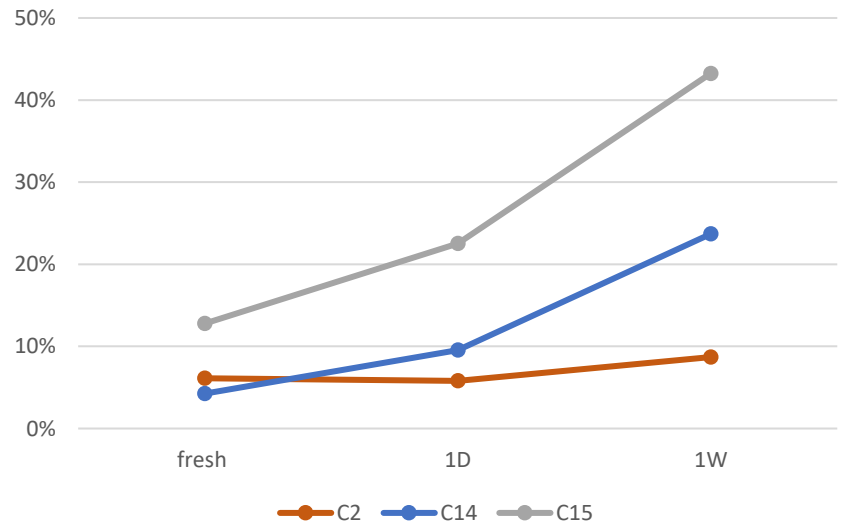

Figure 5.20 Leakage profile overtime at rT for C2, C14, C15.

Here we can notice how the absence of solubilizer results in a decrease of perfume loss which, especially for 90:10 core:shell capsules (C14), lies much

closer to the range considered commercially acceptable. For sake of completeness we report, in Figure 5.21, the values of leakage after 1 week at 35 ºC for all the obtained slurries:

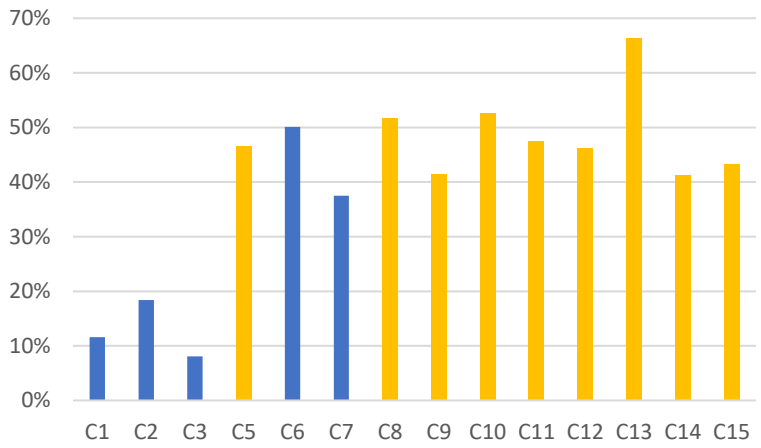

Figure 5.21 Leakage values of all the obtained batches in HDL after 1 week at 35 ºC. The yellow columns represent the levels of leakage from photosensitive capsules batches.

Finally, we need to underline that for all the reported leakage experiments, capsules, in the form of slurry, were in contact with the HDL which is the most aggressive environment in which they can be suspended; it has, indeed, the highest surfactants level if compared with other white bases. Therefore, other formulations and environments, less hostile, could be considered for the capsules, where their stability may me higher and where they may show higher performances.

5.2.7 Light triggered capsules release

The detection of ‘‘odor’’ as the biological, physical and psychological effects caused by the interaction between chemical stimulants, aromas and fragrances and our olfactive systems, is very important because it can be often related to the human perception of comfort and appreciation.[12] Chemical characterization of fragrances is indeed, important and the development and application of methodologies for the determination of the chemical composition of aromas is a challenging task. Gas chromatography coupled to mass spectrometry (GC-MS) is normally employed for the detection of concentration of relevant analytes in fragrance samples. Procedures based on the manipulation of the headspace (HS) in contact with fragrances are very popular and different approaches can

be employed, either using direct static head space (SHS) analysis or by collection of the odorants in the HS using sorbent devices. The light sensitive behaviour of the capsules was tested using Dynamic Head Space (DHS) and thermal desorption. Sample is prepared by adding a known amount of perfume via encapsulates to water; 100 µL of the mixture were added onto a filter paper inside an empty 250 mL volume jar. The measurement of the perfume released into the Head Space is obtained *via* absorption on a trap with a fixed flux and for a fixed time range. The substances absorbed are then released *via* thermal desorption into the GC-MS column. The areas of the identified peaks, characteristic of the PRMs, are reported in the graphs below for a qualitative analysis of the triggered release from photosensitive capsules. The challenge in these measurements was the optimization of the light/dark irradiation time ranges. We report the first experiment of triggered release, performed on photosensitive capsules with 10% of photosensitive monomer and 10% of Soluplus (**C5**). In this experiment two jars were prepared with the same amount of sample (100 µL water + slurry) sampled on a filter paper (3x2 cm). as already explained in the experimental part, one jar was kept in the dark for 30 minutes and the other was exposed to the white light for the same time range. Before starting the measurement, each sample was equilibrated for 30 minutes and, only after that period, the headspace was measured. The results show that after 30 minutes of irradiation, the photosensitive sample release 7% more perfume when compared with the unirradiated one (Figure 5.22).

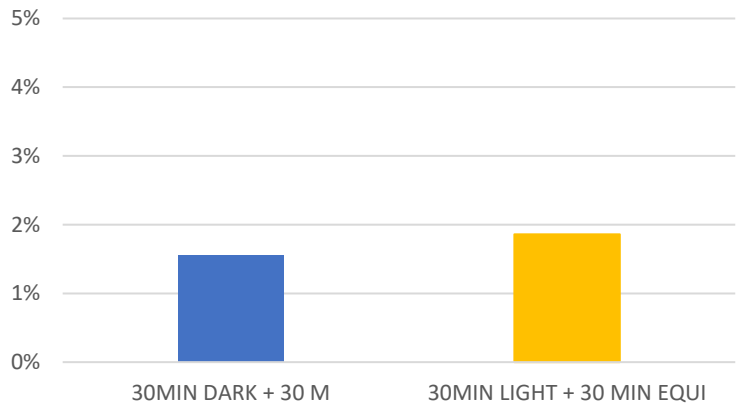

Figure 5.22 DHS measurement of the perfume released from batch C5 kept in the dark (blue) and irradiated with white light (yellow).

In these experiment conditions, a certain difference between the irradiated and unirradiated sample was detected, although it is not very significant. A different setting of the experiment in terms of irradiation and equilibration time was therefore attempted. The measurement of the triggered release can be boosted with several strategies as exposure to more intense light or "real use light conditions", use of freshly prepared samples to avoid the highest levels of leakage, or adjusting the exposure time range according to the isomerization time of the used photosensitive monomer into the polymeric network. We repeated then the same experiment, changing only the irradiation time from 30 minutes to 20- and 10-minutes. Also in these new cases, the photosensitive release of exposed samples is not significantly more pronounced than the one of samples kept in the dark. From a comparison of the release from **C2**, **C5** and **C7** reported in Figure 5.23, we can confirm that the release from photosensitive capsules exposed to light is higher than the one from capsules which do not contain the photosensitive acrylate exposed to the same light conditions. The release from batch C7, non-photosensitive capsules with 10%wt of Soluplus, has an intermediate value due to the high leakage provided by the presence of the amphiphilic polymer.

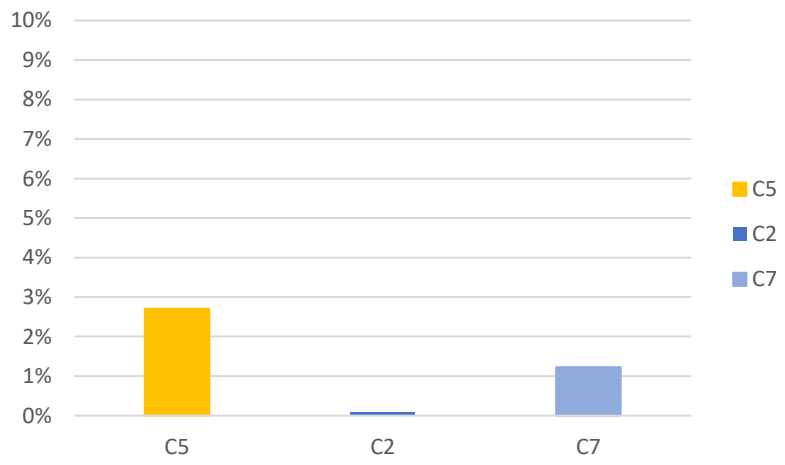

Figure 5.23 DHS measurement of the perfume released from batch C5, C2 and C7 after 10 minutes white light irradiation.

In the next experiment we decided to shorten the range of light irradiation and to eliminate the equilibration time in order to reduce the effect of leakage; in

UV-Visible experiments, indeed, most of the *E-Z* isomerization happens in the first 5 minutes of light exposure and the pps is reached after only 20 minutes. In Figure 5.24, the data are compared between the photosensitive batch **C5** and the corresponding non-photosensitive one, **C7**, so that both contains the same percentage of Soluplus and are affected by the same leakage.

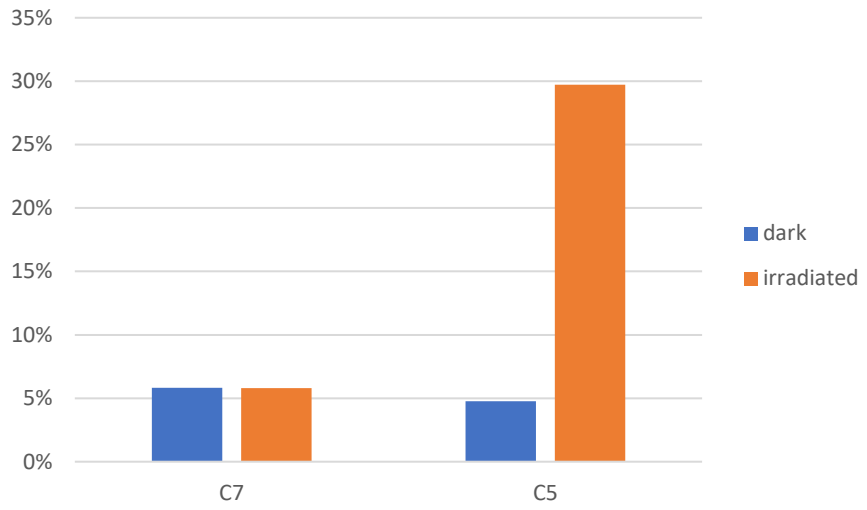

Figure 5.24 DHS measurement of the perfume released from batches C5 (photosensitive) and C7 (non-photosensitive) in dark conditions and after 5 minutes of white light irradiation.

From this experiment it is very clear that the sample containing the photosensitive monomer has a boosted release when irradiated with white light, if compared with non-photosensitive capsules: it releases 5 times more perfume than the non-photosensitive batch under light irradiation. After only 5 minutes of irradiation we can obtain a good balance between the leakage and photosensitive release due to isomerization; after this time range, the leakage is not very high and, at the same time, the percentage of conversion of the *E* isomer into the *Z* form, is at the pss so that, exactly in this first moments, the difference between the behavior of the two batches is evident. Probably, after 5 or 10 minutes of irradiation, when the pss is reached, release from photosensitive capsules, remains high but constant, while the leakage, which has an ascending behavior, takes over and could eventually mask the effect of photoisomerization.

Alternatives cycles of light/dark irradiation could lead to a deeper understanding of the release mechanism and a more pronounced photosensitive release; this approach was explored in the experiment shown below. In this case we measured the perfume released during the equilibration time and we waited 1h before irradiating the sample for 30 minutes; to notice the effect of light on the released perfume which is 5 times higher than the one released from the non-photosensitive sample (Figure 5.25).

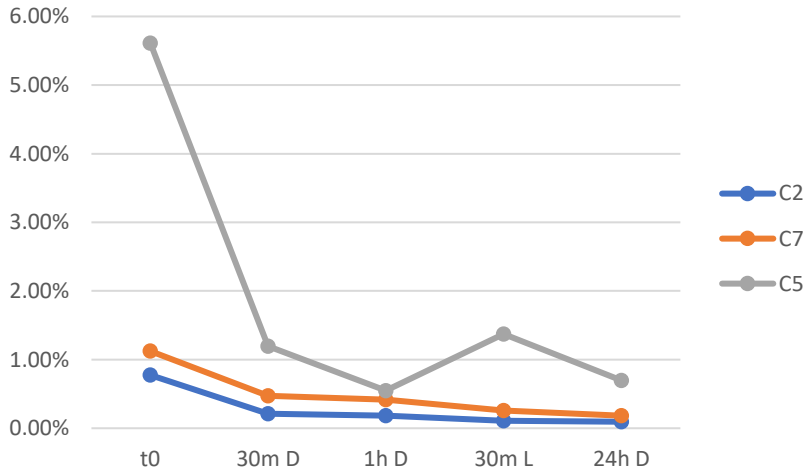

Figure 5.25 DHS measurements of the perfume released from batches C2, C5 and C7 after cycles of light/dark irradiation.

For sake of completeness we report also data of leakage also from other obtained capsules; we only selected batches with a good encapsulation efficiency and with the lower leakage profile. In Figure 5.26 the vales of perfume release from batches **C9** and **C10** are reported.

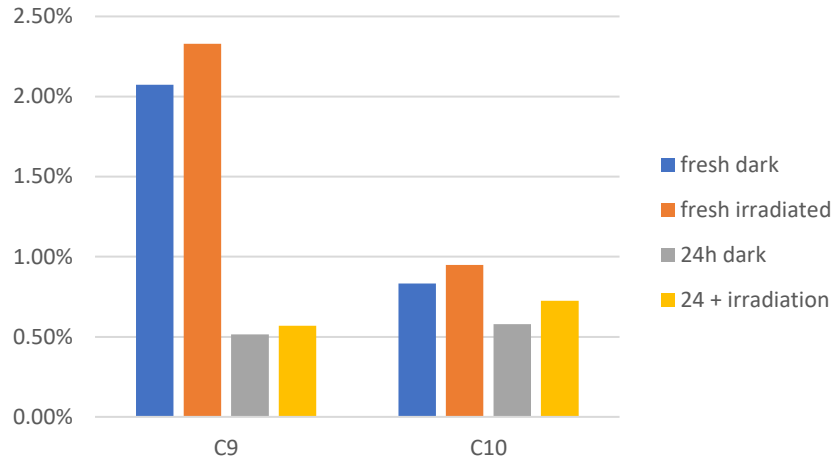

Figure 5.26 HDS measurement of the perfume released from batches C9 and C10 at 4 different moments: t=0, 10 minutes light irradiation, 24h, 24h + 10minutes light irradiation.

The obtained microcapsules have several drawbacks and among all, the most important is the difficult balancing between leakage and controlled release; this is affected by the level of permeability of the capsules shell which also depend on the crosslinking level and in the free volume, and the level of solubilizer and surfactants in the FP.

We decided to accompany the experiments of perfume release via DHS with sensory test for smell detection performed in the sensory laboratories from the Brussels Innovation Center. Sensory tests on curtains in home care rooms were thus, performed to test the applicability of capsules in detergents for the dry cleaning. Olfactive assessment by external panelists were performed to investigate the influence of the acrylate monomer into PACs and registered fresh, after 2h, after 24h; for this purpose, capsules with and without the photosensitive molecule were tested. Samples with 0.1 and 0.5% activity, were prepared by dilution of the slurries in milliQ water. Deposition of the sample on curtains was obtained by a spray dispenser; the rooms are in light conditions. The results from the assessment show that the olfactive difference between different samples is not very big and considered not relevant for commercial applications.

5.3 Conclusions

Light sensitive polyacrylate capsules (PAC) containing modified azobenzene in the shell were successfully prepared *via* in-situ polymerization. In order to understand whether it is possible to form more compact shells without losing the photosensitivity, polyacrylate (PAC) chemistry was selected and carefully designed to introduce a modified azobenzene light sensitive moiety into the shell. The obtainment of a light sensitive compact PAC has several challenges: the synthesis of the acrylate monomer containing the light sensitive modified azobenzene, the solubility of this monomer in the selected perfume for the microencapsulation process and the optimal percentage of the photosensitive moiety in the microcapsules' shell.

It was possible to successfully synthesize a photosensitive methacrylate, the bis(2-(methacryloyloxy)ethyl)4,4'-(diazene-1,2-diyl)(E)-bis(3-methoxybenzoate), called Azo acrylate, and containing the ortho-substituted azobenzene moiety as core structure; the photosensitive molecule was obtained with 80% yield, while NMR studies confirmed that the molecule obtained is monofunctionalized. Its photosensitive behavior was studied by means of UV-Visible spectroscopy: first, the absorption in the visible range was confirmed, as for its parent compound; second the *E-Z* isomerization was induced *via* white light irradiation, reaching the pss after 15 minutes exposure; the conversion *E* to *Z* resulted slightly lower compared with the parent molecule. The thermal *Z* to *E* conversion was also successfully induced at 70 °C and with almost complete recovery of *E* isomer. These monomers were successfully tested in radical polymerization with other commercially available acrylates, leading to a crosslinked network which can encapsulate the selected core material.

Light sensitive perfume capsules were obtained without using any solvent and therefore were considered suitable for testing in detergents applications. In the procedure reported for capsules preparation, besides the three initiators, the monomers and the PVA used as emulsifier, other two species were present in the composition: IPM, which is an anti-solvent that helps the precipitation of the acrylates and drives the precipitation at the interface, and the Soluplus, which is used as solubilizer to overcome the challenging solubilization of the Azo-

acrylate into the perfume without the use of any additional solvents. Concerning the use of IPM, from previous studies we know that the higher the level of IPM the more compact is the capsule shell; as for the Soluplus, we noticed its direct influence on the encapsulation efficiency, on the morphology of the external wall of the capsules and on performances such as the leakage. Capsules morphology was analyzed via OM and SEM; the core – shell morphology was confirmed. The mean size was analyzed and found to be around 20 µm. Finally, the precipitate deposited on the capsule surface when the solubilizer was used, was identified as Soluplus. Leakage experiments showed that the higher the Soluplus content, the higher the leakage and the lower the EE because of the formation of less compacted shells. A good approach for the obtainment of more stable capsules can be the reduction or complete elimination of Soluplus, taking into account that a good balance with the amount and solubilization of Azo-acrylate is required, or the increase of IPM; since IPM is the most expensive component and material and it needs to be at the very limit to obtain affordable and competitive capsules so that we cannot go above the 30%.

The amount of Azo acrylate was, thus, optimized to maximize the performances; good EE values were reached when no or low (5 wt%) Soluplus was used (batches C8, C9, C10, C13, C14 and C15) both for 90:10 and 95:5 core:shell ratio.

Via DHS measurements, we were able to underline the enhanced photosensitive release of capsules batches with lower leakage and good EE.

When compared with non-photosensitive batches, the release from light-sensitive capsules appear to be significantly enhanced by irradiation of light during the first 5 minutes. The cyclic light-dark behavior, of the released perfume, is not visible due to the high levels of leakage which overcome the triggered release. For an improvement of the DHS measurement the introduction of a purge gas such as, for example, helium, nitrogen, or synthetic air can be considered to improve the measurement of volatiles and the method of absorption, but also to avoid possible deposition of the fragrance on the surface of the jars. Also, an increase in the percentage of photosensitive molecule with a decrease of the solubilizer used, and thus, of the leakage, would surely lead to more noticeable triggered release of perfume. A change in the perfume/active used, with the selection of one which follow in a smaller HSP

sphere centered in the Azo acrylate, or the selection of a less aggressive solubilizer, can be valuables options to consider for a good optimization of the system and the obtainment of systems which can really release the active in an effective way, and only when light is applied.

Sensory panel testing proved that release from photosensitive capsules is too fast and that the concentration after 24h is too low to be noticeable for consumers.

Bibliography

1. Dihora, J. O., Smets, J. N., Schwantes, T. A. *U.S. Patent No. 9,186,642*. Washington, DC, Delivery Particle. (2015).
2. Foris, P. L., Brown, R. W., Jr, P. S. P. U.S. Patent No. 4,001,140. Washington, DC, Capsule manufacture. (1978).
3. Schwantes, T. A. U.S. Patent Application No. 14/104,307. Microcapsule particles. (2014).
4. Nicolescu, F. A., Jerca, V. V., Draghici, C., Vuluga, D. M., Vasilescu, D. S. Synthesis and characterization of novel azobenzene methacrylate monomers. Designed monomers and polymers, 12(6), 553-563, (2009).
5. Tylkowski, B., Giamberini, M., Underiner, T., Prieto, S. F. Smets, J. Photo-Triggered Microcapsules. *Macromol. Symp.* **360**, 192–198 (2016).
6. Evans, S. B., Mulvaney, J. E., Hall, H. K. On the synthesis of pure (meth) acrylate esters and their corresponding homopolymers. *J. Polym. Sci. Part Polym. Chem.* **28**, 1073–1078 (1990).
7. Jahns, E., Freundschuh, U. *U.S. Patent No. 5,292,835*. Washington, DC: U.S. Patent and Trademark Office. Microcapsules. (1994).
8. Ballard, N., Asua, J. M. Radical polymerization of acrylic monomers: An overview. *Prog. Polym. Sci.* **79**, 40–60 (2018).
9. Su, W.-F. Radical Chain Polymerization. in *Principles of Polymer Design and Synthesis* (ed. Su, W.-F.) 137–183, Springer, (2013).
10. Zhu, S., Tian, Y., Hamielec, A. E., Eaton, D. R. Radical trapping and termination in free-radical polymerization of methyl methacrylate. *Macromolecules* **23**, 1144–1150 (1990).
11. Hansen, C. M. *Hansen solubility parameters: a user's handbook*. Second Edition.CRC press. (2002).
12. Augusto, F., Leite e Lopes, A., Zini, C. A. Sampling and sample preparation for analysis of aromas and fragrances. *TrAC Trends Anal. Chem.* **22**, 160–169 (2003).

6. General conclusions

Conventional capsules used nowadays in consumer goods products are able to release perfume due to mechanical breakage resulting in a fast and constant release over time. Chemical and technological trends are, today, addressing the microencapsulation process; chemical trend focuses on the research of new chemistries for the obtainment of sustainable capsules, or the possibility to trigger the release of the active encapsulated ingredient, depending of the final usage of the capsules, choosing among different triggers as enzymes, light or temperature. The objective is to give response to the need of reaching a temporal delivery in specific applications. The second important aspect is the technological process trend and the exploration of new techniques for capsules preparation, where the capsules size and the speed of capsules formation, are more and more controlled.

In applications where no or low mechanical stress is involved, for example in beauty care applications or sprays for the home care, it is important to reach a controlled release of the perfume over time. We developed, in this work, chemical species which are not only sensitive to external stimuli (light and temperature) but can also be used to encapsulate an active ingredient. We focused on the preparation of light sensitive, core-shell capsules for the encapsulation of a perfume with business interest for the Procter & Gamble Company (P&G), *via* several strategies and techniques to enrich commercial capsules with light-triggered release.

The photosensitive activity of the polymeric capsules developed in this work, is achieved thanks to the presence, into the capsule shell, of azobenzene-based moieties which are, thus, used as photochromic material. The isomerization of these molecules, triggered by light irradiation, is associated, indeed, to geometrical, spatial changes of the molecule itself, that will influence the morphology and the geometry of the capsule shell, leading to shrinking and untightening of the network (opening of “pores”) into the shell, for the passage of the active.

The main achievements of this thesis are as follow:

- We successfully synthesized several photosensitive moieties that were used, with different techniques, to obtain microcapsules: the Azo-acid (4,4′-bis(chlorocarbonyl)-2,2′-dimethoxy azobenzene, yield 49%) and the Azo-chloride (azobenzene-2,2′-dimethoxy-4,4′-dicarboxylic acid, yield 92%) as parent compounds used for the subsequent obtainment of the Azo-oligomer ($1.4 \cdot 10^3$-$2.6 \cdot 10^3$ g/mol, 4-20% yield) and the Azo-acrylate (bis(2-(methacryloyloxy) ethyl)4,4'-(diazene-1,2-diyl)-bis(3-methoxybenzoate), yield 80%).

  All the obtained moieties were characterized by NMR analysis, to check their purities, while their isomerization was studied by both NMR spectroscopy at high temperature and UV-Visible spectroscopy. The study of the isomerization was used not only to confirm that geometrical and spatial changes were associated to light irradiation, but also to calculate the isomerization kinetics and to understand how rapidly these changes would happen. By monitoring the absorbance of the $\pi-\pi^*$ absorption band at 400 nm of the Azo-acid, we learned that during *E-Z* isomerization, the photostationary state (pss) is reached after 30 minutes with 40% conversion. The *Z-E* thermal back isomerization at 70°C leads to 50% reconversion of the *Z* isomer in 30 minutes. For the oligomeric species the isomerization is slightly slower, as expected, and the pss is reached after 20 minutes of white light irradiation with 20% conversion; in this case the *E* isomer is completely recovered with thermal back isomerization, heating the sample in the darkness at 70°C for 20 minutes. As for the Azo-oligomer, also the Azo-acrylate reaches the pss after 20 minutes of light irradiation with 30% conversion; this content of *Z* isomer is completely reverted to *E* after 30 minutes in darkness at high temperatures. The reversibility of the isomerization under different stimuli (visible light, temperature), opens interesting perspectives to the application of these molecules.

- Capsules were obtained with two different approaches. I) The photosensitive oligomers were used to prepare capsules *via* the physical method of phase inversion precipitation, which do not require any chemical reaction to form the shell. Due to the low molecular weight of the photosensitive oligomer and to its mechanical instability, capsules were

obtained blending it with the commercially available polysulfone. This technique requires the use of solvents and leads to capsules with porous shells, high leakage and low encapsulation efficiency (60-80 wt%).

A second approach for the obtainment of capsules was also explored. II) Chemical encapsulation techniques were applied with the aim of leading to more compact shell, lower leakage and good performances in the finish product (FP). In-situ polymerization was used to create polymeric shells containing the azobenzene-based moieties; Azo-acrylate was used for the obtainment of polyacrylic capsules, while the Azo-chloride was used for the formation of capsules based on melamine resins. In both cases, capsules sized around 30 µm were successfully formed with core:shell ratio 90:10 and 95:5 and high encapsulation efficiencies (90-99 wt%). This chemical encapsulation technique not only is solvent free but is already extensively used in industrial processes of microencapsulation.

- OM and AFM analyses confirmed, for all the crosslinked capsules obtained, that photoirradiation induces a change in capsules surface morphology and size. Both theoretical and experimental studies suggest that a squeezing effect, together with the untightening of the network due to isomerization of the photosensitive sections, can be responsible for photo-triggered increased release. The combination of AFM, on the capsules surface, and NMR, for the isomerization study, put into evidence that the initial morphology and size of the microcapsules are restored as a consequence of thermal back-isomerization at high temperatures.

Especially with the chemical encapsulation technique it is possible to modulate and easily change the percentages of photosensitive oligomer/monomer inserted into the shell and tune the properties of the final capsule. Also, with this approach and with the help of a good and effective molecular design, it is possible to obtain good capsules, changing the chemistry of the shell, without greatly modifying the industrial process. Once selected the chemistry of the crosslinking reaction, it is possible to functionalize the stimuli-responsive molecule accordingly and incorporate it into the net. This strategy based on the combination of different chemical blocks in one single network, could help not

only in the preparation of a wide range of stimuli-responsive systems, but could be also used to fulfil additional desired final shell characteristics, such as, for instance, biodegradability.

Appendixes

Appendix A – List of abbreviations

ADF - Amsterdam density functional

AFM – atomic force microscopy

d-CDCL3 - deuterated chloroform

DCM – dichloromethane

d-DMSO - deuterated DMSO

DHS – Dynamic Head Space

DMF - dimethylsulfoxide

DMSO - dimethyl sulfoxide

Ea - activation energy

Ff – flow focusing

FP – finish product

FP – finished product

HDL – heavy duty liquid

HOMO - highest occupied molecular orbital

IR - Infrared

LUMO - lowest un-occupied molecular orbital

MF – melamine-formaldehyde

NMP – n-methyl pirrolidone

NMR - Nuclear Magnetic Resonance

OPD - optical path difference

P&G – Procter & Gamble

PAC – polyacrylate capsules

PAGs – photoacid generators

PES - potential energy surface

PMC – perfume microcapsules

ppm – parts per million

pss – photostationary state

PSD – Particle Size Distribution

PSD – particle size distribution

PSf - polysulfone

PU – polyurethane

SG – Spray Gun

TDDFT - spin flip time-dependent density functional theory

TDDFT – Time dependent density functional theory

TGA – thermogravimetric analysis

TLC – thin layer chromatography

TMS - tetramethylsilane

TS - Transition state

UF - urea-formaldehyde

UV – Ultraviolet

VZ – Voyager Zen

XG – Xanthan gum

Appendix B – List of Figures and Tables

Appendix C - Congresses and contributions

Authors: R. Del Pezzo, N. A.G. Bandeira, A. Trojanowska, S. Fernandez Prieto, T. Underiner, M. Giamberini, B. Tylkowski
Title: **Ortho-substituted azobenzene: shedding light on new benefit**. *Pure Appl. Chem., 91(9), 1533-1546, 2018*.

Authors: D.Pirone, V.Marturano, R.Del Pezzo, S.Fernandez Prieto, T.Underiner, M. Giamberini, B. Tylkowski
Title: Molecular design od microcapsule shell for visible light-triggered release, *Polymers, 1(5), 904, 2019*.

Authors: D. Pirone, R. del Pezzo, T. Underiner, S. Fernandez Prieto, A. Trojanowska, M. Giamberini, B. Tylkowski
Title: Photo-triggered microcapsules, *in book Microencapsulation, DeGruyter Publisher, Berlin/Boston, in press.*

Authors: R.del Pezzo, A. Trojanowska, D.Pirone, N.A.G. Bandeira, K.A. Boganowicz, M. Giamberini, B. Tylkowski,
Title: Light sensitive microcapsules based on un-modified azobenzene moieties, *in book Microencapsulation, DeGruyter Publisher, Berlin/Boston, in press.*

Authors: R. del Pezzo, M. Giamberini, S. Fernandez Prieto
Title: Stimuli responsive membranes for the targeted delivery of actives
Congress: 15th Doctoral day 2018
Format (poster or oral): Poster
Date: 23 May 2018 **Place**: Tarragona, Spain

Authors: R. del Pezzo, M. Giamberini, S. Fernandez Prieto
Title: Stimuli responsive membranes for the targeted delivery of actives
Congress: *16th NYM (Network Young Membrains) 2018 conference*
Format (poster or oral): Oral presentation
Date: 5-7 July 2018.**Place**: Valencia, Spain

Authors: R. del Pezzo, M. Giamberini, S. Fernandez Prieto
Title: Stimuli responsive membranes for the targeted delivery of actives
Congress: *Georgia Tech 93rd ACS colloid & surface science symposium*
Format (poster or oral): Oral presentation
Date: 16-19 June 2019.**Place**: Atlanta, Georgia

Authors: R. del Pezzo, M. Giamberini, S. Fernandez Prieto
Title: Photo-responsive polyesters for the preparation of triggered devices
Congress: *International symposium on encapsulation technology*
Format (poster or oral): Oral presentation
Date: 22-24 October 2018.**Place**: Tarragona, Spain

Authors: R. del Pezzo, M. Giamberini, S. Fernandez Prieto
Title: Stimuli responsive membranes for the targeted delivery of actives
Congress: *Polymer World Congress – advancement of materials for global excellence*, *21st assembly of Advanced Materials Congress*
Format (poster or oral): Oral presentation
Date: 03-06 September 2018.**Place**: Stockholm, Sweden
Award: best oral presentation

Authors: M. Ammendola, J. Ma, D. Pirone, R. del Pezzo, G. Colace
Title: SMARTMEM: Bridging the emerging technology platform around smart-membranes and consumer goods products
Congress: 2019 MCAA General Assembly & Conference
Format (poster or oral): Poster
Date: 24-25 February 2019 **Place**: Vienna, Austria

Authors: R. del Pezzo, M. Giamberini, S. Fernandez Prieto
Title: Light sensitive thermosetting gates: opportunities for payload-controlled release
Congress: 7th edition of Baekeland Conference
Format (poster or oral): Oral presentation
Date: 15-18, 2019. **Place**: Tarragona, Spain

UNIVERSITAT
ROVIRA i VIRGILI